Glucosylceramide Maintains Colon Epithelial Barrier Integrity During Enterotoxigenic *Bacteroides fragilis* Challenge

Logan Dane Patterson

Roanoke, Virginia

B.S., Biochemistry, Virginia Polytechnic Institute and State University, 2014

B.S., Biology, Virginia Polytechnic Institute and State University, 2014

M.S., Biological and Physical Sciences, University of Virginia, 2016

A Dissertation presented to the Graduate Faculty of the University of Virginia in Candidacy for the Degree of Doctor of Philosophy

Department of Pathology

University of Virginia

November, 2020

Dissertation Abstract

Bacteroides fragilis is a human commensal bacterium that colonizes the majority of adults. There are two subtypes of this bacterium, Nontoxigenic *Bacteroides fragilis* (NTBF) and Enterotoxigenic *Bacteroides fragilis* (ETBF), which differ based on the production of *Bacteroides fragilis* toxin (BFT) by ETBF. ETBF may asymptomatically colonize humans, but it may also cause diarrheal illness. Early microbiome studies of patients with colorectal cancer (CRC) revealed that 90% of patients were colonized with ETBF, suggesting that ETBF was involved in cancer formation or progression. Indeed, *in vivo* studies in genetically susceptible mice showed that colonization with ETBF could lead to tumor formation in the colon within 4 weeks. Tumor formation is dependent on a pro-inflammatory signaling cascade that begins with E-cadherin cleavage in colon epithelial cells (CECs). T helper 17 (Th17) cells producing IL-17A are recruited to the area and stimulate STAT3 and NFκB in CECs, leading to aberrant expression of cytokines and, eventually, the formation of tumors. The initial host response to BFT has not been fully characterized, so we focused on early changes in CECs that could promote inflammatory disease. To do this, we measured sphingolipids, a class of lipids with a sphingoid backbone that play a wide number of roles in cells, from growth and differentiation to cell death. We found that normal C57BL/6J mice colonized with ETBF for one week had increased levels of glucosylceramide in their distal colon. Glucosylceramide is a critically important lipid in the intestines because of its role in

maintaining the epithelial cell barrier. In order to determine the purpose of BFT-induced glucosylceramide increases in the colon, we utilized colon organoids (colonoids) derived from the distal colons of C57BL/6J mice. Colonoids treated with BFT showed higher levels of glucosylceramide, consistent with our previous *in vivo* findings. We assessed the importance of glucosylceramide in CEC response to BFT by using pharmacological inhibitors of glucosylceramide synthase (GCS), the enzyme responsible for generating glucosylceramide, and glucocerebrosidase (GBA), the enzyme responsible for breaking down glucosylceramide. We found that inhibition of GCS caused colonoids to burst, a phenomenon that could be prevented by blocking GBA. The prevention of colonoid bursting was due to the stabilization of tight junction protein 1 (TJP1), an important mediator of tight junctions that regulate paracellular permeability. In addition, we found that glucosylceramide was released from CECs in extracellular vesicles (EVs), although the role of glucosylceramide in EVs is unclear at this point. Together, we have shown for the first time a novel mechanism that CECs use to protect the epithelial barrier from bacterial toxins.

Acknowledgements and Dedication

The work presented within this document would have been impossible to achieve without the help and support from a large group of individuals.

First, I would like to thank my graduate mentor, Dr. Mark Kester, for giving me the opportunity to be in this position. You believed in me, and this project, even when I didn't. Thank you for all of the support that you provided me, and for allowing me to pursue my interests, even if they were outside the normal scope of the lab. You always made time for me when I was struggling, you were eager to celebrate my successes, and you advocated for me when nobody else would. I am forever grateful for all that you have done for me.

Dr. Cynthia Sears, you accepted a random collaboration request when we began this project and without hesitation, provided the expertise and guidance that we needed for this project to succeed. Not only that, but you treated me like one of your own graduate students, even letting me come to Johns Hopkins to learn and work with members of your lab. Thank you for always making the time for me and for all of your support.

To Dr. Melinda Poulter, thank you for introducing me to clinical microbiology, and for fostering my interest in the field. You provided me with invaluable career advice and

taught me something new each day. Because of you, I was able to obtain a fellowship and begin my career as a clinical microbiologist. Thank you for everything.

Dr. Nicholas Zachos, we would not have been able to complete this study without the media components that you supplied us. Growing colonoids was an incredibly challenging task, but your assistance made it possible. Thank you.

To my graduate committee (Dr. Janet Cross, Dr. Tom Loughran, Dr. Bill Petri, and Dr. Melanie Rutkowski), thank you for your tremendous patience over the years. This project did not always have a clear direction or promising results, but you allowed me the time and flexibility to achieve success. Dr. Cross, thank you for serving as the head of the committee, but more importantly, thank you for being such a strong advocate throughout my graduate career.

Dr. Scott Verbridge, thank you for giving me my first opportunity in academic research as an undergraduate at Virginia Tech. I wish that more academic researchers shared your willingness to think outside the box and pursue new and “risky” projects.

Thank you to all of the Kester Lab and Sears Lab members, past and present, (Dr. Tye Deering, Dr. Andrei Khokhlatchev, Zach Davis, Alexis Gademsey, Brett Moseley, Isabella Posey, Jason Smith, and Susan Walker) for your assistance and friendship over the past six years. Dr. Shaoguang Wu, thank you for all of your advice and assistance designing and running experiments. To Dr. Todd Fox, thank you for lending your knowledge on

sphingolipid metabolism to the project and for analyzing hundreds (or thousands) of samples for me.

Thank you to the other graduate students in the Kester Lab and the Sears Lab for being such great friends. Dr. Jawara Allen, we first met when you hosted me on a trip to visit Johns Hopkins, when you opened your home for a stranger to come visit your lab. You always treated me like a good friend, taking me out to eat and introducing me to your friends when I was in Baltimore, and I greatly appreciate that. In addition to your kindness, you were an enormous help providing advice on experiments and results, and your influence on this project was significant. Dr. Kelly Drews, although we knew each other previously from THE University of Virginia, Virginia Tech, we became even closer during grad school. Although my productivity increased after you graduated, I missed having someone to talk with about the random things outside of science that made going to lab more fun. Pedro Costa-Pinheiro, thank you for always making time to talk about work and life in general. I have learned a lot from you and appreciate your friendship. Jeremy Shaw, thank you for always making me laugh and for our late-night vent sessions about life as a grad student. Our road trips with Pedro were some of my favorite memories from grad school.

To my best friends, Josh Cunningham and Ethan Holder, thank you for supporting me throughout graduate school. Josh, you were there for me every single night to play videogames and just talk about life. We're both much different people now than we

were six years ago, but our friendship has continued to grow stronger. I look forward to where life will take us next, knowing that we will always be there to support each other. Ethan, my best friend since high school, we have been through quite a lot together over the last 14 years. We have shared many important life and career milestones, from graduating college, to each getting married, to moving new places and starting our careers. Although you moved about as far away from me as you possibly could have, the distance never prevented you from being an incredibly supportive friend. I appreciate and cherish both of you greatly.

Thank you to my parents, Dane and Marcia Patterson, who fostered my curiosity from a young age and challenged me to be the best person that I could be. You gave me the tools and freedom to chase my dreams and I would have never made it to this point in life without your love and support. To my sister, Haley Patterson, for becoming a great friend. You have always had my back and I look forward to being there for you as you start the next chapter of your life. To my second family, George, Jean, and Andrew Brammer, thank you for always treating me like part of the family and for always being there to cheer me on. To my grandparents, Nell "Granny" Patterson, Jimmy Payne, Bette "Mocha" Saunders, and Robbie Johnson, thank you for everything that you have done for me throughout my life. I love you all and am incredibly grateful to have such a loving and supportive family.

Finally, I would like to dedicate this work to my wife, and biggest supporter, Meredith Patterson. You have sacrificed so much for me to be able to get to this point, and it did not go unnoticed. I appreciate you putting up with me during this incredibly stressful experience, as I know I wasn't always the easiest person to deal with. I would have never been able to achieve my successes without you, and as we embark on a new journey, I am comforted knowing that I will have you by my side. I love you.

Table of Contents

List of Figures

List of Abbreviations

Abbreviations	Definition
Apc	Adenomatous polyposis coli
AV	Annexin V
BFT	*Bacteroides fragilis* toxin
BHI	Brain heart infusion
C1P	Ceramide-1-phosphate
C6-CNL	C6-ceramide nanoliposomes
CBE	Conduritol B epoxide
CCS	Cold chelating solution
CD	Crohn's disease
CDase	Ceramidase
CECs	Colon epithelial cells
CMGF-	Complete medium without growth factors
CMGF+	Complete medium with growth factors
CRC	Colorectal cancer
DMEM	Dulbecco's modified eagle medium
DMSO	Dimethyl sulfoxide
DSS	Dextran sodium sulfate
E-cadherin	Epithelial cadherin

EDTA	Ethylenediaminetetraacetic acid
EGF	Epidermal growth factor
EHEC	Enterohemorrhagic Escherichia coli
ETBF	Enterotoxigenic *Bacteroides fragilis*
EVs	Extracellular vesicles
FBS	Fetal bovine serum
FITC	Fluorescein isothiocyanate
FPS	Frames per second
FVD	Fixable Viability Dye
GBA	Glucocerebrosidase
GCS	Glucosylceramide synthase
GI	Gastrointestinal
GSLs	Glycosphingolipids
HBSS	Hank's Balanced Salt Solution
IBD	Inflammatory bowel disease
iNKT	Invariant natural killer T cells
JACOP	Junction-associated coiled-coil protein
JAMs	Junctional adhesion molecules
MAGI	Membrane-associated guanylate kinase inverted proteins

Muc2	Mucin 2
MUPP1	Multi-PDZ domain proteins
MVs	Microvesicles
mβCD	Methyl-β-cyclodextrin
N-cadherin	Neural cadherin
NFκB	Nuclear Factor kappa-light-chain-enhancer of activated B cells
NLRs	Nod-like receptors
NTBF	Nontoxigenic *Bacteroides fragilis*
PATJ	PALS1-associated tight junction protein
PBS	Phosphate-buffered saline
P-cadherin	Placental cadherin
PRRs	Pattern recognition receptors
PS	Phosphatidylserine
qPCR	Quantitative real-time polymerase chain reaction
R-cadherin	Retinal cadherin
S1P	Sphingosine-1-phosphate
SARS-Cov-2	Severe acute respiratory syndrome virus 2
SMS	Sphingomyelin synthase
Th17	T-helper 17 cell

TJP1	Tight junction protein 1
TJP2	Tight junction protein 2
TJP3	Tight junction protein 3
TLRs	Toll like receptors
Treg	Regulatory T cell
UC	Ulcerative colitis

Chapter 1: Introduction

1.1: Colon Physiology

1.1.1: Function of the Colon

The human intestinal tract contains two major divisions: the small intestine and the large intestine.[1–3] Digested food from the stomach enters the small intestine where it is digested further and nutrients are absorbed.[1] The small and large intestines are divided by the cecum,[3] which serves as the first of four major components of the large intestine, along with the colon, the rectum, and the anus.[1] The colon, which is the primary focus of our studies, is responsible for reabsorbing water and electrolytes from undigested material.[2,4,5] In addition to absorbing water and electrolytes from dietary components, the colon also absorbs short-chain fatty acids and other nutrients produced by the resident microbiota (the microorganisms that reside in the gastrointestinal tract).[4,6] The colon also contains the majority of the intestinal microbiota, which consists of the bacteria, fungi, viruses, and bacteriophages that reside there.[7,8]

1.1.2: Cellular Composition of the Colon

The colon is lined with a single layer of epithelial cells, which are further organized by function within crypts (Figure 1.1).[1–3,9] Cells are organized into three main categories: stem cells, transit-amplifying cells, and differentiated cells. In the colon, the stem cell population is located at the bottom of the crypts, and gives rise to all of the other cell types in the crypt.[9,10] As new cells are created, they move up the crypt into the transit-amplifying zone, where they continue to divide while differentiating into more specific

cell types, such as enterocytes (referred to as colonocytes) or goblet cells (which secrete mucus to protect the epithelium).[1,2,9,10] The majority of cells at the top of the crypt are colonocytes, which no longer divide, and eventually undergo apoptosis before being replaced by newer cells.[1] Cell turnover within the colon occurs every four to five days,[1,9,11] which helps cells avoid mutations caused by exposure to toxins or carcinogens within the gastrointestinal (GI) tract.[1,2]

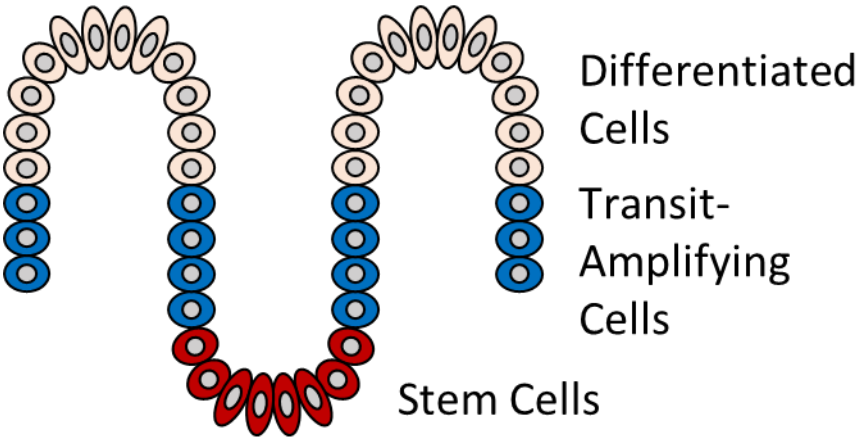

Figure 1.1: Graphical representation of a colon crypt.

1.1.3: Maintenance of the Epithelial Barrier

One of the most important roles of the colon epithelium is to provide a barrier between the intestinal contents, including the resident microorganisms, and the underlying tissue. However, in addition to serving as a physical barrier, epithelial cells must also permit the passage of ions and nutrients from the environment.[12,13] This delicate

balance is maintained by two main groups of proteins: tight junctions and adherens junctions.[13–15]

Tight junctions are primarily found at the apical side of the epithelial membrane (the side closest to the intestinal lumen), and serve two main functions: establishing polarity within the membrane and regulating the passage of molecules through the paracellular space between cells.[12–15] The first function, establishing membrane polarity, results in the segregation of membrane proteins to the areas in which they are needed. Proteins located at the apical side of the membrane are exposed to the external environment, and are therefore responsible for the uptake of materials from the environment as well as to serve as an initial line of defense from the resident microbiota.[12,13] Meanwhile, proteins on the other side of tight junctions are involved in cell-to-cell adhesion, intercellular communication, and attachment to the basement membrane.[12] The second function, regulating paracellular uptake of molecules, allows cells to uptake water, ions, and small molecules from the environment while prohibiting bacteria from translocating through the epithelial barrier.[12,13,16]

Tight junctions are structurally formed by the attachment of transmembrane proteins, which span the paracellular space, to cytoplasmic proteins within cells that serve to anchor the junctions.[13] The three main transmembrane protein(s) involved in forming tight junctions are occludin, the claudin family of proteins, and junctional adhesion molecules (JAMs).[12–15] Occludin, which was the first transmembrane protein to be

identified,[14] helps to regulate paracellular permeability.[12,13,15] However, an occludin knockout mouse model demonstrated that this protein is not required for tight junction formation.[17] Claudins, which are a family of at least 24 proteins,[14] are transmembrane proteins that form channels to allow paracellular transport of molecules.[13,15] Claudins are differentially expressed throughout the body, and even change within the colon, with different expression patterns in the proximal colon (closest to the cecum) and the distal colon (adjacent to the rectum).[18] JAMs are the third set of transmembrane proteins found in tight junctions, and they help to regulate paracellular permeability and reinforce cell-to-cell contact.[12,13]

Cytoplasmic proteins help to stabilize the membrane spanning proteins (occludin, claudins, JAMs), and also serve as anchor points to mediate the attachment to the actin cytoskeleton of cells.[12,13,15] While there are numerous cytoplasmic proteins involved in the formation and stabilization of tight junctions, such as multi-PDZ domain proteins (MUPP1), membrane-associated guanylate kinase inverted proteins (MAGI), PALS1-associated tight junction protein (PATJ), junction-associated coiled-coil protein (JACOP), and cingulin,[14,19] the most well-studied are the zonula occludens (herein referred to as tight junction proteins, or TJP).[12–15,19] The tight junction protein family consists of three members (TJP1, TJP2, and TJP3), and are able to bind to the transmembrane proteins (occludin, claudins, and JAMs).[13–15] Each TJP has different binding domains, and as such, they have different binding partners and functions within cells.[13,15,19–21] Interestingly,

TJP1 and TJP2 knockout mice are embryonic lethal, while TJP3 knockout mice display no phenotypic changes, suggesting that TJP3 is dispensable or that TJP1 or TJP2 can compensate for the loss.[19–21]

Adherens junctions are located below tight junctions, towards the basolateral side of the epithelium, and mediate cell-to-cell adhesion.[12–15,22] Adherens junctions are comprised of nectins or cadherins, which form weak or strong cell-to-cell attachments, respectively.[13] Nectin binds to afadin, which connects to the actin cytoskeleton and stabilizes the cell-to-cell interactions.[13,23,24] Cadherins are a family comprised of at least 80 different proteins, each with varying functions and expression profiles within the organism.[25,26] The cadherin proteins are divided into three main subgroups: classical cadherins, protocadherins, and atypical cadherins.[27,28] The classical cadherins were the first to be identified, and are the most well-studied.[26,27] Members of the classical cadherin family include E-cadherin (epithelial cadherin), N-cadherin (neural cadherin), R-cadherin (retinal cadherin), and P-cadherin (placental cadherin)[26–28] As might be obvious, the classical cadherins were named according to the tissue in which they were found to be highly expressed. However, it is now understood that the classical cadherins can be expressed in other tissue types and are not confined to their namesake tissue.[26]

In the colon, E-cadherin is the most widely expressed cadherin, and is vitally important for establishing and maintaining adherens junctions.[22] Within the colonic crypt, E-

cadherin expression is relatively low towards the base of the crypt and becomes higher in the differentiated cells at the top of the crypt.[22,29] While there are numerous theories for why expression of E-cadherin varies within the crypt, the most accepted is that low E-cadherin expression at the base of the crypt allows cells to divide and migrate up the crypt, while high expression at the top of the crypt allows cells to maintain tight cell-to-cell interactions that provide a strong barrier against the luminal stressors.[22,29] In addition to forming cell-to-cell contacts, E-cadherin also has numerous cytoplasmic binding partners, most notably the catenin family of proteins (α-catenin, β-catenin, and p120-catenin).[12,13,15,25–28,30] p120-catenin and β-catenin both bind E-cadherin directly, and can do so simultaneously, while α-catenin associates with E-cadherin indirectly by binding to β-catenin.[15,26] Each catenin has its own role within cells. α-catenin binds to actin filaments and alters cytoskeletal dynamics, p120-catenin stabilizes cadherin junctions, and β-catenin functions as a signaling factor that can dissociate from E-cadherin and enter the nucleus where it interacts with transcription factors.[13,15,26]

In conjunction with its interactions with the catenin family, E-cadherin also interacts with tight junction proteins.[12,13,15,22] During the establishment of cell-to-cell adhesion, E-cadherin and TJP1 co-localize at the intercellular junction.[31,32] As the adherens junctions begin to form, E-cadherin and TJP1 begin to move apart from one another, and TJP1 interacts with tight junction proteins, such as occludin, to begin the formation of tight junctions.[33] This process is thought to be mediated by α-catenin, which is able to bind

to TJP1, as well as associate with E-cadherin through its interaction with β-catenin.[13,15,32] This idea is further supported by evidence that tight junctions do not form if α-catenin is unable to bind TJP1.[34] E-cadherin is essential for the formation of tight junctions, but loss of E-cadherin in cells does not disrupt existing tight junctions.[35] Despite differences between tight junctions and adherens junctions, there is clearly some degree of functional redundancy as well as cooperation between these two groups in the establishment and maintenance of the epithelial barrier in the colon.

1.2: Sphingolipids

Sphingolipids are a class of lipids that contain sphingosine, an 18-carbon monounsaturated amino alcohol moiety, which differentiates them from other types of lipids.[36] There are four main sphingolipids in mammalian cells: ceramide, sphingosine, sphingomyelin, and glucosylceramide. Through a number of different enzymes, each of these sphingolipids can be reused, or recycled, into any of the other sphingolipid species. Further, additional modifications to these base sphingolipids can generate more complex sphingolipids, such as sphingosine-1-phosphate (S1P), ceramide-1-phosphate (C1P), and higher order glycosphingolipids.[37–41] Sphingolipids are vital for normal cellular function, with roles in growth, differentiation, cell death, inflammation, adhesion, metabolism, and cell signaling.[38,40,41]

Ceramide is the first major sphingolipid generated from *de novo* synthesis, and can be converted into sphingomyelin (through sphingomyelin synthase, or SMS), sphingosine (through ceramidase, or CDase), or glucosylceramide (through glucosylceramide synthase, or GCS).[38] A visual representation of the pathway can be found in Figure 1.2. Ceramide is generally thought to be a pro-apoptotic lipid, which makes it an important mediator of normal cell turnover.[36,38] Sphingosine has also been shown to mediate cell death.[37] In contrast, sphingomyelin and glucosylceramide are important membrane sphingolipids that provide structural support and promote cell survival.[37,38,41] Importantly, sphingolipid dysregulation has been shown in a number of cancers.[36–39,42–44]

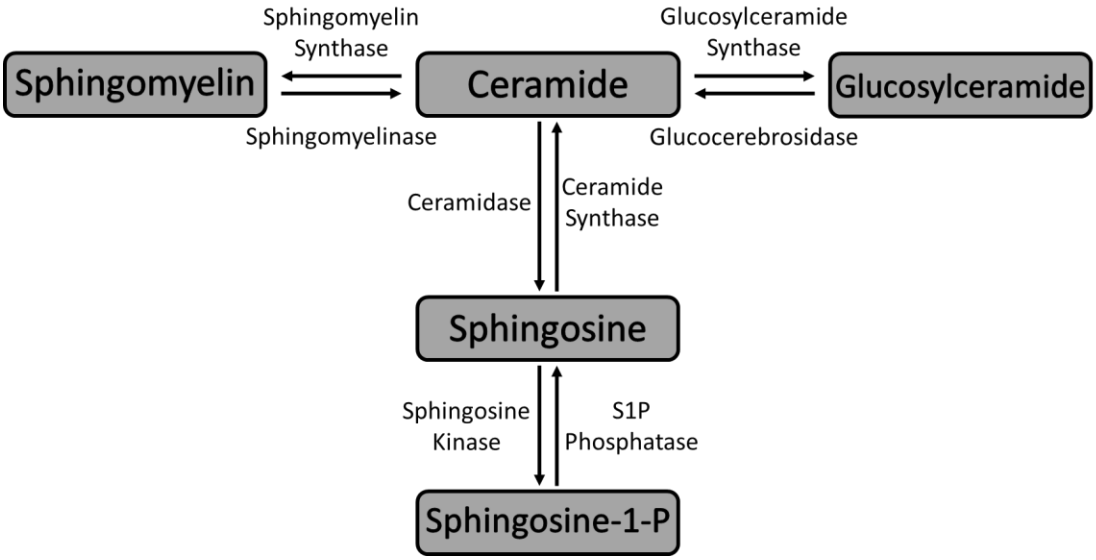

Figure 1.2: Graphical representation of the sphingolipid pathway. Sphingolipids are located inside of the bubbles, while the text adjacent to the arrows represents the enzymes involved in the formation or breakdown of each lipid.

Glucosylceramide is generated by glucosylceramide synthase (GCS), which adds a glucose molecule to ceramide, or is recycled back into ceramide by glucocerebrosidase (GBA), which removes the glucose molecule.[45] Gaucher disease, a lysosomal storage disease that results in the accumulation of glucosylceramide, is caused by a mutation in GBA.[46] Glucosylceramide is a necessary component for animal survival, demonstrated by studies that have shown embryonic lethality of GCS knockout in mice.[47] GCS expression is much higher in the skin, stomach, small intestine, and colon than other tissues, demonstrating the importance for glucosylceramide in maintaining epithelial barriers throughout the body.[41,48–50]

In the intestines, sphingomyelin and glucosylceramide are both highly expressed in the plasma membrane where they support barrier function, aid in the absorption of nutrients, and prevent invasion from pathogens.[45,48,50,51] Targeted knockout of GCS in mouse intestinal epithelial cells led to defects in nutrient absorption and cellular differentiation, that was followed by increased diarrhea and, shortly after, death.[52] Because glucosylceramide is such a critical regulator of intestinal health, dysregulation of the lipid may promote disease, such as inflammatory bowel disease (IBD) and colorectal cancer (CRC).[38,48,51] The addition of dietary glucosylceramide to mice enhances epithelial barrier function, at least in part by increasing the expression of tight junction proteins such as claudin-1, and reduces tumor formation in CRC mouse models.[39,50,51,53,54] Recently, researchers demonstrated that targeted glucosylceramide

knockout in T cells (using a Cre-Lox system to delete GCS in thymocytes) significantly reduced the formation of invariant natural killer T (iNKT) cells, which are critically important for protecting the host from pathogens.[55]

1.3: The Intestinal Microbiota

The intestinal microbiota is comprised of bacteria, fungi, viruses, and bacteriophages that generally live in symbiosis with the host.[7,8] Estimates have suggested that the human microbiota contains over 1,000 different bacterial species, amassing nearly 10^{13} cells, which is roughly equivalent to the number of human cells throughout the body.[56–59] The colon is the largest repository for bacteria, containing nearly 70% of all microbes in the human body.[57] It is no surprise then that the resident bacteria have a huge influence on normal gut health, as well as in the development and progression of disease throughout the body. Bacteria in the colon aid in digestion, breaking down complex carbohydrates that may be indigestible by the host. The result of this process is the release of short chain fatty acids, such as butyrate, propionate, and acetate, which serve as a major energy source for colonocytes.[8,57,60–62] Dysregulation of the intestinal microbiota, which is characterized by alterations in, and diversity of, the resident microorganisms, has been shown to play a role in IBD, obesity, autism, cardiovascular disease, and colorectal cancer, among other diseases.[8,56–59,61,63–70] Genetic predisposition, diet, and age are also important factors that determine the response of

the host to microbial changes that may promote disease.[61,71,72]

The intestinal epithelium is physically separated from the resident microbiota by two mucosal layers. The most immediate is a dense layer that prevents the colonization of bacteria, which prevents the bacteria from coming into direct contact the epithelium. The second is a more fluid layer of mucus that permits the colonization of bacteria.[57,60,62,73] The second, permeable layer is formed as endogenous proteases slowly break down the first mucosal layer, causing it to become porous and expand outwards.[74] Goblet cells continuously generate the mucins that form these layers, and turnover is rapid due to mechanical loss from normal digestion and chemical breakdown by the resident microbes.[16,56,73,75] Colonizers of the mucosal layer typically have the ability to degrade mucins, which allows them to use the released carbohydrates as an energy source as well as to form a niche in which they can reside.[76–78] Importantly, mice with a Muc2 knockout (the predominant mucin found in the mucosal layer), develop spontaneous colitis, highlighting the importance of the mucosal layer as a protective barrier in the colon.[16,60]

While the bacteria and host epithelium are physically separated from one another, biological and chemical signals allow for crosstalk to occur. The host samples bacterial antigens and metabolites as a way to monitor the microorganisms present in the microbiota through a variety of receptors. These include pattern recognition receptors (PRRs), like the toll like receptor family (TLRs), as well as NOD-like receptors (NLRs) present in epithelial cells.[8] Due to the large volume of microorganisms present, the

intestinal tract has the largest quantity of immune cells of any site in the body.[60,79] The epithelial cells are able to communicate information about the microbiota with immune cells that reside below the epithelium in the lamina propria.[8,16] If pathogenic bacteria are detected during invasion, epithelial cells produce chemokines to recruit immune cells to clear the infection.[9,80] If the infection is severe, colonocytes may undergo programmed cell death to prevent the bacteria from crossing the epithelial barrier.[9] During this process, apoptotic cells signal to the surrounding cells, which allows them to reorganize their cellular junctions and establish contact with one another to preserve the barrier as the apoptotic cell is extruded from the membrane.[81] Sustained inflammation caused by pathogenic bacteria can have detrimental effects for the host. Inflammation in the intestines can lead to an increase in paracellular permeability due to disruption of adherens and tight junctions.[56,82] Along the same lines, disruption of tight junctions may promote inflammation by inappropriately allowing the passage of bacteria and other materials through the epithelial barrier.[60,83] In a healthy individual, the epithelium will reseal, and any bacteria that breach the barrier are typically dealt with by immune cells in the lamina propria.[66]

Successful pathogens have the ability to manipulate host cells in a number of different ways that allow them to colonize and invade new areas. One of these mechanisms is to enhance paracellular permeability of the epithelium by degrading adherens or tight junction proteins.[66,73] Degradation of the junctional complexes allows translocation of

bacteria into the lamina propria and beyond, which, as mentioned previously, could lead to systemic inflammation that may promote disease.[60,83] While some bacteria have the ability to break down tight junctions, other commensal organisms have the ability to reinforce them by inducing expression of tight junction proteins in epithelial cells.[73] Indole, a molecule that can be produced by commensal bacteria in the colon, activates anti-inflammatory signaling pathways and reinforces the epithelial barrier.[84]

1.4: Bacteroides fragilis

Bacteroides fragilis is a unique intestinal bacterium that is comprised of two different subtypes, each with opposing effects on human health. The two subtypes, nontoxigenic *Bacteroides fragilis* (NTBF) and enterotoxigenic *Bacteroides fragilis* (ETBF), are separated from one another based on their ability to produce a metalloprotease toxin, termed *Bacteroides fragilis* toxin (BFT).[85] Previous studies have suggested that 40-70% of humans are colonized with NTBF.[86] NTBF is considered to be a beneficial organism in the intestines, largely due to its ability to illicit an anti-inflammatory immune response through the stimulation of T-regulatory cells (Treg).[87]

ETBF colonization is less frequent, only colonizing between 2-30% of humans.[88,89] ETBF was originally discovered as a cause of diarrhea in farm animals, but later studies demonstrated that ETBF played a role in diarrheal illness in humans as well.[85,88] ETBF

strains can express one of three toxin isotypes: BFT1, BFT2, or BFT3.[90] BFT2 is considered to be the most virulent, although BFT1 is the most common.[88,90] ETBF strains expressing BFT1 or BFT2 are found globally, while strains expressing BFT3 are typically found in Southeast Asia.[85] Thanks to the advent of microbiome sequencing, researchers discovered that patients with colorectal cancer (CRC) were frequently colonized with ETBF expressing BFT2. Remarkably, one study found that ETBF was present in approximately 90% of patients with CRC, suggesting a potential causative relationship between ETBF and CRC.[91] Independent studies have revealed that ETBF can indeed promote CRC progression in genetically susceptible *Apc*$^{min/+}$ mice.[92] The formation of tumors in mice requires a signaling cascade that includes activation of pro-inflammatory T-helper 17 cells (Th17) that produce the cytokine IL-17A, activation of NF-κB, and Stat3 activation.[91] Importantly, production of BFT is required for the formation of tumors in this model, as ETBF strains with a chromosomal deletion of *bft* did not increase tumor formation when compared to sham controls.[93]

BFT is able to alter colon epithelial cells in a number of different ways that may also promote tumor formation. One of the first events, which takes place within minutes of BFT addition to cells, is the cleavage of E-cadherin.[90,94] Following this cleavage, cells undergo rounding and paracellular permeability is increased.[95–97] TJP1 is also impacted by BFT, with one study suggesting that BFT decreased its expression while another suggested that localization of the protein was altered.[94,97] Beyond disruption of the

epithelial barrier, BFT stimulates pro-tumorigenic signaling, including the activation of the Wnt signaling pathway, possibly as a result of E-cadherin cleavage and subsequent release of β-catenin.[98] While the effects of BFT have been extensively studied in cancer cell lines and in cancer mouse models, few studies have focused on its effects on healthy colon epithelial cells.

1.5: Colon Pathophysiology

1.5.1: Diseases of the colon

Dysregulation of the intestinal barrier is one of the biggest risk factors for disease development in the colon. Breakdown of epithelial tight junctions between cells has been implicated in inflammatory bowel disease (IBD) and colorectal cancer.[22,51,60,83,99–102] Loss of cell-to-cell adhesion increases paracellular permeability, which allows luminal contents to enter the lamina propria, triggering the release of pro-inflammatory cytokines and the recruitment of immune cells to the area.[51,99,100] Inflammatory cytokines may further disrupt cellular repair, causing sustained damage to the colon.[99]

IBD, which includes Crohn's Disease (CD) and Ulcerative Colitis (UC), is a chronic disease that affects nearly 3 million Americans.[103] CD can develop along the entire gastrointestinal (GI) tract, while UC is limited to the colon.[100,103] The cause of these diseases is still unknown, but it is now appreciated that genetics, diet, and the gut microbiota each play an important role in disease development.[100,101,103] Patients with

IBD present with increased intestinal permeability, likely due in part to the downregulation of TJP1, E-cadherin, occludin, and claudins.[83,104] Additionally, overexpression of GBA decreased glucosylceramide levels in the colon, further enhancing barrier defects due to an increase in ceramide.[51,105,106] While increased epithelial permeability is important for IBD progression, it is not sufficient to cause the disease.[101,102] Recently, the intestinal microbiota has been implicated as a driver of the disease. Dysbiosis, or a shift away from the normal, healthy, microbiota, is frequently seen in patients with IBD.[107] Further, childhood antibiotic use, which reduces bacterial diversity in the microbiota, increases the risk of developing CD.[103,108] The combinatorial effect of decreased barrier function and a dysregulated microflora is a sustained inflammatory response that defines the disease.[100]

Colorectal cancer is the second leading cause of cancer deaths in the United States.[109] The initial step in CRC development is the formation of polyps, or groups of cells growing abnormally on the epithelial surface.[110] Untreated, polyps may acquire mutations in adenomatous polyposis coli (Apc), leading to the formation of adenomas, or a group of cells with altered cellular organization.[110–112] From an adenoma, progression of cancer continues with mutational activation of KRAS, PIK3CA, and the inactivation of TP53, eventually becoming a carcinoma.[113–115] Carcinomas are malignant and possess the ability to spread throughout the body (referred to as metastasis), requiring the need for immediate medical intervention.[115,116]

Similar to IBD, environmental factors play a significant role in the development of CRC.[117] Due to the sheer number of toxins and bacterial antigens that the colon is exposed to on a daily basis, it should be no surprise then that a breakdown of the epithelial barrier increases the risk for cancer development. As in IBD, Muc2 expression is decreased in CRC, exposing the underlying epithelial cells to the bacteria and luminal contents of the colon.[75,118] Bacterial invasion of the mucosal space promotes the breakdown of tight junctions, triggering pro-inflammatory cytokine release and immune activation, which further disrupts the epithelial barrier.[119,120] Chronic inflammation is a risk factor for CRC, illustrated by the observation that patients with IBD are at an increased risk of developing cancer.[3,121]

Sphingolipid metabolism is frequently dysregulated in cancer, and CRC is no different.[38,50,122–126] In CRC, ceramide and sphingosine, both pro-apoptotic lipids, are decreased, favoring the formation of S1P and glucosylceramide.[38,50,122,127,128] S1P promotes cell survival, inhibits apoptosis, and is involved in immune cell recruitment to the colon, which increases the pro-tumorigenic potential of this lipid.[128,129] GCS overexpression in the colon is thought to promote CRC by reducing levels of ceramide, a pro-apoptotic lipid that would prevent cancer progression.[36,122] However, other studies have shown that GCS may have additional roles in CRC. GCS overexpression has been associated with multidrug resistance, affording cancer cells protection from chemotherapeutics.[38,50,122] This process can be reversed using inhibitors of GCS to block

its activity, sensitizing CRC to treatment again.[127,130] Addition of exogenous glucosylceramide reduces carcinogenesis in CRC mouse models, illustrating a multifactorial role for glucosylceramide in the development of CRC.[39,50]

1.5.2: Colonoids as an *ex vivo* Model to Study Colonic Disease

Intestinal diseases have long been studied in cancer cell lines, derived from patient samples many years ago, and grown indefinitely across the world.[131] While these cell lines are cheap to maintain and easy to grow, they pose many limitations for translational research.[132] For starters, these cell lines are tumor-derived, and thus are not representative of healthy tissue.[133,134] Additionally, these cell lines consist of only one cell type from the colonic crypt (typically colonocytes).[134] Results in cell lines often do not translate well to animal models, which reduces their utility in translational research.[133,135] Further, inherent dysregulation of sphingolipid metabolism in cancer cell lines potentially masks shifts within the pathway that might be informative for disease progression or treatment.[122]

Within the past 10 years, researchers have developed methods to grow colon organoids (termed colonoids), an *ex vivo* model of colonic crypts isolated from humans or animals.[10,136] Colonoids possess all of the epithelial cell types found in the crypt, including the stem cell population.[10] Unlike primary cell culture from tissue-derived samples, colonoids can be passaged indefinitely, without undergoing genetic or

phenotypic changes.[10,133,134] However, in order to maintain long-term culture of colonoids, specific growth conditions must be met. Colonoids are typically grown in an extracellular matrix, such as Matrigel, where the basolateral layer of the epithelium can attach to the matrix. The apical layer of the epithelium faces the interior of the colonoid, creating the lumen within the structure.[10,135,136] Specific growth factors, such as Wnt3A, R-spondin 1, Noggin, and EGF, must be added to the medium to maintain the stem cell population.[136] If these growth factors are removed, the cells will differentiate into colonocytes, and the stem cell population will be lost.[10]

The utility of colonoids is still being fully discovered, but many researchers have already adapted the model. One of the most intriguing uses of colonoids is the study of pathogen interactions with the intestinal eptihelium.[10,133,135,137] Already, researchers have found novel mechanistic changes caused by enterohemorrhagic *Escherichia coli* (EHEC), *Salmonella enterica*, and *Clostridium difficile*.[10,133,135,138] Our collaborators at Johns Hopkins have used colonoids to assess epigenetic changes caused by BFT.[139] In this study, we utilized colonoids to study the effects of BFT on sphingolipid metabolism, paracellular permeability, tight junction structure and composition, and cell-signaling in a non-transformed colon epithelium.

Chapter 2: Materials and Methods

2.1: Animal experiments

Animal experiments were approved by the Johns Hopkins University Institutional Animal Care and Use Committee and performed at Johns Hopkins University School of Medicine. Five-week-old C57BL/6J mice (Jackson Laboratory) were given a 1-week course of antibiotics, 0.1mg/mL clindamycin and 2mg/mL streptomycin delivered orally through the drinking water, to enhance bacterial colonization. After a 1-week course of antibiotics, mice were colonized with $1x10^8$ CFU/100µL ETBF (86-5443-2-2),[140] ETBF*Δbft*,[91] or 100µL of phosphate-buffered saline (PBS, Gibco 10010023) via oral gavage. After 1 week, mice were euthanized, and colons were extracted for lipid analysis.

2.2: Lipidomic analysis

Lipids were extracted as previously described,[141] and analyzed by ultra-performance liquid chromatography-electrospray tandem mass spectrometry (Waters Acquity Xevo TQ-S) based on the method described by Merrill *et al.*[142] Briefly, tissue was homogenized using a BeadBug bead homogenizer (Thomas Scientific D1030-E), sonicated, and resuspended in 0.1X PBS. Colonoids were isolated from 3D-growth matrix, pelleted, and resuspended in 0.1X PBS. Resuspended colonoids were then lysed by sonication. Total protein was determined and quantified using the Bio-Rad DC Protein Assay (Bio-Rad 5000116). For each experiment, all samples submitted for mass

spectrometry analysis contained the same amount of protein (typically a minimum of 40µg/sample). Resuspended tissue/cells were added to 2mL of lipid extraction mixture (isopropanol:water:ethyl acetate at 30:10:60 v/v/v), vortexed, sonicated, and then incubated for one hour with shaking. Samples were centrifuged and the upper organic layer was collected. Remaining sample was re-extracted using the above methods and the resulting organic layers from the two extractions were combined. The combined organic layers were dried using nitrogen gas and then resuspended in mobile phase buffer. Mobile phase A consisted of 70:30 w/w water:acetonitrile with 0.2% formic acid, 10mM ammonium formate, and 1mM methylphosphic acid. Mobile phase B was comprised of 90:10 w/w isopropanol:methanol with 0.2% formic acid, 10mM ammonium formate, and 1mM methylphosphic acid. Samples were filtered using a 96 well 0.45µm hydrophilic MultiScreen Solvinert Filter Plate (Milipore Sigma MSRLN0410) and stored at -20°C until they were analyzed. Data from tissue or cell lysates is represented as picomoles of lipid per milligram of protein.

2.3: Colonoid isolation and culture

Colonoids were isolated from the distal colons of C57BL/6J or *Apc*$^{min/+}$ mice (Jackson Laboratory). The isolation protocol and media components have both been described previously.[143,144] Briefly, the distal colon was extracted and cut into 1-mm pieces, washed 5-6 times in cold chelating solution (CCS),[144] and incubated in in CCS with 10mM

EDTA to release colon tissue crypts. Fetal bovine serum (FBS) was added to aid in collection of the crypts. Crypts were pelleted and resuspended in Matrigel (Corning 356231). Resuspended crypts were plated within 3D domes using 25µL Matrigel/well on a pre-warmed 24-well plate (Genesee Scientific 25-107) and placed at 37°C for 15 minutes to allow the Matrigel to solidify. Once solidified, 500µL complete medium with growth factors (CMGF+) was added to each well and refreshed every other day. By day 3, crypts began forming colonoids. After 1 week, colonoids were passaged and expanded for experimental use.

Complete medium without growth factors (CMGF-) and CMGF+ growth media were prepared fresh weekly. CMGF- basal media consisted of Advanced DMEM/F12 (Gibco 12634010), GlutaMAX (2mM; Gibco 35050061), HEPES (10mM; Gibco 15630080), Penicillin/streptomycin (100U/mL; Gibco 15140122). CMGF+ growth media consisted of CMGF- (17.5% v/v), L-Wnt3A-conditioned media (50% v/v; provided by the Zachos Laboratory), R-Spondin-conditioned media (20% v/v; provided by the Zachos Laboratory), Noggin-conditioned media (10% v/v; provided by the Zachos Laboratory), B27 (1X; Invitrogen 17504-044), N-acetylcysteine (1mM; Sigma A9165), epidermal growth factor (EGF; 50ng/mL; R&D 236-EG-01M), [Leu15] Gastrin (10nM; Sigma G9145), A83-01 (500nM; Tocris 2939), SB202190 (10µM; Sigma S7067), and Primocin (100µg/mL; Invivogen ant-pm-2).

2.4: Bacterial culture and preparation of concentrated bacterial culture supernatants

Enterotoxigenic *Bacteroides fragilis* (ETBF, 86-5443-2-2),[140] enterotoxigenic *Bacteroides fragilis Δbft* (ETBF*Δbft*),[91] recombinant ETBF*Δbft* expressing BFT2 (rETBF*Δbft bft-2*; unpublished), non-toxigenic *Bacteroides fragilis* (NTBF, NCTC 9343),[145] recombinant NTBF expressing BFT2 (rNTBF *bft-2*),[145] and recombinant NTBF expressing a mutated and inactive form of BFT (rNTBF *bft-2* H352Y)[146] were all obtained from the Sears Lab and grown in brain heart infusion broth (BHI; BD Bacto 237200) with hemin (Sigma H9039), vitamin K1 (Sigma V3501), and clindamycin hydrochloride (Sigma C5269) under anaerobic conditions. To generate concentrated bacterial culture supernatants from *B. fragilis* strains, bacteria were grown in 500mL BHI media for 24 hours. The bacterial suspension was centrifuged at 4,000G for 20 minutes to pellet the cells. The supernatant was collected and the bacterial pellet was discarded. The resulting supernatant was then filtered using a 0.45µm syringe filter (GE Healthcare 6780-2504) to remove residual cells or debris. After this, the filtered supernatant was added to a 10kDa centrifuge filter tube (Amicon UFC901024) and centrifuged at 4,000G for 30 minutes according to the manufacturer's protocol. The flowthrough was discarded and the remaining media is referred to as concentrated bacterial culture supernatant. In this study, concentrated bacterial culture supernatant from ETBF is referred to as BFT, while concentrated bacterial culture supernatant from ETBF*Δbft* is referred to as

control. Protein content of concentrated bacterial culture supernatants was determined and quantified using the Bio-Rad DC Protein Assay (Bio-Rad 5000116).

2.5: Validation of toxin presence and activity in concentrated bacterial culture supernatants

To confirm that concentrated bacterial culture supernatant from ETBF contained BFT, a western blot was performed using an anti-BFT antibody to detect the 20kDa protein. BFT was detected only in our ETBF preparation, as expected (Figure 3.3A). Next, we sought to determine whether the concentrated supernatant contained active toxin. Based on previous studies showing that BFT triggers cleavage of E-cadherin in HT29/C1 colonic carcinoma cells,[147] we treated HT29/C1 cells with our concentrated bacterial culture supernatants and measured cleaved E-cadherin by western blot. We found that our concentrated ETBF culture supernatant effectively cleaves E-cadherin, while the concentrated ETBF*Δbft* culture supernatant shows only minimal cleavage (Figure 3.3B). We evaluated BFT activity by measuring E-cadherin cleavage with numerous dilutions of concentrated bacterial culture supernatants and found that 100µg/mL (total protein/mL concentrated bacterial culture supernatant) delivered a sufficient amount of biologically active BFT to cells, and all subsequent experiments used this concentration. To further confirm that observed responses were due to the presence of toxin, and not due to other bacterial proteins or factors in the media, we visualized colonoids using confocal

microscopy and tracked colonoid morphology changes to assess toxin activity. To enhance the activity of BFT on colonoids, CMGF+ medium was replaced with CMGF- basal cell medium containing concentrated bacterial culture supernatants for the first six hours. After six hours, media was removed and fresh growth media without concentrated bacterial culture supernatant was added to colonoids. Colonoids treated with BFT display dramatic morphology changes, highlighted by rounding of cells and an overall lack of epithelial cell membrane structure as soon as 1 hour, and persisting for up to 48 hours. Figure 3.3C shows an example of the morphology changes that occur after addition of concentrated bacterial culture supernatant from ETBF for six hours. In comparison, addition of concentrated ETBF*Δbft* bacterial culture supernatant does not alter the appearance of the colonoids (Figure 3.3D). Using concentrated bacterial supernatant from a recombinant ETBF*Δbft* strain expressing *bft* (rETBF*Δbft bft-2*), morphology changes similar to those in the BFT treatment were observed (Figure 3.3E). Since ETBF and ETBF*Δbft* strains are identical except for the expression of *bft*, we next investigated a non-toxigenic strain that cannot produce toxin (NTBF; NCTC 9343). Concentrated bacterial culture supernatant from the NTBF alone does not cause any morphology changes (Figure 3.3F). Next, we used concentrated bacterial culture supernatant from a recombinant NTBF strain expressing *bft* (rNTBF *bft-2*) and saw morphology changes similar to our BFT treatment (Figure 3.3G). Finally, we used concentrated bacterial supernatant from a recombinant NTBF strain with a mutated and inactivate form of BFT (rNTBF *bft-2* H352Y) and found that it no longer causes

morphology changes (Figure 3.3H). Taken together, concentrated bacterial supernatants derived from wild-type ETBF strain 86-5443-2-2 expressing chromosomal *bft*, or *B. fragilis* strains genetically engineered to express *bft* from a plasmid, led to dramatic cell morphology changes. In contrast, concentrated bacterial supernatants from NTBF strains that lack the *bft* gene or express a mutant *bft* or ETBF strains with an in-frame chromosomal *bft* deletion do not yield cellular changes.

2.6: Colonoid treatment and glucosylceramide modulation

Colonoids were treated with concentrated bacterial supernatants at a concentration of 100µg protein/mL or 5nM purified BFT2 (Obtained from the Sears Laboratory, and purified as previously described).[95] For treatment, CMGF+ medium was removed, and basal CMGF- medium containing concentrated bacterial culture supernatant or purified BFT was added for up to six hours, depending on the experiment. Concentrated bacterial supernatants or purified BFT were both added in basal media to enhance the activity of BFT, as early experiments showed that serum, present in CMGF+ medium, reduced its activity (data not shown). At six hours, media was removed and replaced with CMGF+ media for the remainder of the experiment.

In order to inhibit glucosylceramide synthase (GCS) in colonoids, ibiglustat (Venglustat, Sanofi Genzyme; obtained from MedChemExpress HY-16743) was resuspended in

DMSO, diluted using CMGF- media, and used at a final concentration of 5µM. For experiments using ibiglustat, a vehicle control of DMSO was used for all conditions not receiving the drug. Typically, ibiglustat was added 24 hours before the addition of concentrated bacterial culture supernatant so that glucosylceramide lipid levels would be decreased by the start of the assay. When concentrated bacterial supernatant, resuspended in CMGF- media, was added to the colonoids, fresh ibiglustat was added again to maintain inhibition of GCS.

In order to inhibit glucocerebrosidase (GBA), Conduritol B Epoxide (Cayman Chemical 15216) was resuspended in water, diluted using CMGF- media, and added at a final concentration of 20µM. For experiments using CBE, a vehicle control of water, diluted in CMGF- media, was used. A subset of colonoids were cultured with CBE indefinitely, with fresh drug added every other day during passages or media changes.

Glucosylceramide synthase activity was measured by adding C6-ceramide nanoliposomes (C6-CNL, a generous gift from KeyStone Nano, State College, PA) to colonoids for one hour. Ghost nanoliposomes were used as a vehicle control for these experiments. The formulation of the ghost nanoliposomes is identical to that of CNL, but lacks ceramide.

2.7: Cell culture of HT29/C1

HT29/C1 cells were grown at 37°C and 5% CO2 in Dulbecco's modified Eagle medium (DMEM, Gibco 11965092) with 10% fetal bovine serum (FBS) and 1% Pen/Strep (Gibco 15140122).

2.8: Confocal microscopy

Colonoid images were captured using an Olympus FV3000RS confocal microscope (Johns Hopkins University School of Medicine), an Operetta CLS High-Content Analysis System (University of Virginia Advanced Microscopy Facility, RRID:SCR_018736), or a Zeiss LSM 700 (University of Virginia Advanced Microscopy Facility). Images were illuminated and captured using brightfield at 20x (Olympus FV3000RS) or 10x (Operetta CLS HIGH-Content Analysis System) magnification. Images were captured every 20 minutes after addition of concentrated bacterial supernatant. At six hours, between image captures, media was removed and CMGF+ media was added. Imaging experiments lasted 48 hours and resulting images were processed with ImageJ[148] in order to generate videos. Frames per second (FPS) in all videos was set to 15. In experiments using ibiglustat, cells were pre-treated for 24 hours before observations began.

For the FITC-Dextran permeability assay, images were captured using a Zeiss LSM 700 confocal microscope (University of Virginia Advanced Microscopy Facility) at 10x

magnification. In order to prepare samples for imaging, the Matrigel was dissolved using 500µL of Cultrex Organoid Harvesting Solution (R&D Systems 3700-100-01) for 20 minutes with shaking at 4°C. After 20 minutes, the colonoid suspension was collected and centrifuged at 500G for 5 minutes. After centrifugation, the supernatant was aspirated and the remaining cells were resuspended in 30µL FITC-Dextran solution (4 kDa FITC-Dextran resuspended at 2mg/mL in CMGF+ growth medium; FITC-Dextran obtained from Sigma-Aldrich 46944-100MG-F). Colonoids were immediately mounted onto a microscope slide and imaged. Double-sided tape was used to raise the coverslip to prevent the coverslip from crushing the colonoids. For samples treated with EDTA, 2mM EDTA was prepared from 0.5M EDTA (Thermo Fisher AM9260G) in ice-cold Hank's Balanced Salt Solution (HBSS; Gibco 14175095). Quantification of fluorescent signal was performed using ImageJ, and interior colonoid fluorescence was normalized to the exterior signal surrounding the colonoid.

For immunofluorescence imaging, images were captured using a Zeiss LSM 700 confocal microscope (University of Virginia Advanced Microscopy Facility) using the 63x oil-immersion lens. Colonoids were removed from the Matrigel, as in the FITC-Dextran permeability assay above, and centrifuged at 1000G for 5 minutes. Colonoids were resuspended in 2% paraformaldehyde in 100mM phosphate buffer (pH 7.4) for 30 minutes at room temperature. After fixation, cells were washed in PBS with rocking for 5 minutes at room temperature and then pelleted at 1000G for 5 minutes. The wash

step was repeated two more times. After three washes, colonoids were resuspended in 1X PBS/0.3% Triton X-100 for 15 minutes with rocking at room temperature. After this, colonoids were pelleted and resuspended in blocking buffer (1X PBS/5% normal goat serum/0.3% Triton X-100) for one hour with rocking at room temperature. After blocking, colonoids were pelleted and resuspended in the primary antibody solution (1X PBS/1% normal goat serum/0.1% Triton X-100) and left overnight, with rocking, at 4°C. The next day, colonoids were washed with 1X PBS/0.1% Triton X-100 with rocking for 5 minutes, repeated two more times for a total of three washes. Colonoids were then resuspended in the secondary antibody solution (1X PBS/1% normal goat serum/0.1% Triton X-100) for one and a half hours, at room temperature with rocking. Colonoids were washed three times with 1X PBS/0.1% Triton X-100 before the addition of Alexa Fluor 633 Phalloidin (resuspended in 1X PBS/1% normal goat serum/0.1% Triton X-100) for one hour at room temperature with rocking (Note: phalloidin was only used in conjunction with DAPI, and was excluded from experiments with E-cadherin and TJP1 antibodies due to overlapping fluorescence). Following this, colonoids were washed twice with 1X PBS and then 300nM DAPI was added for 5 minutes at room temperature. Cells were pelleted, resuspended in 1X PBS, and immediately centrifuged to wash the colonoids. These quick washes were repeated two more times, for a total of three washes. Colonoids were pelleted and resuspended in 15µL mounting solution (90% glycerol/0.5% N-propyl gallate/20mM Tris) overnight at room temperature. On the third day, 7µL of colonoids in mounting solution was added to a slide, surrounded by

two pieces of double-sided tape (3M 665-2P12-36), stacked, to prevent the coverslip from crushing the colonoids. The coverslip/sample was sealed using clear nail polish and then imaged. Primary antibodies used for this project were: E-cadherin (Cell Signaling Technology 14472; 1:100) and TJP1/ZO-1 (Novus Biologicals NBP1-85046; 1:100). Secondary antibodies used were: Goat anti-mouse Alexa Fluor 488 (Thermo Fisher Scientific A-11001; 1µg/mL) and Goat anti-rabbit Alexa Fluor 594 (Thermo Fisher Scientific A-11012; 2µg/mL). Dyes/stains used were: Alexa Fluor 633 Phalloidin (Thermo Fisher Scientific A22284) and DAPI (Thermo Fisher Scientific D1306). Phalloidin and DAPI were resuspended according to the manufacturer's instructions. Other reagents used were: Normal goat serum (Abcam ab7481), N-propyl gallate (Fisher Scientific MP210274780), and Triton X-100 (Sigma-Aldrich TX1568-1).

2.9: Quantitative real-time PCR

At the indicated time points, colonoids were harvested and RNA was extracted using the TRIzol reagent following the manufacturer's instructions (Thermo Fisher Scientific 15596018). cDNA was created using an iScript cDNA Synthesis Kit (Bio-Rad 1708891) according to the manufacturer's instructions. Quantitative PCR (qPCR) was performed on a Bio-Rad CFX384 following the instructions outlined in the iTaq Universal SYBR Green Supermix Kit (Bio-Rad 1725121). Primers used for this project were purchased

from Bio-Rad: GCS (qMmuCID0010046) and reference gene GAPDH (qMmuCED0027497).

2.10: Western blot

Colonoids were lysed using RIPA buffer (Alfa Aesar J62524) and protein was quantified using the Bio-Rad DC Protein Assay (Bio-Rad 5000116). Lysed protein samples were loaded onto a NuPAGE 4-12% Bis-Tris protein gel and run at 100V for two and a half hours. Proteins were transferred to a PVDF membrane using the Trans-Blot Turbo PVDF Transfer Kit (Bio-Rad 1704275) following the manufacturer's instructions. Membranes were probed using the primary antibodies (listed below) and visualized using Alexa Fluor IgG secondary antibodies (Rabbit Invitrogen A11012, Mouse Invitrogen A11005; 1:10000) on a Syngene G:BOX. Protein levels were quantified using ImageJ software and normalized to levels of β-actin (Sigma-Aldrich A5441; 1:10000). Bio-Rad Precision Plus Protein Dual Color Standards ladder was used for all experiments (Bio-Rad 1610374; 5µL/lane). Primary antibodies used for this project were: E-cadherin (Cell Signaling Technology 14472; 1:1000), TJP1/ZO-1 (Novus Biologicals NBP1-85046; 1:1000), caspase-3 (Cell Signaling Technology 9662; 1:1000), claudin-3 (Abcam ab15102; 1:1000), occludin (Novus Biologicals NBP1-87402; 1:1000), and BFT (Sears Lab; 1:1000).

2.11: Flow cytometry

Colonoids were treated with concentrated bacterial culture supernatant +/- 5µM ibiglustat, as described previously. At six- or 24-hours post-treatment, colonoid media was aspirated and the Matrigel was dissolved using Cultrex Organoid Harvesting Solution (R&D Systems 3700-100-01) with gentle shaking for 20 minutes at 4°C. After 20 minutes, the suspension was pipetted up and down ~30 times in order to break apart the colonoids. Colonoids were moved to 1.7mL microcentrifuge tubes (Olympus Corporation 24-282) and spun at 1000G for 5 minutes at 4°C. The supernatant was aspirated and the pellet was resuspended in 250µL TrypLE Express (Gibco 12605010) for 30 minutes at 37°C, with occasional vortexing. Once a single cell suspension was obtained, cells were pelleted and 500uL of eBioscience Fixable Viability Dye eFluor 780 (Thermo Fisher Scientific 65-0865-14) was added for 30 minutes at 4°C according to the manufacturer's instructions. After 30 minutes, cells were spun down, media was aspirated, and cells were resuspended in 100µL 1X Annexin V Binding Buffer (BD 556454) with 5µL FITC Annexin V (BD 556419). Samples were incubated for 15 minutes and then 150µL of 1X Annexin V Binding Buffer was added to each tube. Samples were then immediately run on the Attune Nxt (Life Technologies). Gates were established using forward and side scatter to isolate singlets and eliminate debris.

2.12: Statistics

Statistics were performed using GraphPad Prism 8.0.1 for Windows (GraphPad Software, San Diego, California USA). All experiments were performed with a minimum of three replicates unless otherwise stated. Single comparisons were made using an unpaired t-test while group comparisons were performed using a one-way ANOVA and Tukey's multiple comparisons test. Statistical significance is indicated by asterisks: * ($p<0.05$), ** ($p<0.01$), or *** ($p<0.001$). NS indicates non-significant results. Error bars represent the standard deviation of the mean.

2.13: Extracellular vesicle isolation

Media collected from colonoids was centrifuged at 300G for 10 minutes. The resulting supernatant was transferred to a new tube and centrifuged at 20,000G for 30 minutes, while the initial pellet (residual cells/debris) was discarded. The supernatant was transferred to a new tube and the remaining pellet was saved. Next, the supernatant was then filtered using a 0.45µm syringe filter (GE Healthcare 6780-2504). The filtered supernatant was transferred to a 0.8mL Open-Top Thinwall Ultra-Clear Tube (344090 Beckman Coulter) and placed in a Beckman Coulter SW55 Ti swinging bucket rotor. Samples were spun at 100,000G for two hours at 4°C. Once the spin completed, the supernatant was discarded and the remaining pellet was resuspended in 700µL PBS and centrifuged at 100,000G

for an additional hour at 4°C. After the spin, the supernatant was discarded and the remaining pellet (extracellular vesicles) was resuspended in 150µL PBS and stored at -80°C until use.

2.14: Measuring size and concentration of extracellular vesicles

The size and concentration of extracellular vesicles was determined using dynamic light scattering on a Malvern NanoSight (Malvern Panalytical NanoSight LM10). Samples were diluted 1:1,000 in PBS and injected into the chamber to be evaluated.

2.15: Measurement of cellular viability

Cell viability of HT29/C1 cells was measured using an MTS assay according to the manufacturer's instructions (Promega G1111).

Chapter 3: Glucosylceramide production maintains colon integrity in response to *Bacteroides fragilis* toxin-induced colon epithelial cell signaling

The text in this chapter has been adapted from the following publication:

Glucosylceramide production maintains colon integrity in response to *Bacteroides fragilis* toxin-induced colon epithelial cell signaling

Logan Patterson, Jawara Allen, Isabella Posey, Jeremy Joseph Porter Shaw, Pedro Costa-Pinheiro, Susan J. Walker, Alexis Gademsey, Xinqun Wu, Shaoguang Wu, Nicholas C. Zachos, Todd E. Fox, Cynthia L. Sears, Mark Kester

The FASEB Journal, 2020; https://doi.org/10.1096/fj.202001669R

3.1: Abstract

Enterotoxigenic *Bacteroides fragilis* (ETBF) is a commensal bacterium of great importance to human health due to its ability to induce colitis and cause colon tumor formation in mice through production of *Bacteroides fragilis* toxin (BFT). Formation of tumors is dependent on a pro-inflammatory signaling cascade, which begins with the disruption of epithelial barrier integrity through cleavage of E-cadherin. Here, we show that BFT increases levels of glucosylceramide, a vital intestinal sphingolipid, both in mice and in colon organoids (colonoids) generated from the distal colons of mice. When colonoids are treated with BFT in the presence of an inhibitor of glucosylceramide synthase (GCS), the enzyme responsible for generating glucosylceramide, colonoids become highly permeable, lose structural integrity, and eventually burst, releasing their contents into the extracellular matrix. By increasing glucosylceramide levels in colonoids via an inhibitor of glucocerebrosidase (GBA, the enzyme that degrades glucosylceramide), colonoid permeability was reduced, and bursting was significantly decreased. In the presence of BFT, pharmacological inhibition of GCS caused levels of tight junction protein 1 (TJP1) to decrease. However, when GBA was inhibited, TJP1 levels remained stable, suggesting that BFT-induced production of glucosylceramide helps to stabilize tight junctions. Taken together, our data demonstrates a glucosylceramide-dependent mechanism by which the colon epithelium responds to BFT.

3.2: Introduction

Bacteroides fragilis is a human commensal bacterium with two main molecular subtypes, each with opposing effects on human health. The first, non-toxigenic *Bacteroides fragilis* (NTBF), is a beneficial symbiote that promotes the expansion of anti-inflammatory regulatory T-cells (Treg) while also suppressing pro-inflammatory T-helper 17 (Th17) cells known to aid in colon tumorigenesis.[118,149] The second subtype, enterotoxigenic *Bacteroides fragilis* (ETBF), promotes colitis and colon tumorigenesis through a Th17-dependent mechanism.[92] The main difference between the NTBF and ETBF subtypes is the production of *Bacteroides fragilis* toxin (BFT) by ETBF strains.[90] BFT is a 20kDa zinc-dependent metalloprotease that binds to an unknown receptor on colon epithelial cells and triggers a cascade of pro-inflammatory signaling events.[150] One of the first events is the cleavage of E-cadherin, which leads to an increase in paracellular epithelial permeability.[96,147] This increased permeability causes loss of barrier function in the colon and stimulates an immune response that is required for ETBF-induced tumorigenesis.[91]

Beyond E-cadherin, tight junctions also play a critical role in maintaining epithelial cell barrier function, and additionally serve to control the passage of molecules through the paracellular space.[13] Tight junctions are comprised of several proteins,[12,13] but we focused on three tight junction-associated proteins that are highly expressed in the distal colon: claudin-3, occludin, and tight junction protein 1 (TJP1, also known as zonula

occludens-1, or ZO-1.[18] Claudin-3 belongs to the claudin family of transmembrane proteins that regulate paracellular permeability and, similar to occludin, has the ability to bind to TJP1.[12,13] Occludin is another transmembrane protein that binds to TJP1 and regulates tight junctions.[15] TJP1 serves as a scaffolding protein, holding together transmembrane tight junction proteins (such as occludin and claudins) while also anchoring them to the colon epithelial cell (CEC) cytoskeleton.[14] Importantly, in response to epithelial cell damage, TJP1 and E-cadherin colocalize and reestablish cell-to-cell junctions.[31]

Herein, we focused on sphingolipids, a class of lipids containing a sphingoid backbone that have a wide range of roles in healthy cells such as controlling growth and differentiation, regulating apoptosis, and maintaining structural integrity.[38,41] Of particular interest in the intestines is glucosylceramide, a sphingolipid involved in inflammation, cell adhesion, and enterocyte function.[41,151] Glucosylceramide is generated by glucosylceramide synthase (GCS) and broken down by glucocerebrosidase (GBA). These enzymes attach (GCS) or remove (GBA) a glucose molecule to or from the sphingolipid, ceramide.[45] Although global GCS knockout in mice is embryonic lethal, targeted GCS knockout in mouse enterocytes leads to intestinal distress, dysfunction, and soon after, death.[47,151] In colon cancer, GCS is frequently overexpressed and can lead to multidrug resistance, evasion of apoptosis, and increased cellular proliferation.[37,38,41,50,51,122,152]

Considering the epithelial-specific signaling events caused by BFT, and the importance of glucosylceramide in maintaining structural integrity of the intestinal epithelium, we hypothesized that BFT may alter glucosylceramide synthase levels. To test this hypothesis we utilized colon organoids (or "colonoids"), an *ex vivo* model for healthy colon.[10] Utilization of colonoids afforded us the ability to interrogate the importance of sphingolipids in healthy CECs exposed to BFT. Using pharmacological inhibitors of GCS and GBA, we have defined a novel and functionally significant role for glucosylceramide in cells undergoing BFT challenge.

3.3: Results

ETBF, through production of BFT, increases glucosylceramide levels in mouse distal colon and colonic epithelial cells

We colonized normal C57BL/6J mice with ETBF (strain 86-5443-2-2) vs. a strain with a chromosomal deletion of *bft* (86-5443-2-2*Δbft*, herein referred to as ETBF*Δbft*), or a PBS sham control to determine if BFT alters sphingolipids in the colon. Since previous studies have shown that ETBF-induced tumors occur primarily in the distal colon,[91,153,154] we focused on the role of sphingolipids in this location to determine how *B. fragilis* impacts the colon epithelium. After 1 week, ETBF, but not ETBF*Δbft* or PBS, nearly doubled glucosylceramide levels in the distal colon (Figure 3.1A). Examination of other

major sphingolipid species in the distal colon showed that ceramide and sphingomyelin levels were unchanged across all treatments in the distal colon (Figure 3.2A and 3.2B, respectively). This finding suggests that increased glucosylceramide is a specific event in response to ETBF, dependent on its secreted metalloprotease toxin, BFT.

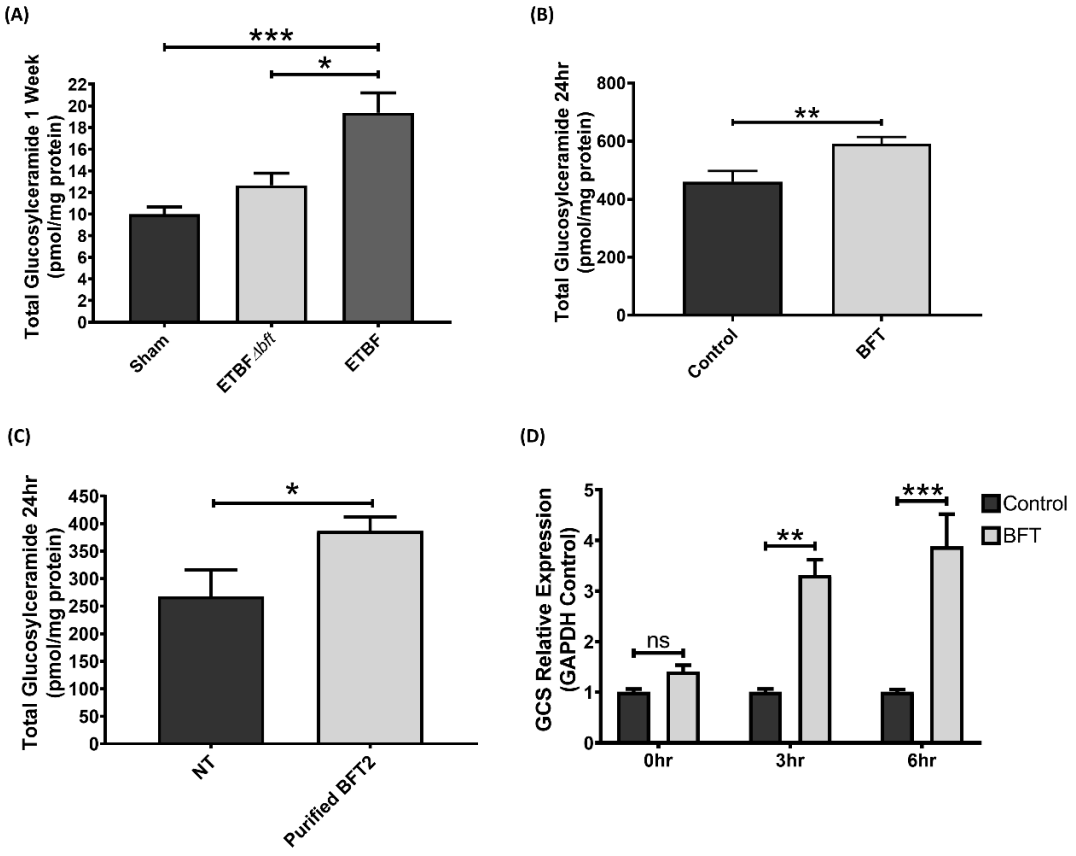

Figure 3.1: ETBF, through BFT, increases glucosylceramide levels in mice and in colonoids. Colonization with C57BL/6J mice for 1 week with ETBF increases glucosylceramide levels in the distal colon (A). Treatment of colonoids with concentrated bacterial culture supernatant from ETBF (BFT) significantly increases glucosylceramide levels at 24hr when compared to concentrated bacterial supernatant from ETBF*Δbft* (Control) (B). Addition of purified *Bacteroides fragilis* toxin (Purified BFT2, isolated from ETBF strain 86-5443-2-2, see Materials and Methods for details) to colonoids increases glucosylceramide production (C). Treatment of colonoids with BFT increases mRNA expression of glucosylceramide synthase (GCS) at three and six hours, as measured by qPCR (D). Group comparisons were performed using a one-way

ANOVA and Tukey's multiple comparisons test, while single comparisons were made using an unpaired t-test. Statistical significance is indicated by asterisks: * ($p<0.05$), ** ($p<0.01$), or *** ($p<0.001$). Error bars represent the standard deviation of the mean. Sham represents a PBS control. NT indicates no treatment was added. Control represents concentrated bacterial culture supernatant from ETBF*Δbft*, BFT represents concentrated bacterial culture supernatant from ETBF, and Purified BFT2 represents purified BFT from ETBF strain 86-5443-2-2 (see Materials and Methods).

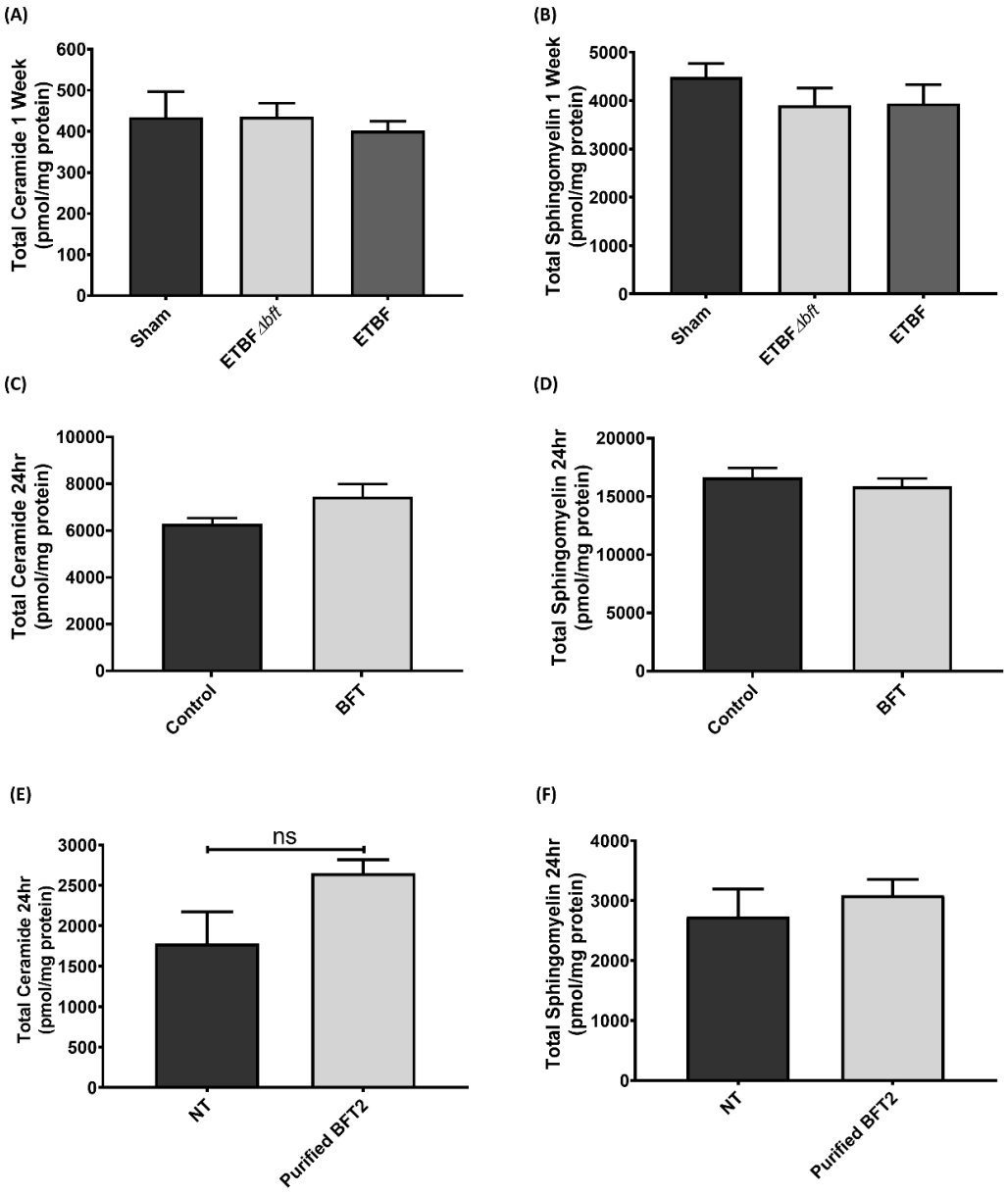

Figure 3.2: BFT does not significantly alter levels of other major sphingolipid species. Mass spectrometry analysis of colon (A and B), colonoids treated with concentrated bacterial culture supernatant (C and D), and colonoids treated with purified BFT2 (E and F) determined that the total levels of ceramide (A, C, E) and sphingomyelin (B, D, F) do not change significantly in response to treatment. All results were collected in the same experiments used to produce the data shown in Figure 3.1. Group comparisons were performed using a one-way ANOVA and Tukey's multiple comparisons test while single comparisons were made using an unpaired t-test. NS indicates non-significant results. Error bars represent the standard deviation of the mean. Sham represents a PBS control. NT indicates no treatment was added. Control represents

concentrated bacterial culture supernatant from ETBF*Δbft*, BFT represents concentrated bacterial culture supernatant from ETBF, and Purified BFT2 represents purified BFT from ETBF strain 86-5443-2-2 (see Materials and Methods).

We next sought to investigate sphingolipids in CECs after BFT treatment. Due to the inherent dysregulation of sphingolipid metabolism present in cancer cell lines,[38,50,123–126] we utilized colonoids from distal colons of C57BL/6J mice as an *ex vivo* model for normal, healthy CECs.[10,133] Colonoids were grown in 3D culture, embedded in Matrigel, following the established protocol by Dr. Hans Clevers' Laboratory.[136] In order to replicate our *in vivo* findings from Figure 3.1A, we concentrated cell-free bacterial culture supernatants from ETBF as a method to deliver BFT to colonoids (herein referred to as BFT). Furthermore, to focus on BFT-specific changes caused by our concentrated bacterial culture supernatants, and to prevent any non-toxin bacterial factors from impacting our results, we utilized concentrated bacterial culture supernatants from ETBF*Δbft* as the control for all of our colonoid experiments (herein referred to as Control). Concentrated bacterial culture supernatant preparation details, as well as validation of BFT presence and activity, are detailed in Materials and Methods (Validation of toxin presence and activity in concentrated bacterial culture supernatants; Figure 3.3). We treated colonoids with our concentrated bacterial culture supernatants, and, similar to our *in vivo* results (Figure 3.1A), BFT significantly increased glucosylceramide levels by ~28% in colonoids (Figure 3.1B). To validate that these results were due to BFT, and not any other bacterial factors present in our concentrated

bacterial culture supernatant preparations, colonoids were treated with 5nM purified BFT2, which was obtained from the Sears lab after an extensive purification process to isolate BFT from ETBF bacterial culture supernatants (see Methods for purification information).[95] Importantly, purified BFT alone was sufficient to increase glucosylceramide levels by ~44% in colonoids (Figure 3.1C).[95] We also measured ceramide and sphingomyelin levels in response to concentrated bacterial culture supernatants (Figure 3.2C and 3.2D) or purified BFT (Figure 3.2E and 3.2F), and did not observe any significant changes in either condition. Next, we assessed the mRNA expression of GCS shortly after treatment with BFT (Figure 3.1D). Consistent with mass spectrometry results showing increased glucosylceramide levels, GCS mRNA expression increased over time in the presence of BFT when compared to the control (Figure 3.1D). Taken together, these data highlight a BFT-specific increase in glucosylceramide lipids and GCS expression.

Pharmacological reduction of glucosylceramide in the presence of BFT causes colonoids to burst

In order to determine the purpose of increased glucosylceramide in CECs after exposure to BFT, we next utilized a GCS inhibitor to reduce the levels of glucosylceramide and then measured cellular responses. Ibiglustat, an allosteric inhibitor of GCS, currently entering phase III clinical trials for the treatment of autosomal dominant polycystic

kidney disease (ClinicalTrials.gov Identifier: NCT03523728), was used. In order to align with our BFT treatment timeline, colonoids received 5µM ibiglustat for 24 hours in normal growth medium, then medium was aspirated and replaced with basal medium containing ibiglustat for six hours, which was subsequently replaced with growth medium containing ibiglustat again for the remainder of the experiment (18 or 42 hours for 24 or 48 hour time points, respectively). A schematic representation of the treatment regimen can be found in Figure 3.4A. Using this treatment regimen, we verified through mass spectrometry that levels of glucosylceramide were significantly decreased by nearly 80% at 24 and 48 hours when compared to the vehicle control (DMSO; Figure 3.4B). To confirm GCS activity was inhibited by ibiglustat, we added 5µM C6-ceramide, a non-physiological form of ceramide, using C6-ceramide nanoliposomes (C6-CNL) or ghost liposomes (vehicle control that lacks ceramide) to colonoids for one hour after a 24-hour pre-treatment with ibiglustat or vehicle control. Conversion of C6-ceramide into C6-glucosylceramide was completely blocked in the presence of ibiglustat, demonstrating that ibiglustat is inhibiting GCS activity (Figure 3.4C). As expected, ghost liposomes did not return a signal for any C6-sphingolipids (data not shown). Finally, we visualized colonoids treated with 5µM ibiglustat using confocal microscopy and did not observe any overt morphological changes (Figure 3.4D).

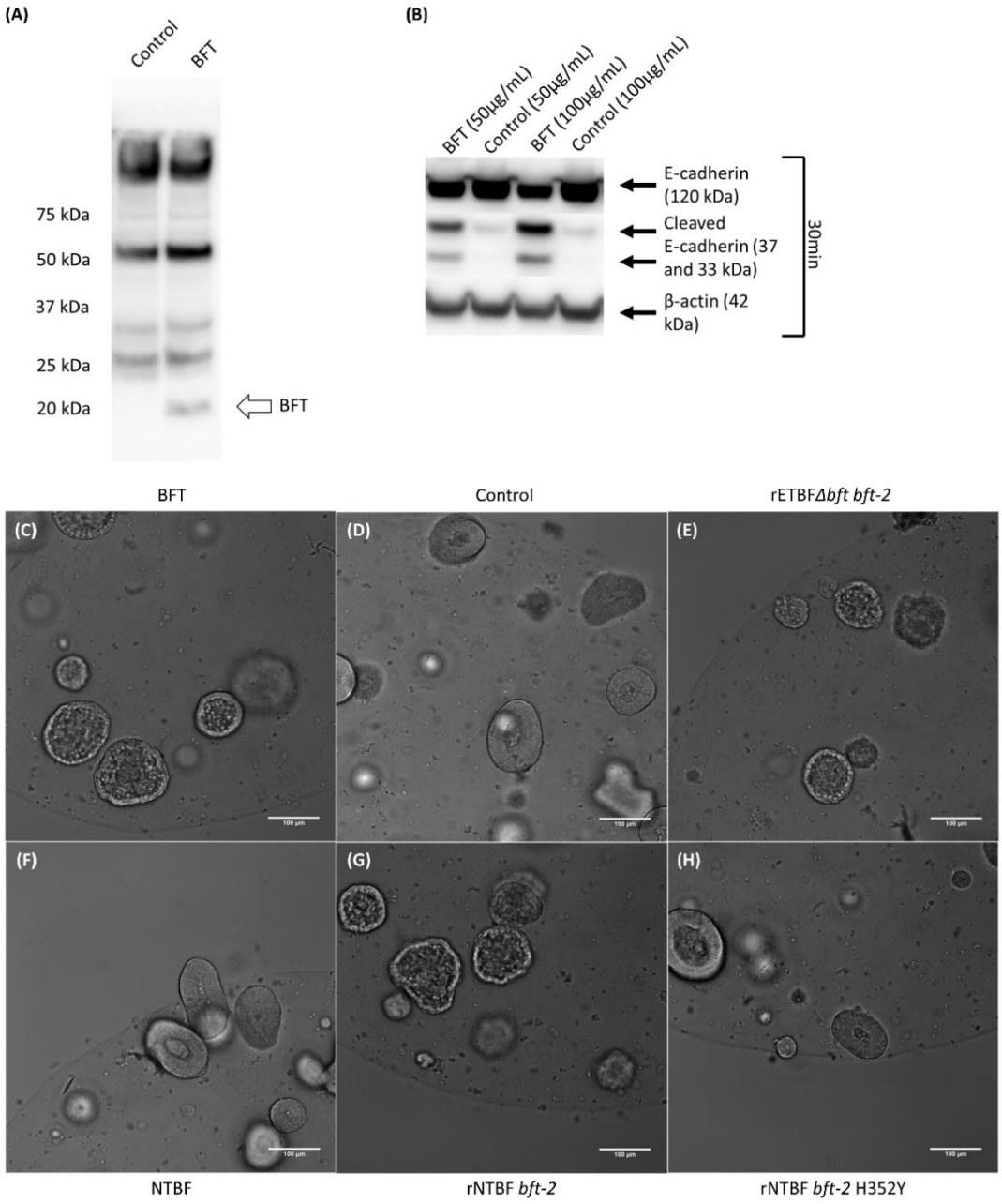

Figure 3.3: Concentrated bacterial culture supernatant from ETBF contains *Bacteroides fragilis* toxin and BFT is biologically active. Western blot of concentrated bacterial culture supernatants (200µg protein) using an anti-BFT antibody shows presence of toxin in concentrated bacterial culture supernatant from BFT but not control (A). Addition of BFT to HT29/C1 cells for 30 minutes leads to E-cadherin cleavage, illustrating toxin activity in our BFT preparations (B). Confocal imaging of colonoids treated for six hours with different concentrated bacterial culture supernatant preparations demonstrates that presence of toxin leads to morphology changes (C-

H). Concentrated ETBF bacterial culture supernatant, containing BFT, dramatically alters colonoid morphology (C). Concentrated bacterial culture supernatant from ETBF*Δbft* does not alter colonoid morphology (D), but when a recombinant version of this strain that produces BFT2 is used (rETBF*Δbft bft-2*), morphology changes are similar to those seen with BFT (E). Concentrated bacterial culture supernatant from NTBF (NCTC 9343), which does not produce BFT, does not cause morphology changes in colonoids (F). In contrast, a recombinant NTBF strain that produces BFT2 (rNTBF *bft-2*) alters morphology, similar to BFT (G). A recombinant NTBF strain, which secretes a biologically inactive mutant of BFT2 (rNTBF *bft-2* H352Y) no longer causes morphology changes (H). Confocal images were captured using 10x magnification. Scale bar indicates a distance of 100µm.

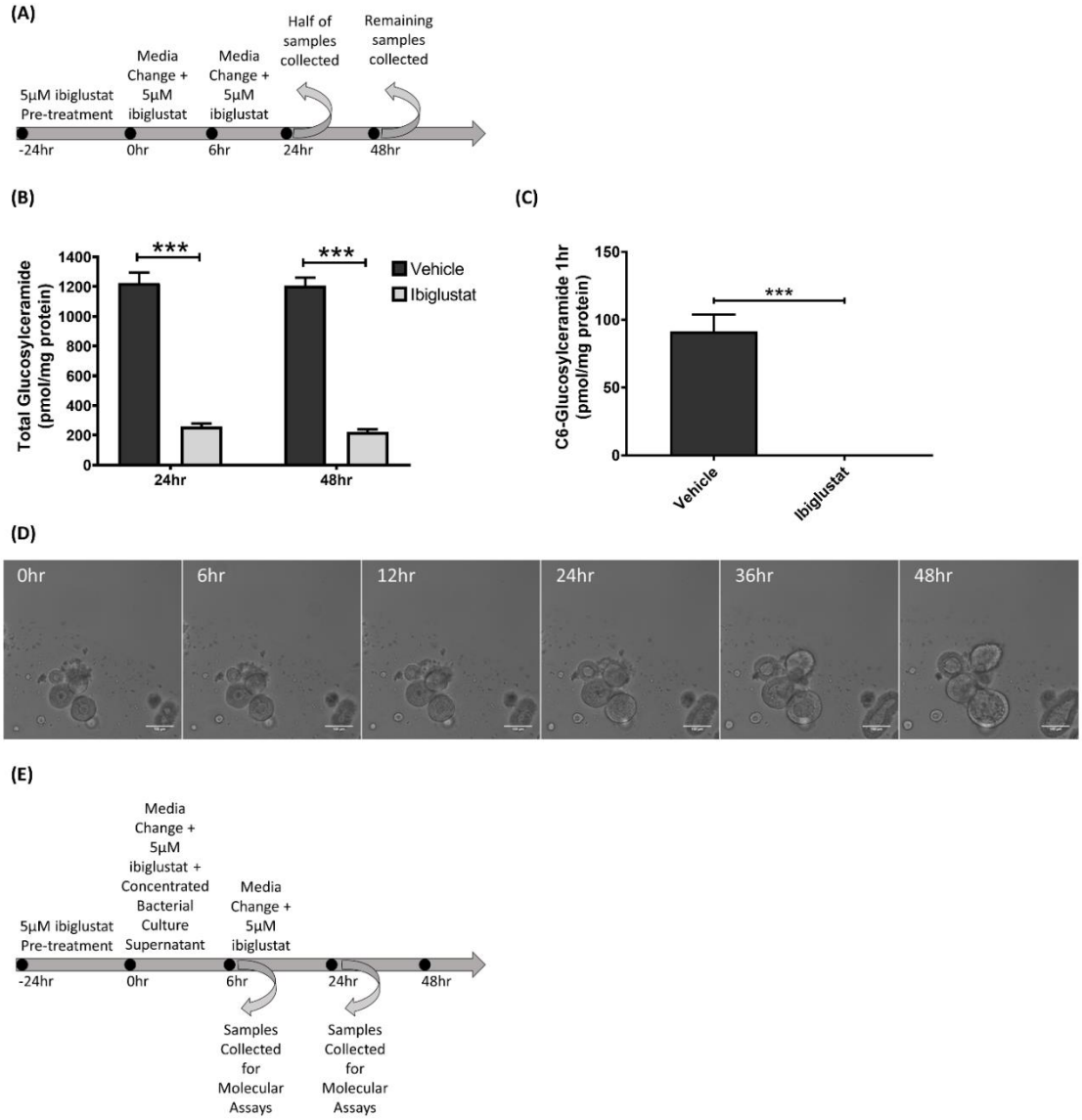

Figure 3.4: A selective inhibitor of glucosylceramide synthase (GCS) decreases glucosylceramide lipid levels. The treatment regimen for administration of 5µM ibiglustat to colonoids is depicted (A). Addition of 5µM ibiglustat effectively reduced total levels of glucosylceramide (B). Colonoids were pre-treated with 5µM ibiglustat for 24 hours and then treated with C6-ceramide nanoliposomes (CNL) for one hour to determine the effectiveness of ibiglustat in blocking GCS activity. Colonoids were collected and lipids were extracted. Presence of ibiglustat completely blocks the ability for colonoids to process C6-ceramide into C6-glucosylceramide, demonstrating the efficacy of ibiglustat at inhibiting GCS activity (C). Pre-treatment of colonoids with 5µM ibiglustat followed by addition of concentrated bacterial supernatant from ETBF*Δbft* does not alter colonoid morphology, visualized by confocal microscopy (D). The treatment regimen for administration of 5µM ibiglustat and concentrated bacterial culture supernatant is depicted (E).

Single comparisons were made using an unpaired t-test. Statistical significance is indicated by asterisks: *** ($p<0.001$). Error bars represent the standard deviation of the mean. Vehicle represents a vehicle control (see Materials and Methods). Confocal images were captured using 10x magnification. Scale bar indicates a distance of 100µm.

Once we validated the efficacy of ibiglustat in our model, we added our concentrated bacterial culture supernatants to the treatment regimen mentioned previously (detailed in Materials and Methods; schematic representation shown in Figure 3.4E) to determine the effects of BFT while glucosylceramide levels were reduced. We visualized the colonoids for 48 hours using confocal microscopy, taking images every 20 minutes. Videos were assembled and images from 0, 6, 12, 24, 36, and 48-hour time points are shown in Figure 3.5A-D (corresponding videos can be found in Supplemental Videos 1-4; online manuscript). Figure 3.5A shows normal colonoid morphology after the control treatment. Similar to Figure 3.5A, treatment with control and 5µM ibiglustat did not induce morphological alterations over 48 hours (Figure 3.5B). However, when BFT was added for six hours, colonoids underwent a rapid expansion and cells began to round. This was followed by a recovery and reorganization of the epithelial membrane structure around 36 hours, and a return to normal morphology by 48 hours (Figure 3.5C). In stark contrast, when BFT is added for six hours in the presence of ibiglustat, colonoids lose their structure, and luminal contents escape into the extracellular matrix (Figure 3.5D). We refer to this phenomenon as “colonoid bursting” to represent the overall loss of colonoid structural integrity and displacement of cells and other luminal content into the extracellular matrix. When bursting events across all treatments were

quantified, BFT and ibiglustat treatment led to a significantly higher level of bursting events (14.77% average) when compared to all other treatments (0.45% average in control, 3.98% average in control + ibiglustat, and 1.06% average in BFT; Figure 3.5E). Colonoid bursting during BFT and ibiglustat treatment demonstrates that BFT-induced cellular production of glucosylceramide is important for colonoid survival.

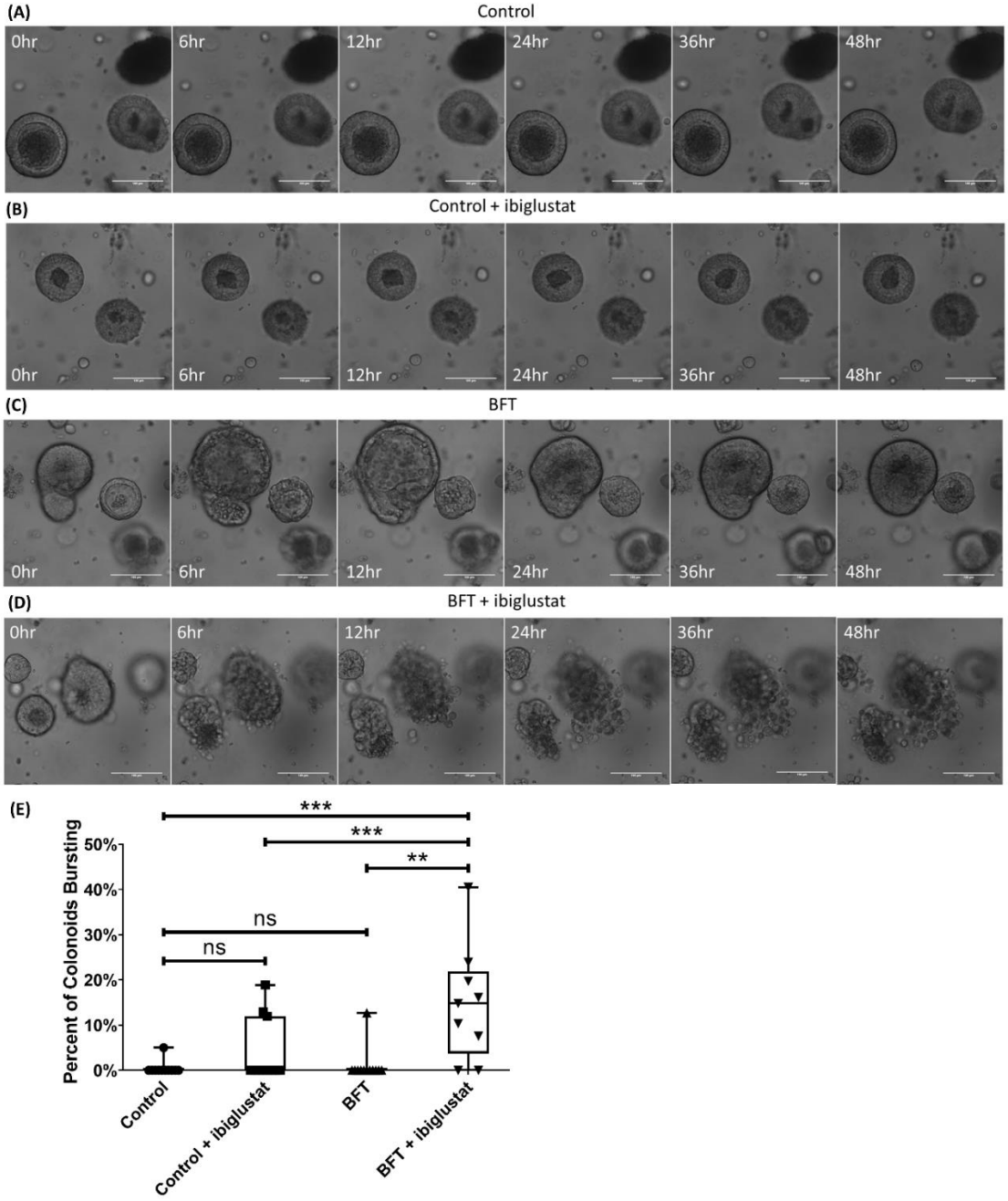

Figure 3.5: Combination of BFT and ibiglustat causes colonoids to burst. Colonoids treated with concentrated bacterial culture supernatant from ETBF*Δbft* (Control) (A) or control + 5μM ibiglustat (B) show no obvious morphology changes when visualized by confocal microscopy. Colonoids treated with BFT undergo dramatic swelling and bubbling by six hours before returning to normal morphology by 48 hours (C). Colonoids treated with BFT and 5μM ibiglustat burst open, spilling contents into the extracellular matrix (D). Colonoids in all videos were tracked and bursting events were counted (E). Colonoids were considered bursting if by 48

hours they had lost overall structure and there was no evidence that the outer epithelial membrane was reforming. We counted all of the colonoids in the well and calculated the percentage of colonoids that burst within 48 hours (n=12). Group comparisons were performed using a one-way ANOVA and Tukey's multiple comparisons test. Statistical significance is indicated by asterisks: ** ($p<0.01$) or *** ($p<0.001$). NS indicates non-significant results. Control represents concentrated bacterial culture supernatant from ETBF*Δbft* and BFT represents concentrated bacterial culture supernatant from ETBF. Confocal images were captured using 20x magnification. Scale bar indicates a distance of 100µm. Compiled 48-hour time-lapse videos can be found in Supplemental Videos 1-4 (online manuscript).

Pharmacological inhibition of glucocerebrosidase increases glucosylceramide levels in colonoids but does not alter colonoid morphology

To further examine the importance of glucosylceramide in our model, we utilized conduritol B epoxide (CBE), an inhibitor of glucocerebrosidase (GBA),[155] to prevent the breakdown of glucosylceramide and, therefore, increase cellular levels of glucosylceramide. After culturing colonoids for 24 hours with 20µM CBE, a ~22% increase in glucosylceramide levels was observed (Figure 3.6A). We maintained a subset of colonoids in 20µM CBE, refreshed every other day. After one week, glucosylceramide levels were over two-fold higher than colonoids cultured without CBE (Figure 3.6A). We then measured sphingolipid changes in colonoids cultured in CBE after treatment with control or BFT with or without ibiglustat. We observed that in the presence of CBE, while both the control and the BFT treated colonoids had elevated levels of glucosylceramide, in contrast to colonoids cultured without CBE (Figure 3.1B), BFT no longer significantly increased glucosylceramide (Figure 3.6B). Moreover, ibiglustat

remained effective at reducing the levels of glucosylceramide in both treatments, albeit to a lesser degree than that seen in colonoids without CBE (Figure 3.4B). We visualized colonoids cultured in CBE during treatment with concentrated ETBF*Δbft* culture supernatant using confocal microscopy, and did not observe morphology changes (Figure 3.6C). Therefore, treatment with CBE is an effective way to increase glucosylceramide levels in colonoids that does not disrupt normal morphology.

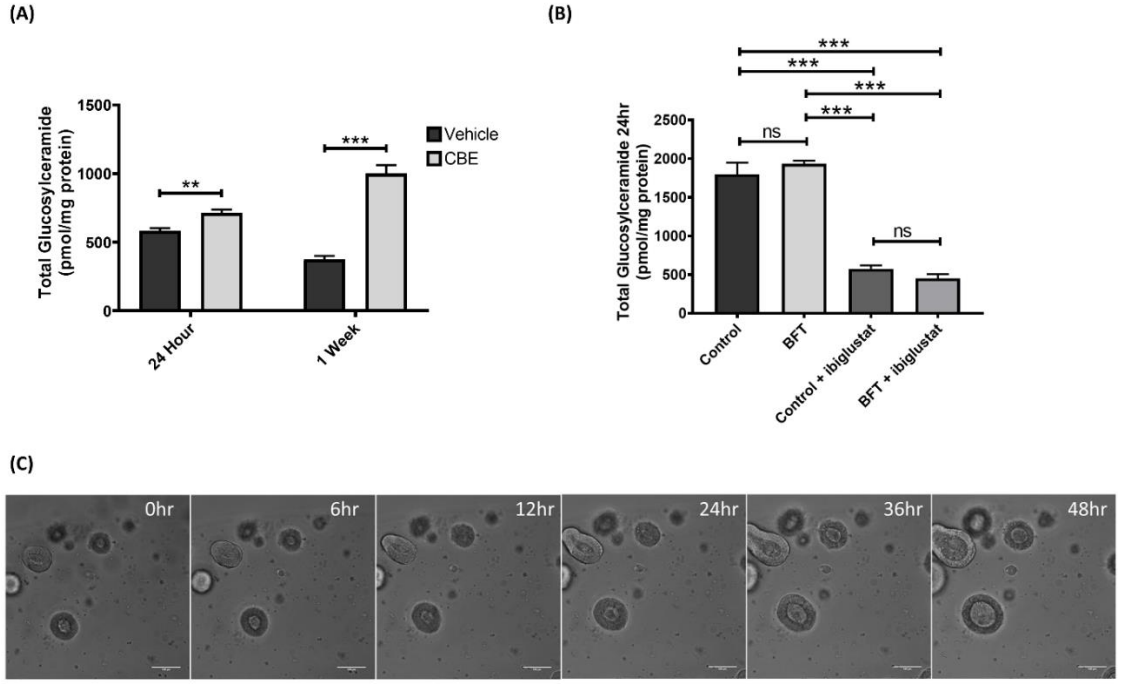

Figure 3.6: Inhibition of GBA increases glucosylceramide levels but does not alter colonoid morphology. Colonoids treated with 20μM CBE for 24 hours or 1 week have increased levels of glucosylceramide (A). Colonoids cultured in CBE were treated according to the treatment regimen in Figure 3.4E and collected at 24 hours post-concentrated bacterial culture supernatant addition for lipid analysis. Total glucosylceramide levels were similar between control and BFT treatments, but were significantly decreased in the presence of 5μM ibiglustat (B). Colonoids treated with concentrated bacterial culture supernatant from ETBF*Δbft* and cultured in CBE did not display any obvious morphological changes when visualized by confocal microscopy (C). Group comparisons were performed using a one-way ANOVA and Tukey's multiple comparisons test while single comparisons were made using an unpaired t-test. Statistical significance is indicated by asterisks: ** ($p<0.01$) or *** ($p<0.001$). NS indicates non-

significant results. Error bars represent the standard deviation of the mean. Vehicle indicates a vehicle control was used (see Materials and Methods). Control represents concentrated bacterial culture supernatant from ETBF*Δbft* and BFT represents concentrated bacterial culture supernatant from ETBF. Confocal images were captured using 10x magnification. Scale bar indicates a distance of 100µm.

Inhibition of GCS enhances BFT-induced early apoptosis

To better understand the bursting events taking place in colonoids treated with ibiglustat and BFT, we next investigated markers of apoptosis and cell viability. We treated colonoids using the same regimen outlined above (Figure 3.4E), extracted protein from cells collected six hours after treatment, and measured cleaved caspase-3, a marker of apoptosis,[156] by western blot. Because CBE colonoids were cultured with CBE in perpetuity, and maintained and passaged separately from the normal subset, we treated them as if they were a different cell line. As such, quantified results from normal and CBE colonoids were normalized to the control treatment within each group. Levels of cleaved caspase-3 were significantly increased in both the BFT and BFT + ibiglustat treatments (Figure 3.7A,C), indicating an increase in apoptosis. Colonoids cultured in CBE also displayed high levels of cleaved caspase-3 with BFT and BFT + ibiglustat treatment (Figure 3.7A,C). Total caspase-3 levels were decreased by BFT in normal and CBE colonoids, but this decrease was non-significant (Figure 3.7A,B).

To determine if caspase-3 cleavage resulted in a decrease in cell viability, and to confirm the increase in apoptosis in response to BFT, cells were stained using a fixable viability

dye (FVD; cell viability) and Annexin V (AV; apoptosis) and measured with flow cytometry. At six hours, cell viability was significantly reduced in the BFT (~17%) and BFT + ibiglustat (~22%) treatments when compared to control (Figure 3.7D). Normal and CBE colonoids treated with BFT + ibiglustat had a greater number of cells entering early apoptosis, as indicated by AV+ staining (Figure 3.7F). None of the treatments affected the numbers of cells undergoing late stage apoptosis/necrosis, indicated by cells positive for AV and FVD, in normal or CBE colonoids (Figure 3.7G). Interestingly, the control + ibiglustat treatment significantly reduced viability (~35%; Figure 3.7D), although the number of cells entering early apoptosis or late apoptosis/necrosis were similar to control (Figure 3.7F,G). Although BFT + ibiglustat increased early apoptosis, this did not significantly reduce viability when compared to BFT alone, suggesting that induction of early apoptosis is not sufficient for the colonoid bursting events seen in Figure 3.5D.

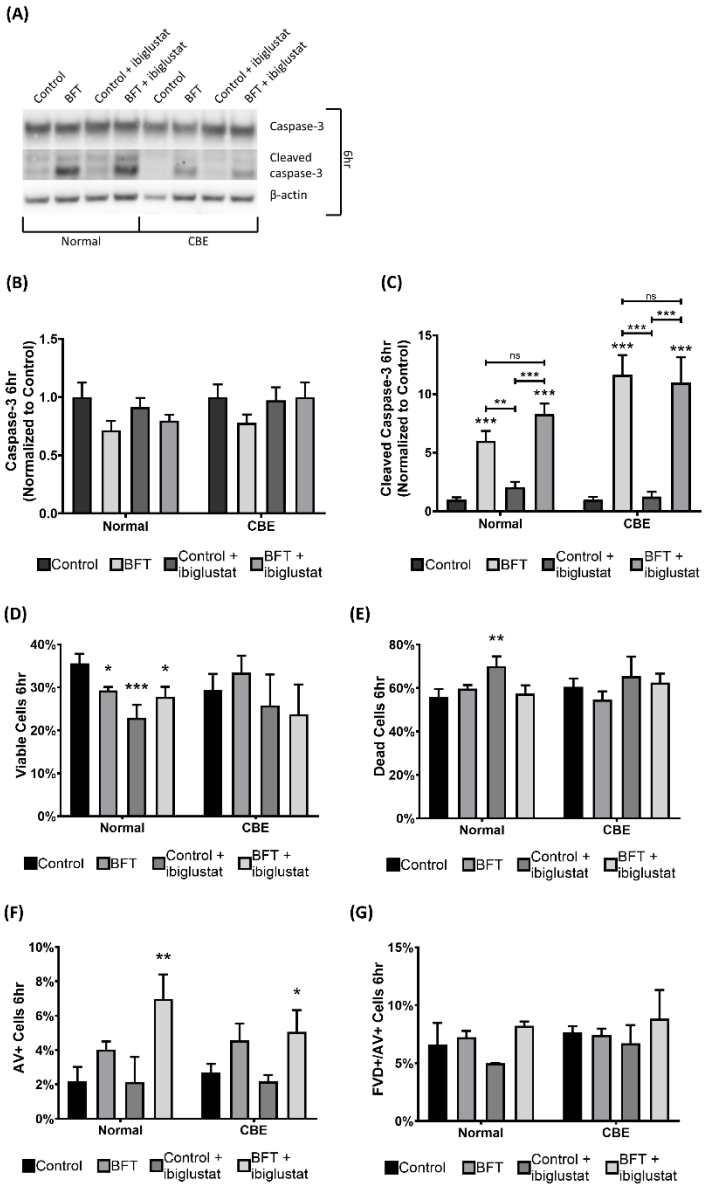

Figure 3.7: BFT increases caspase-3 cleavage and reduces cell viability in colonoids. As measured by western blots, levels of full-length caspase-3 were unaltered in all conditions in normal and CBE colonoids (A,B). BFT and BFT + 5µM ibiglustat-treated colonoids have increased levels of cleaved caspase-3 at six hours in normal and CBE colonoids (A,C). Cell viability and apoptosis were determined by flow cytometry using a fixable viability dye (FVD) and Annexin V (AV) staining, respectively. At six hours, BFT, control + 5µM ibiglustat, and BFT + 5µM ibiglustat caused significant reductions in the number of viable cells in normal colonoids, but did not significantly decrease viability in CBE treated colonoids (D). The percentage of dead cells was significantly increased in the control + ibiglustat treatment group, but other treatments did not impact the population of dead cells (E). BFT + ibiglustat treatment increased the number of AV+

cells, representing cells undergoing early apoptosis, in normal and CBE colonoids (F). FVD+/AV+ cells, representing cells in late apoptosis/necrosis, were not significantly altered by any of the treatments in either group (G). Western blot results were compiled among multiple experiments (n=6 biological replicates), normalized to their respective β-actin to control for loading, and then normalized to the average of their respective controls, where the control value was arbitrarily set to one (normal colonoids were normalized to the average of all control treatments, while CBE colonoids were normalized to the average of all CBE controls). Representative blots are shown for each target. Group comparisons were performed using a one-way ANOVA and Tukey's multiple comparisons test. Statistical significance of each individual treatment when compared to the respective control is indicated by asterisks: * ($p<0.05$), ** ($p<0.01$), or *** ($p<0.001$). Statistical significance between treatment conditions is shown by an asterisk above a line. NS indicates non-significant results. Error bars represent the standard deviation of the mean. Control represents concentrated bacterial culture supernatant from ETBF*Δbft* and BFT represents concentrated bacterial culture supernatant from ETBF.

Most early cellular responses to BFT are not dependent on glucosylceramide

The morphology changes that occur in colonoids exposed to BFT are highlighted by colonoid swelling (shown previously in human intestinal epithelial cells)[157] and cell rounding (Figure 3.5C). These changes preclude the loss of cell-to-cell adhesion and eventual colonoid bursting when BFT is added in the presence of ibiglustat (Figure 3.5D). These additional morphological variations, namely colonoid bursting, that occurred when ibiglustat was added prompted us to interrogate whether glucosylceramide in the epithelial membrane of colonoids might contribute to the maintenance of cell adhesion. Membrane polarity of colonoids grown in 3D culture and embedded in Matrigel, according to the established protocol by Dr. Hans Clevers' Laboratory,[136] is reversed from the orientation typically found in an intact colon. The apical domain, which is exposed to the digestive tract in the colon, faces the interior of the colonoid and is

protected from extracellular factors. Meanwhile, the basolateral membrane, which interacts with the extracellular matrix and is generally protected from environmental factors in the colon, faces the exterior of the colonoid and is exposed to the environment.[10] Using confocal microscopy, we stained colonoids with Alexa Fluor 633 phalloidin and confirmed that the apical domain was facing the interior of the colonoid, illustrated by the presence of actin there (Figure 3.8A,B).

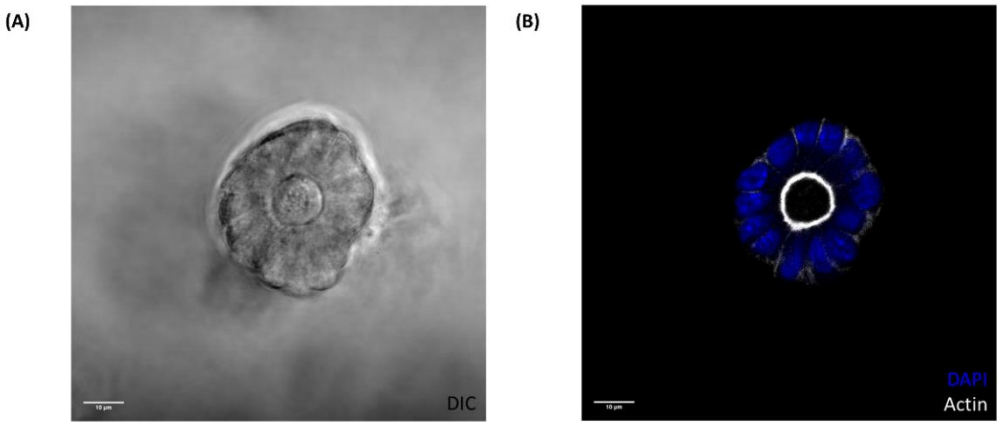

Figure 3.8: Confocal immunofluorescence of actin demonstrates the apical membrane faces the interior of the colonoid. Colonoids were extracted from the Matrigel, fixed using 2% paraformaldehyde in 100mM phosphate buffer (pH 7.4), and stained using Alexa Fluor 633 phalloidin (actin) and DAPI (nuclear stain). A representative colonoid is shown with DIC imaging (A). Confocal immunofluorescence of Alexa Fluor 633 (white) and DAPI (blue) is shown with strong actin staining at the apical ring (B). Confocal images were captured using a 63x oil-immersion lens. Scale bar indicates a distance of 10µm.

One of the first molecular events that occurs after BFT treatment is the cleavage of E-cadherin,[147] and previous studies have shown that BFT displays biological activity on the basolateral side of CEC membranes. Thus, we questioned if glucosylceramide levels

would affect E-cadherin cleavage. We examined E-cadherin cleavage via western blot and found that after a six-hour treatment with our concentrated bacterial culture supernatants, cultured with or without ibiglustat, E-cadherin was only cleaved in the presence of BFT (Figure 3.9A,B). BFT-induced E-cadherin cleavage was similar in the presence or absence of ibiglustat (Figure 3.9B). Similarly, when colonoids were cultured with CBE, levels of E-cadherin were decreased in both BFT treatments (Figure 3.9A,B). To confirm these findings, we used confocal immunofluorescence imaging on colonoids treated for six hours (as above) and removed from the Matrigel (see Materials and Methods for a detailed protocol). Consistent with our protein data, E-cadherin was expressed in control and control + ibiglustat treatments (Figure 3.9F,G middle panel). Further, in the BFT and BFT + ibiglustat treatments, E-cadherin signal was almost completely eliminated (Figure 3.9H,I middle panel). Collectively, this data suggests that BFT-induced E-cadherin cleavage does not rely on glucosylceramide, as increases or decreases did not prevent or enhance cleavage, respectively.

Since E-cadherin cleavage was indistinguishable between BFT and BFT + ibiglustat treatments, alteration of E-cadherin alone could not explain the significant difference seen in colonoid bursting events in the presence of ibiglustat (Figure 3.5E). Thus, we next examined tight junction proteins claudin-3, occludin, and TJP1, as they are located at the apical membrane of cells and function as both a barrier for extracellular factors as well as a CEC structural component to maintain cell polarity.[13] Colonoids were cultured

with or without CBE, treated as above (Figure 3.4E), and protein changes of claudin-3, occludin, and TJP1 were measured at six hours by western blot. In normal and CBE treated colonoids, levels of claudin-3 (Figure 3.9A,C), occludin (Figure 3.9A,D), and TJP1 (Figure 3.9A,E) were not changed significantly by any of the treatments.

A previous study by the Sears Lab showed that one hour BFT treatment did not alter TJP1 levels in HT29/C1 cells, but did impact membrane localization of TJP1.[94] Therefore, we sought to determine if membrane localization of TJP1 was different among our treatments using confocal immunofluorescence imaging for TJP1. We observed strong TJP1 signal at the apical barrier in control (Figure 3.9F, right panel) and control + ibiglustat (Figure 3.9G, right panel) treatments. BFT treatment did not seem to modify the levels of TJP1, but we noticed that TJP1 expression at the apical membrane was less consistent in normal colonoids when compared to control treatments (Figure 3.9H, right panel). In the BFT + ibiglustat treatment, TJP1 expression was normal but appeared to be extremely disorganized, with no obvious apical localization (Figure 3.9I, right panel). Although TJP1 levels appeared consistent across all conditions, inappropriate localization of the protein during BFT + ibiglustat treatment could increase membrane permeability, making colonoids more susceptible to bursting.

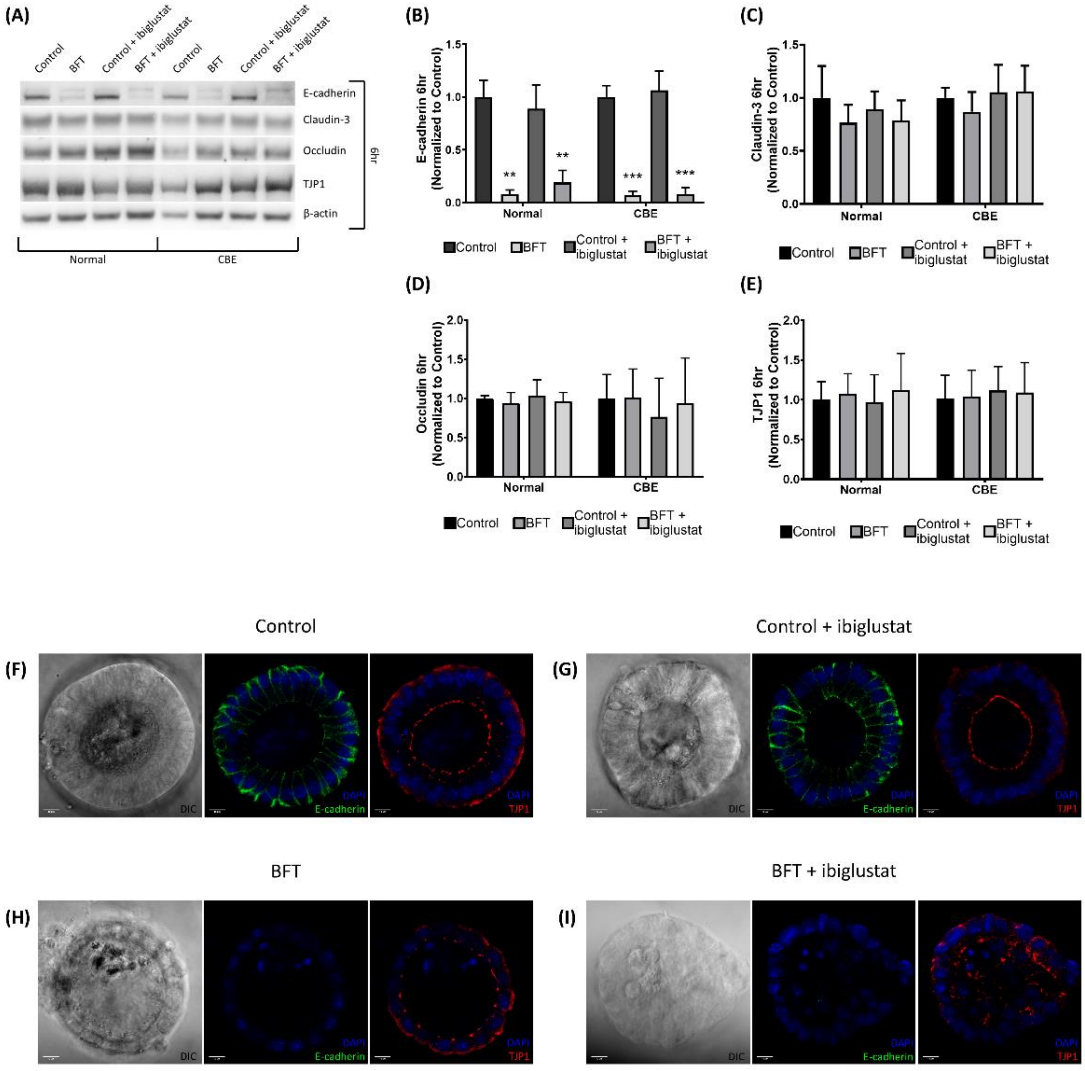

Figure 3.9: BFT decreases E-cadherin levels in colonoids at six hours and disrupts TJP1 localization. Colonoids treated with BFT show reduced levels of full-length E-cadherin at six hours via western blot, but claudin-3, occludin, and TJP1 levels are not significantly impacted by any treatment in normal or CBE colonoids (A). Quantification of E-cadherin western blots shows that BFT significantly decreased levels of full-length E-cadherin in normal and CBE-treated colonoids when compared with their respective controls (B). Claudin-3 (C), occludin (D), and TJP1 (E) levels were all quantified and did not change significantly when compared to the control treatments. Confocal immunofluorescence of colonoids for E-cadherin, TJP1, and DAPI (nuclear stain) confirms western results. Control treated colonoids displayed normal E-cadherin and TJP1 expression (F). The addition of ibiglustat did not impact E-cadherin or TJP1 expression when compared to the control (G). In colonoids treated with BFT, the E-cadherin signal was almost entirely eliminated. TJP1 localization at the apical membrane was less consistent than in the control treatments (H). BFT + ibiglustat treatment resulted in almost no E-cadherin expression,

while TJP1 localization was disorganized and irregular (I). Western blot results were compiled among multiple experiments (n=6 biological replicates for all targets except occludin, n=3). Values for each target were normalized to their respective β-actin value to control for loading variability. Finally, adjusted values were then normalized to the average of their respective control, where the control value was arbitrarily set to one (normal colonoids were normalized to the average of all control values, while CBE colonoids were normalized to the average of all CBE control values). Representative blots are shown for each target. Group comparisons were performed using a one-way ANOVA and Tukey's multiple comparisons test. Statistical significance of each individual treatment when compared to the respective control is indicated by asterisks: ** ($p<0.01$) or *** ($p<0.001$). Error bars represent the standard deviation of the mean. Confocal images were captured using a 63x oil-immersion lens. Scale bar indicates a distance of 10µm. Normal represents colonoids grown under normal conditions, while CBE represents colonoids grown in CBE. Control represents concentrated bacterial culture supernatant from ETBF*Δbft* and BFT represents concentrated bacterial culture supernatant from ETBF.

Colonoid viability and tight junction proteins are influenced by glucosylceramide levels 24 hours after BFT treatment

The bursting events seen in the BFT + ibiglustat treatment (Figure 3.5D) could not be explained by increases in early apoptosis or E-cadherin cleavage, as these events occurred similarly in normal and CBE treated colonoids. Because of this, we hypothesized that increasing glucosylceramide could be a protective mechanism by colonoids in response to the rapid cellular damage caused by BFT. To test this, we monitored cell viability using flow cytometry 24 hours after BFT treatment. Colonoids were treated using the treatment regimen outlined in Figure 3.5E, and cell viability was determined using flow cytometry. At 24 hours, the number of viable cells in normal colonoids was significantly decreased by BFT (~32%) and BFT + ibiglustat (~47%) when compared to control (Figure 3.10A). In colonoids cultured with CBE, the number of

viable cells was decreased to a greater degree by BFT (~47%) and BFT + ibiglustat (~56%) when compared to control, but the percentage of viable cells remaining was similar to each respective treatment in normal colonoids (Figure 3.10A). In general, colonoids treated with CBE had more viable cells (Figure 3.10A), and less dead cells (Figure 3.10B), at 24 hours when compared to colonoids cultured normally. Early apoptosis, indicated by AV+ staining, was relatively low in normal and CBE colonoids across all treatments (Figure 3.10C). Late stage apoptosis/necrosis increased in response to BFT and BFT + ibiglustat (Figure 3.10D), which was likely the resulting population of cells undergoing early apoptosis at six hours (Figure 3.7F). Taken together, CBE treatment increases colonoid viability, but this increase does not prevent BFT or BFT + ibiglustat-induced death.

Next, we evaluated E-cadherin, claudin-3, occludin, and TJP1 levels using a western blot as a way to monitor the adherens and tight junctions within the epithelial membrane 24 hours after initial BFT treatment. E-cadherin levels were still returning to baseline in normal colonoids (Figure 3.10E,F), and had largely recovered in CBE colonoids (Figure 3.10E,F) at 24 hours. Claudin-3 (Figure 3.10E,G) and occludin (Figure 3.10E,H) levels were mostly unaltered by any of the treatments in normal and CBE colonoids, similar to our results at six hours (Figure 3.9A,C,D). Surprisingly, although TJP1 levels did not change at six hours (Figure 3.9A,E), BFT + ibiglustat treatment in normal colonoids caused a significant drop in TJP1 (Figure 3.10E,I). This drop was not seen in colonoids

cultured with BFT alone, or in any treatment when CBE was present (Figure 3.10E,I), indicating that glucosylceramide may stabilize TJP1, helping to prevent BFT-induced colonoid burst.

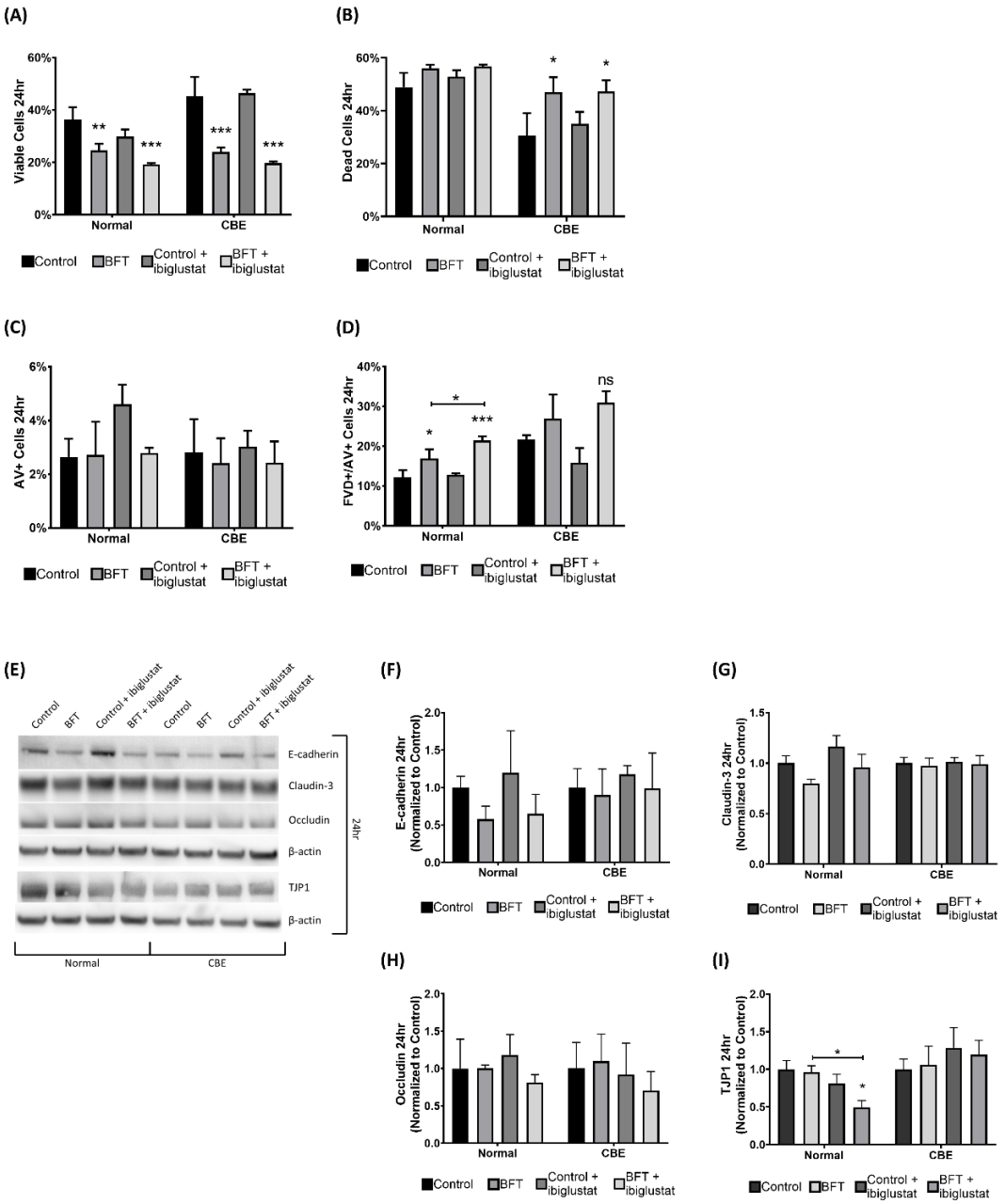

Figure 3.10: BFT-treated colonoids are less viable and have decreased TJP1 expression when GCS is inhibited. Cell viability and apoptosis were determined by flow cytometry using a fixable viability dye (FVD) and Annexin V (AV) staining, respectively. At 24 hours, BFT and BFT + ibiglustat significantly decreased the number of viable cells in both normal, and CBE colonoids (A). BFT and BFT + ibiglustat significantly increased the number of dead cells in CBE colonoids (B). Early apoptotic cells, measured by AV+ staining, were not significantly impacted by any treatment in normal or CBE colonoids (C). Colonoids treated with BFT and BFT + ibiglustat had

significantly higher percentages of cells in the late apoptosis/necrosis stage in normal colonoids, but non-significantly increased levels in CBE colonoids, as indicated by FVD+/AV+ staining (D). Colonoids were collected 24 hours after initial BFT treatment for protein and E-cadherin, claudin-3, occludin, and TJP1 were measured (E) and quantified. E-cadherin levels were non-significantly reduced in normal colonoids treated with BFT, but close to baseline in CBE colonoids (F). Claudin-3 (G) and occludin (H) levels were not significantly altered by any treatment. TJP1 expression was significantly decreased in normal colonoids treated with BFT + ibiglustat when compared to control or BFT alone, but not in CBE colonoids (I). Western blot results were compiled among multiple experiments (n=6 biological replicates for all targets except occludin, n=3). Values for each target were normalized to their respective β-actin value to control for loading variability. Finally, adjusted values were then normalized to the average of their respective control, where the control value was arbitrarily set to one (normal colonoids were normalized to the average of all control values, while CBE colonoids were normalized to the average of all CBE control values). Representative blots are shown for each target. Group comparisons were performed using a one-way ANOVA and Tukey's multiple comparisons test. Statistical significance of each individual treatment when compared to the respective control is indicated by asterisks: * ($p<0.05$), ** ($p<0.01$), or *** ($p<0.001$). Statistical significance between treatment groups is shown by an asterisk above a line. Error bars represent the standard deviation of the mean. Normal represents colonoids grown under normal conditions, while CBE represents colonoids grown in CBE. Control represents concentrated bacterial culture supernatant from ETBF*Δbft* and BFT represents concentrated bacterial culture supernatant from ETBF.

Colonoid permeability increases in colonoids treated with BFT and ibiglustat

To determine if the alterations in TJP1 expression by BFT and ibiglustat were having a functional effect on colonoids, we measured membrane permeability using a modified dextran diffusion assay.[158] Because TJP1 is important for maintaining structural integrity of the membrane, we hypothesized that ibiglustat-induced reduction of TJP1 would increase membrane permeability, an effect which could be prevented by CBE addition. Colonoids were treated as above (Figure 3.4E) and collected at 24 hours. As colonoids with an intact membrane should exclude fluorescent dye, membrane permeability was

determined by measuring the amount of fluorescent dye (FITC-dextran) found within the colonoid. In order to more accurately measure cellular permeability, colonoids that had burst, and would therefore be highly permissive to the dye, were excluded. We quantified the internal fluorescence, and, while control treated colonoids showed very minimal diffusion of FITC-dextran into the lumen (Figure 3.11A,B), all other treatments caused an increase in permeability, although not always significantly. Ibiglustat addition did not increase permeability in normal colonoids (Figure 3.11C,K), but did significantly increase permeability in colonoids cultured with CBE (Figure 3.11D,K). BFT treatment increased permeability in both normal (Figure 3.11E,K) and CBE (Figure 3.11F,K) colonoids. However, when BFT was added in combination with ibiglustat, normal colonoids were significantly more permeable (Figure 3.11G,K), whereas permeability in CBE colonoids was not significantly increased when compared to control (Figure 3.11H,K). As a positive control for increased permeability, we used EDTA to disrupt tight junctions and, as expected, EDTA treatment significantly increased permeability in both the normal and CBE treatment groups when compared to their respective controls (Figure 3.11I,J,K). The increase in colonoid permeability seen with the BFT + ibiglustat treatment further supports our bursting data from Figure 3.5D/E, and highlights the importance of glucosylceramide in regulating the CEC tight junctional complex.

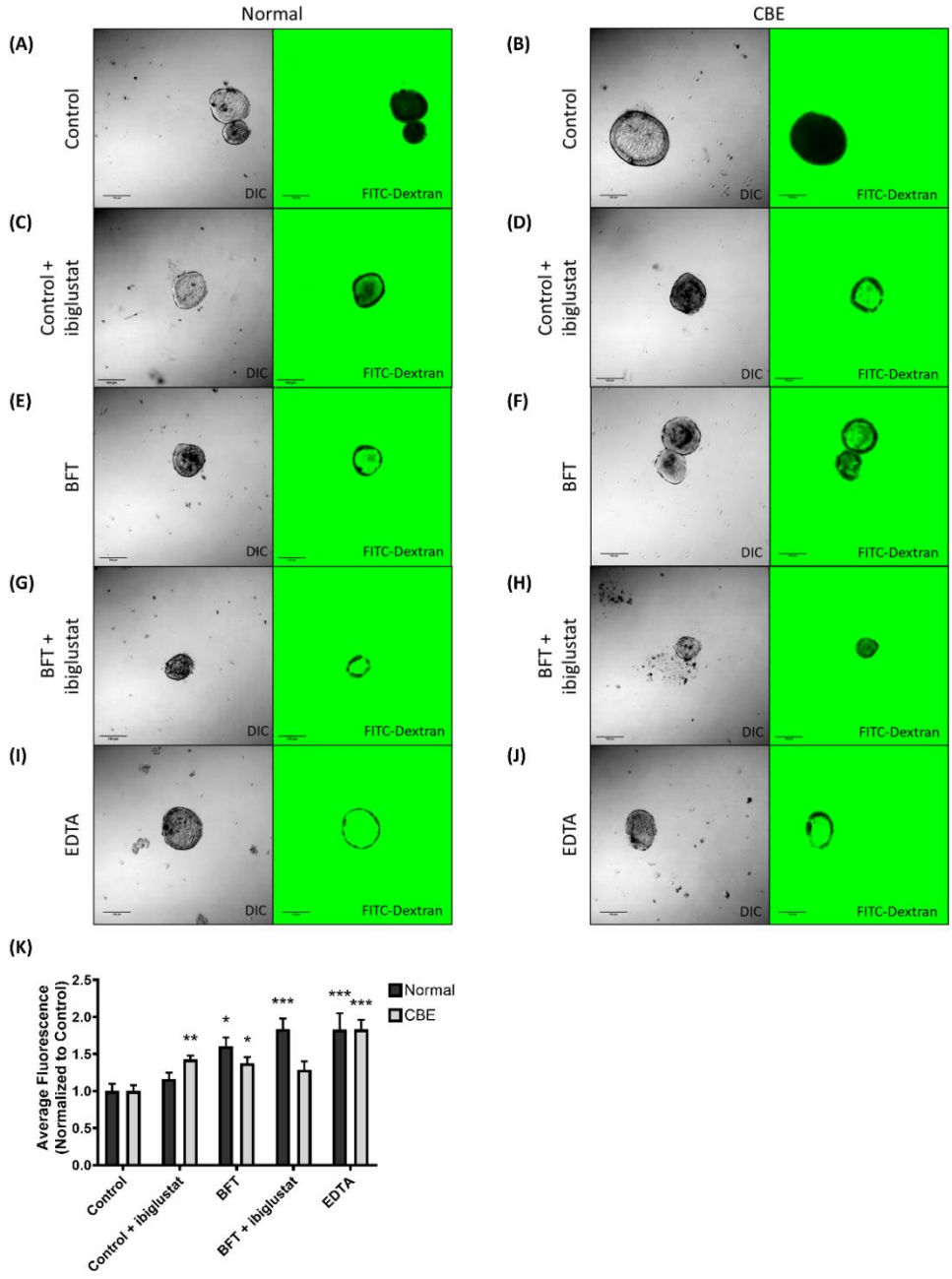

Figure 3.11: BFT treatment increases colonoid permeability, which is enhanced by GCS inhibition. Epithelial barrier integrity of colonoids grown normally or in 20µM CBE was assessed using a FITC-Dextran permeability assay. Colonoids were treated as described previously (Figure 3.4E). Colonoids were removed from the extracellular matrix at 24 hours, pelleted, and resuspended in growth media containing 2mg/mL 4kDa FITC-Dextran. Colonoids were mounted onto a slide and immediately imaged using DIC and confocal microscopy (n=15-29 colonoids/treatment). Control colonoids in normal (A) and CBE (B) groups had very little

internal fluorescence. The addition of ibiglustat significantly increased permeability of CBE colonoids (D), but not normal colonoids (C). BFT treatment caused a significant increase in permeability in normal (E) and CBE (F) colonoids. BFT treatment with ibiglustat caused a significant permeability increase in normal colonoids (G), but not CBE colonoids (H). EDTA-treated colonoids served as a positive control for increased permeability, which was seen in both treatment groups (I,J). Group comparisons were performed using a one-way ANOVA and Tukey's multiple comparisons test. Statistical significance of each individual treatment when compared to the respective control is indicated by asterisks: * ($p<0.05$), ** ($p<0.01$), or *** ($p<0.001$). Error bars represent the standard deviation of the mean. Normal represents colonoids grown under normal conditions, while CBE represents colonoids grown in CBE. Control represents concentrated bacterial culture supernatant from ETBF*Δbft* and BFT represents concentrated bacterial culture supernatant from ETBF.

Increasing levels of glucosylceramide in colonoids prevents BFT-induced bursting

Our data suggest that glucosylceramide synthesis is crucial for the integrity of colonoid structures in the presence of BFT, so we next tested whether increasing glucosylceramide levels protected colonoids from bursting. We visualized colonoids cultured in CBE for 48 hours using confocal microscopy (Figure 3.12A-D; Videos can be found in Supplemental Videos 5-8; online manuscript). In the presence of CBE, colonoids treated with control (Figure 3.12A) or control + 5μM ibiglustat (Figure 3.12B) showed no morphological changes. BFT treatment caused temporary cell rounding and membrane disorganization (Figure 3.12C), similar to that seen in colonoids without CBE (Figure 3.5C). The addition of BFT with ibiglustat caused the typical toxin induced morphology changes, but colonoids did not burst (Figure 3.12D). This was in stark contrast to those grown without CBE (Figure 3.5D). Even more striking, across all treatments in the CBE-pre-treated colonoids, we did not observe colonoids bursting. As

a more rigorous control, while scoring colonoid bursting events, we also kept track of colonoids that appeared to initiate, but not complete, bursting. These colonoids typically released luminal contents into the extracellular space but would appear to either recover and reconnect their outer epithelial membrane or maintain an ordered outer epithelium that did not fully dissociate by the end of the experiment. For these events, we scored them as "potential colonoid bursts," indicating that they may or may not recover, but we could not definitively say that they had burst. Within the CBE treatment group, there were no significant changes in potential bursting events (Figure 3.12E). Further, when compared to colonoids cultured without CBE, it is especially clear that CBE treatment protects colonoids from BFT + ibiglustat-induced burst (Figure 3.12E). Taken together, cellular increase in glucosylceramide in response to BFT appears to serve as a protective mechanism used to maintain structural integrity of the colon epithelium. This is highlighted by the fact that colonoids with reduced glucosylceramide have decreased TJP1 expression, increased permeability, and burst under stress in response to BFT, while those pharmacologically treated to maintain functional glucosylceramide levels are able to stabilize TJP1 levels and withstand the assault.

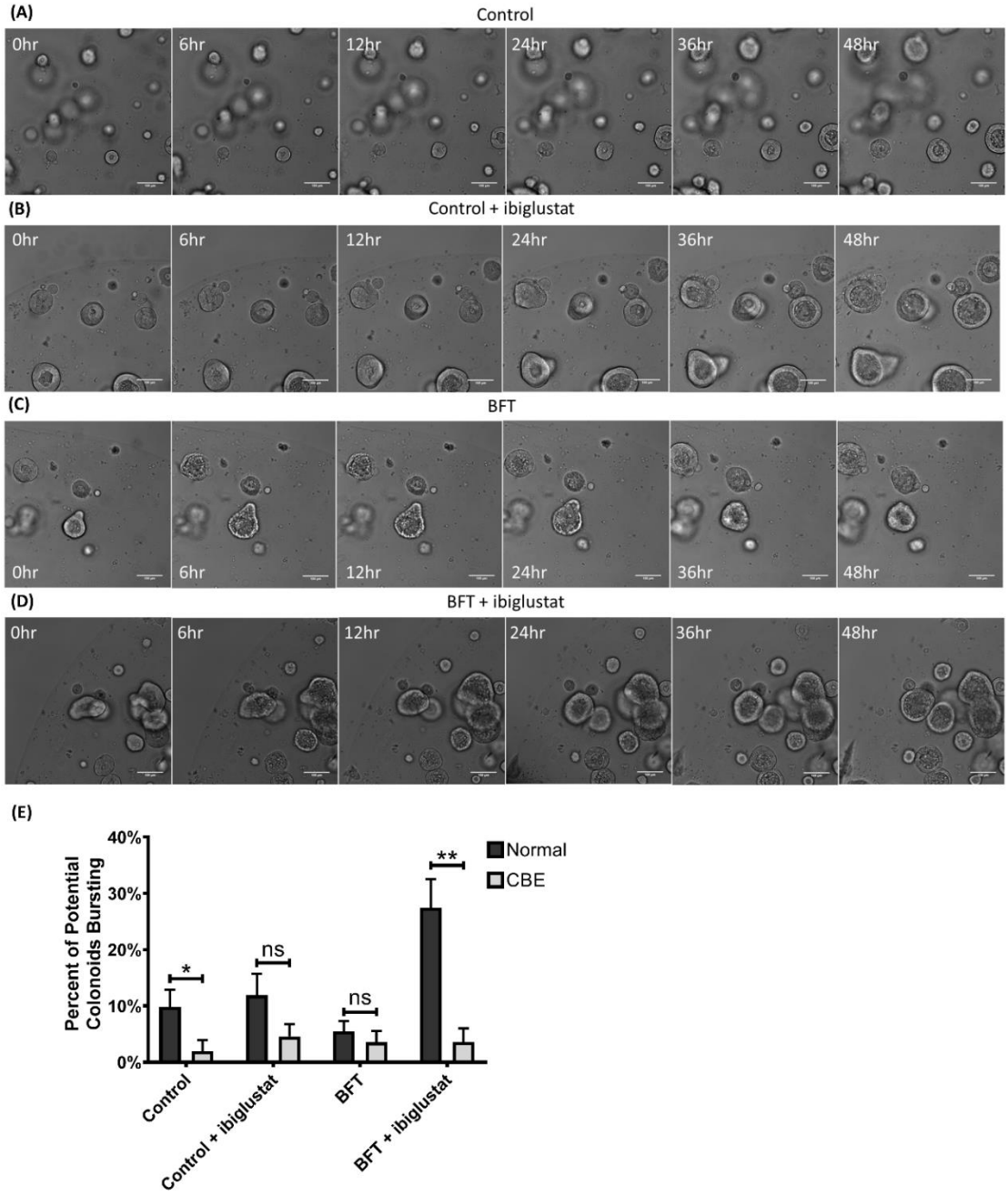

Figure 3.12: Pharmacological inhibition of glucocerebrosidase protects colonoids from BFT and ibiglustat-induced bursting. Colonoids were cultured in CBE and morphology changes were tracked by confocal microscopy. Colonoids treated with concentrated bacterial culture supernatant from ETBF*Δbft* (control) (A) or control + 5µM ibiglustat (B) showed no obvious morphology changes over 48 hours. Colonoids treated with BFT undergo dramatic swelling and bubbling and are still in the process of recovering and returning to normal morphology by 48 hours (C). Colonoids treated with BFT and 5µM ibiglustat also display a normal BFT response

and delayed recovery, but no colonoid bursting (D). Colonoids in all videos were tracked and bursting events were counted. Colonoids that appeared to initiate, but not complete, bursting were scored as a potential colonoid explosion. Potential bursting events from normal colonoids and colonoids cultured in CBE were counted and compared across all conditions (E). CBE-treated colonoids overall had less potential bursting events when compared to colonoids without CBE. Further, BFT + ibiglustat-treated colonoids had significantly less potential bursting events in the presence of CBE. Single comparisons were made using an unpaired t-test. Statistical significance for comparison between treatment groups is indicated by asterisks: * ($p<0.05$) or ** ($p<0.01$). Error bars represent the standard deviation of the mean. Normal represents colonoids grown under normal conditions, while CBE represents colonoids grown in CBE. Control represents concentrated bacterial culture supernatant from ETBF*Δbft* and BFT represents concentrated bacterial culture supernatant from ETBF. Confocal images were captured using 10x magnification. Scale bar indicates a distance of 100µm. Compiled 48-hour time-lapse videos can be found in Supplemental Videos 5-8 (online manuscript).

3.4: Discussion

We have demonstrated that ETBF, through BFT, increases glucosylceramide levels in the murine distal colon following *in vivo* treatments and in colonoids derived from the murine distal colon *in vitro*. These findings suggest that BFT directly impacts glucosylceramide production in colon epithelial cells. Our results support that the BFT-induced increase in glucosylceramide affords cells a protective mechanism by which they can maintain structural integrity of the epithelium in response to BFT. Pharmacological inhibition of GCS causes BFT-treated colonoids to burst. In contrast to this, those treated with an inhibitor of GBA are protected from BFT-induced burst. These findings are consistent with previous studies detailing the importance of glucosylceramide in the intestines.[41,151]

The utilization of colonoids as a model for healthy colon epithelial cells proved to be incredibly useful in this study, but we would like to comment on some of the shortcomings of colonoid experiments. Because colonoids are grown in 3D culture, any experiments must either be performed by first dissolving the Matrigel and collecting the colonoids, or by performing the assays while the colonoids remain in the Matrigel. Although colonoids remain intact during the collection process, excess handling can impact downstream assays, especially in experiments using living cells. In the flow cytometry procedure used in this study, colonoids were resuspended in TrypLE to yield a single-cell suspension which could then be stained and analyzed. In an early pilot experiment using only the fixable viability dye, we found that overall viability was higher than in later experiments when we added Annexin V staining (data not shown). The additional handling, pipetting, and time that this staining added likely introduced additional stresses that may have reduced overall viability. Similarly, in immunofluorescence imaging experiments, colonoids imaged within the Matrigel produced low-quality images, requiring the removal of colonoids from the Matrigel to allow for higher resolution imaging. However, colonoids had to be handled very carefully to avoid smashing the colonoids and disrupting their morphology when mounting them on slides and imaging them. Experiments that could be performed on colonoids within the Matrigel (colonoid bursting events and colonoid morphology changes) or in colonoids immediately lysed after removal from the Matrigel (lipid and protein collection) were inherently less prone to alterations caused by handling.

Growing colonoids in 2D monolayers may alleviate some of the limitations of 3D culture systems, and protocols detailing the methods to grow colonoids in 2D monolayers have been published recently.[137,159]

In C57BL/6J mice colonized with ETBF, we showed a significant increase in glucosylceramide levels in the distal colon. In general, sphingolipid levels in the distal colon were higher than that of the proximal colon (data not shown). To our knowledge, this is a novel finding in itself that warrants further study to determine why sphingolipid levels differ along the colon axis. It has been previously reported that the extracellular sphingolipid sphingosine-1-phosphate (S1P) was upregulated in response to ETBF.[160] While we were unable to replicate this finding (data not shown), results from that study were obtained in a cancer model and may not reflect the early changes shown in our non-cancerous models.

Our primary focus in this publication was glucosylceramide, but ceramide may also be converted into galactosylceramide if a galactose molecule is added instead of glucose.[161] Most of the common methods used for sphingolipid extraction and quantification, including ours, struggle to distinguish galactosylceramide from glucosylceramide.[162] Although this means that our “glucosylceramide” changes could have been galactosylceramide, or a mix of the two, we felt comfortable reporting our results as glucosylceramide for a few reasons. The first is that our "glucosylceramide" levels dropped after ibiglustat addition (Figure 3.4B). Ibiglustat is a specific GCS inhibitor,

which would not block activity of galactosylceramide synthase.[163] Second, when we measured GCS activity by adding a non-physiological form of ceramide (C6-ceramide) and measured its conversion to glucosylceramide, we found C6-"glucosylceramide", but when ibiglustat was present, no signal was detected (Figure 3.4C). Finally, we prevented molecular and phenotypic changes in our model using a GBA inhibitor, which would only impact the GSL pathway at the level of glucosylceramide and any species beyond it (Figures 3.6-3.12). Taken together, although we cannot definitively say that galactosylceramide is not included in our results, we feel confident that our results are glucosylceramide dependent.

In order to study the effects of glucosylceramide in CECs exposed to BFT, we utilized inhibitors for the enzymes responsible for creating (ibiglustat; GCS) or breaking down (CBE; GBA) glucosylceramide. In experiments with CBE-treated colonoids, we continued to use ibiglustat in our treatment groups even though these inhibitors should have opposing effects on cells, effectively canceling out their actions. In fact, for the most part, colonoids treated with both CBE and ibiglustat responded similarly to control colonoids without glucosylceramide manipulation. The one exception was where the CBE control + ibiglustat treatment caused a significant increase in permeability when compared to the control alone (Figure 8K). Although this increase in permeability was surprising, it did not impact colonoid bursting events, as shown in figure 9E. Even though CBE + ibiglustat co-treatment is somewhat counterintuitive, these experiments

support and further strengthen the finding that maintaining homeostatic glucosylceramide levels is critically important for colonoids to retain membrane integrity.

Glucosylceramide may be further modified into higher order glycosphingolipids (GSLs) through the attachment of additional carbohydrates (for further explanation of the synthesis of GSLs, see the review by Schnaar and Kinoshita).[164] Briefly, GSLs exert many of the same roles as traditional sphingolipids, including modulating proliferation, apoptosis, and cell adhesion.[165,166] Perhaps more importantly, however, are the roles that GSLs play in cell-to-cell signaling and pathogen recognition and interaction. GSLs are typically expressed on the outer leaflet of the plasma membrane where they are exposed to the external environment.[164] There, they have been shown to interact with other bacterial toxins, such as cholera toxin, tetanus toxin, and botulinum toxin.[165] Since there is no known receptor for BFT,[150] we hypothesized that GSLs could be serving as a binding partner for the toxin. However, because we still observed toxin activity on cells treated with ibiglustat, which prevents the formation of not only glucosylceramide, but also the higher order GSLs which build upon it, our data suggests the BFT receptor is not a GSL. It is possible that GSLs may help to stabilize the elusive BFT receptor, or simply serve as messengers for cell-to-cell signaling in response to the increased epithelial permeability caused by BFT via cleavage of E-cadherin, but further research will need to be done to confirm these hypotheses.

While this study focused only on intestinal sphingolipids, *Bacteroides fragilis* itself is able to produce sphingolipids.[167–169] These sphingolipids differ from their mammalian counterparts in that their fatty acid chains typically have an odd-chain length (17-19 carbons in length), while mammalian sphingolipids are typically of an even-chain length (18-20 carbons).[168,170] One of the most well-studied sphingolipids produced by *B. fragilis* is α-galactosylceramide that has been shown to influence host invariant natural killer T (iNKT) cells.[167,169] In addition to modulating host immune responses, bacterial sphingolipids also provide the bacteria with a survival advantage when dealing with the stresses encountered in the gut.[168] Since there is already evidence that bacterial sphingolipids can be incorporated into mammalian cells,[170] the incorporation of odd-chain length sphingolipids into the membrane has the ability to influence membrane fluidity and structure. Considering the potential disruptions in membrane function caused by bacterial sphingolipids, combined with our findings on the importance of membrane sphingolipids in maintaining gut homeostasis, inclusion of bacterial sphingolipids into host membranes warrants attention in subsequent studies.

Glucosylceramide modulation in response to BFT-induced epithelial barrier disruption has broad implications for the development of intestinal diseases, such as colitis and colon cancer. ETBF colonization of C57BL/6J mice with ETBF leads to colitis in as little as one week.[93] Others have shown that induction of colitis by dextran sodium sulfate (DSS) increases glucosylceramide levels in the colon.[171] Our finding that glucosylceramide

upregulation protects CECs exposed to BFT is further supported by studies in colitis models where glucosylceramide administration prevented colon epithelial damage and reduced the inflammatory immune response associated with the disease.[172,173] In addition, stabilization of TJP1 by glucosylceramide allows cells to maintain tight junctions, which are critical for reducing epithelial permeability caused by colitis.[174] Persistent colitis caused by ETBF promotes hyperplasia in the colonic crypts of C57BL/6J mice,[93] which in a mouse model for colon cancer (*Apc*$^{min/+}$), leads to tumor formation within four weeks.[153] Additional studies beyond the scope of this project are needed to determine the role of glucosylceramide upregulation in ETBF-induced intestinal disease. However, we can hypothesize that, based on published data, and in conjunction with our results, early glucosylceramide increases are likely serving as a protective mechanism by CECs to prevent colitis. As other studies have shown that increased GCS expression in the colon is pro-tumorigenic,[37,38,41,50,51,122,152] persistent and long-term activation of GCS might actually inadvertently support tumor development. Though this study was limited to early BFT-induced molecular alterations in healthy tissue, we suggest that our findings could be applied to a number of inflammatory diseases in the intestines.

In this study, we identify tight junction protein 1 (TJP1) as a putative mediator of glucosylceramide-induced protection and/or stabilization of the colonoids. While we mainly focused on TJP1, claudin-3, and occludin during this study as markers for changes

in cellular tight junctions, there are many other proteins involved in the assembly, maintenance, and function of tight junctions. Some other examples include junctional adhesion molecules (JAMs) and other claudin family proteins.[13–15] In future studies, we plan to revisit these other cell adhesion proteins to determine if they also play a role in epithelial cell response to BFT and pharmacological inhibition of glucosylceramide metabolism.

We propose a model where healthy CECs, exposed to normal microflora, have intact tight junctions and adherens junctions (Figure 3.13A). However, when ETBF colonizes the gut, *Bacteroides fragilis* toxin is produced and binds to CECs, which triggers E-cadherin cleavage and thus, a reduction of cellular adhesion. Following the loss of E-cadherin, we suggest that glucosylceramide levels are increased and help to stabilize tight junction proteins, mainly TJP1. This stabilization serves as a compensatory response to maintain CEC membrane integrity, cell-to-cell contact, and prevent epithelial breakdown after the loss of E-cadherin (Figure 3.13B). In contrast, if GCS is inhibited in the presence of BFT, tight junctions are destabilized, paracellular permeability increases, and the colon epithelium experiences catastrophic damage, allowing bacteria and bacterial factors to translocate into the lamina propria (Figure 3.13C). However, if glucosylceramide levels are restored, CECs are protected from BFT-induced damage (Figure 3.13D). Taken together, this study shows for the first time the

protective role of glucosylceramide as an important structural element that protects the colon epithelium from toxic bacterial stress.

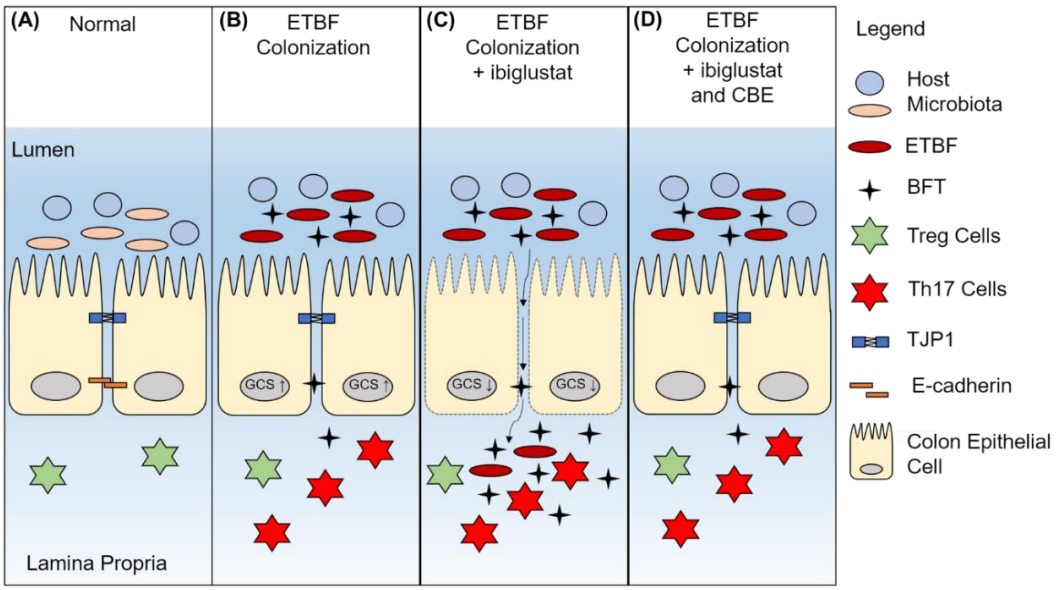

Figure 3.13: A proposed mechanism for the role of glucosylceramide in response to BFT. In a healthy colon, normal microbiota persists, cells maintain normal levels of glucosylceramide, and adherens junctions and tight junctions ensure cell-to-cell adhesion (A). When the host is colonized with ETBF, ETBF joins the microbiota and begins producing BFT, causing a decrease in CEC E-cadherin levels and an increase in glucosylceramide synthase expression (B). If glucosylceramide synthase is inhibited in a host colonized with ETBF, E-cadherin and tight junction protein 1 levels decrease, which leads to an increase in membrane permeability. Bacterial factors are able to pass through the membrane and interact with host immune cells in the lamina propria, triggering a Th17-driven pro-inflammatory immune response (C). Colonization with ETBF in the presence of CBE protects tight junctions and reduces membrane permeability (D).

3.5: Acknowledgements

We would like to thank Dr. Adrian Halme and Dr. Stacey Criswell with the Advanced Microscopy Facility at UVA (RRID:SCR_018736) for their assistance with confocal

imaging. We would also like to thank Michael H. Raymond for his assistance with flow cytometry analysis and Meredith B. Patterson for her help with confocal immunofluorescence imaging and analysis. Confocal imaging with the Operetta was possible thanks to NIH grant S10 OD021723 “Operetta CLS High-content Imaging System,” which funded its purchase. This work used the Zeiss LSM 700 in the Advanced Microscopy Facility which is supported by the University of Virginia School of Medicine. This work was supported by Bloomberg Philanthropies (to CLS). The authors also wish to acknowledge the Integrated Physiology and Imaging Cores of the Hopkins Conte Digestive Disease Basic and Translational Research Core Center (NIH DK-089502) for providing growth factor conditioned media for colonoids and use of Olympus FV3000RS confocal microscope (S10 OD025244).

Chapter 4: Glucosylceramide Beyond the Membrane: Colorectal Cancer and Extracellular Vesicles

4.1: Chapter Introduction

In the previous chapter, we showed that Enterotoxigenic *Bacteroides fragilis*, through production of its toxin (BFT), causes glucosylceramide levels to increase in colon epithelial cells (CECs). We demonstrated that glucosylceramide plays an important role in the response to BFT as it helped cells maintain structural integrity of the epithelium, highlighted by experiments showing a loss of glucosylceramide increased paracellular permeability and caused colonoids to burst. These adverse events were prevented by pharmacologically increasing glucosylceramide levels in cells. Because ETBF is associated with diarrheal disease and cancer, we questioned whether glucosylceramide upregulation by BFT could be involved in other cellular processes beyond epithelial maintenance. In this chapter, we focused on two cellular events that are impacted by sphingolipid alterations: colorectal cancer and the formation and release of extracellular vesicles (EVs) from cells.

4.2: BFT-Induced Glucosylceramide Increases are Absent in Colorectal Cancer Cells

4.2.1: Abstract

Enterotoxigenic *Bacteroides fragilis* (ETBF) is a human commensal that colonizes the colon and, through production of *Bacteroides fragilis* toxin (BFT), can cause inflammatory diarrhea and cancer in $Apc^{min/+}$ mice. We have previously shown that

ETBF colonization of mice increases glucosylceramide levels in the distal colon, the primary location for ETBF-induced tumor formation.[175] Glucosylceramide has previously been shown to be a pro-tumorigenic sphingolipid by reducing ceramide driven apoptosis and promoting multi-drug resistance. Therefore, we sought to determine if BFT-induced glucosylceramide increases in colon epithelial cells (CECs) might promote tumor formation or progression. Using a colorectal cancer cell line and colonoids generated from *Apc*$^{min/+}$ mice, we determined that BFT did not increase glucosylceramide levels in either model, even though glucosylceramide synthase (GCS) activity was increased in *Apc*$^{min/+}$ colonoids. Although we did not observe any significant increases in glucosylceramide, the increases in GCS activity are indicative that BFT is still generating glucosylceramide, but determining where it is going will be an important future direction.

4.2.2: Introduction

We previously showed that normal CECs will increase production of glucosylceramide when they are exposed to BFT. This increase protected cells by helping them to maintain tight junctions and overall membrane integrity after E-cadherin cleavage. However, persistent upregulation of GCS by BFT could disrupt normal, and required, cell turnover in the colon by preventing ceramide-induced apoptosis.[1,2,36,38] The prevention of cell shedding could allow cells to gain mutations, leading to polyp development that is

seen in mice colonized with ETBF.[92] Therefore, we hypothesized that BFT-induced glucosylceramide could be a pro-tumorigenic event.

4.2.3: Results and Discussion

BFT Does Not Increase Glucosylceramide Levels in Cancer CECs

To determine if BFT altered glucosylceramide levels in CRC, we utilized HT29/C1 cells, which were derived from HT-29 cells that were originally established from a patient with colorectal adenocarcinoma.[176] Similar to our experimental methods in colonoids, cells were treated for six hours with ETBF*Δbft* or ETBF concentrated bacterial culture supernatants in basal medium (DMEM without FBS) for six hours, at which point the media was removed and replaced with fresh growth medium (DMEM with 10% FBS) for 18 hours. At 24 hours post-treatment, cells were collected and sphingolipids were extracted. A true NT control was included to ensure that these cells were not being influenced by our concentrated bacterial culture supernatants. Total glucosylceramide levels in control and BFT treatments were nearly identical to the NT control (Figure 4.1A). To further confirm that BFT was not promoting the production of glucosylceramide, we treated cells for six hours (as above) and measured mRNA expression of GCS. In agreement with our lipid data, GCS expression was unchanged across all treatments (Figure 4.1B). Finally, to assess whether BFT addition would

enhance viability of HT29/C1 cells, we treated cells and performed an MTS assay. This assay showed that viability was not altered by any of the treatments (Figure 4.1C).

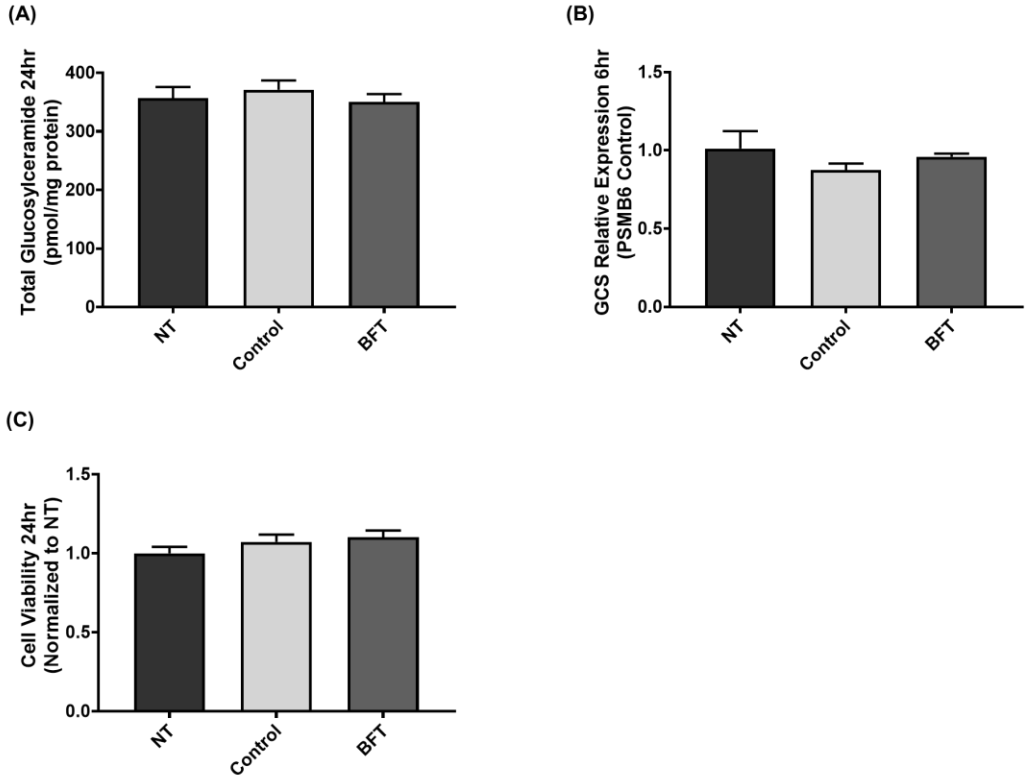

Figure 4.1: BFT does not alter glucosylceramide, GCS expression, or cell viability in HT29/C1 cancer cells. HT29/C1 cells were treated for six hours with concentrated bacterial culture supernatant from ETBF*Δbft* (Control) or ETBF (BFT) or a true no treatment control (NT). At six hours, samples were collected for mRNA extraction, while media was replaced with fresh growth medium on cells used for lipid and protein extractions and incubated for an additional 18 hours. At 24 hours post treatment, remaining cells were collected and sphingolipids or proteins were extracted. BFT did not increase glucosylceramide levels in HT29/C1 cells (A). GCS expression was not significantly changed between the three treatments (B). Cell viability, as measured by an MTS assay, was unchanged across treatments (C). Error bars represent the standard deviation of the mean. NT indicates no treatment was added. Control represents concentrated bacterial culture supernatant from ETBF*Δbft* and BFT represents concentrated bacterial culture supernatant from ETBF.

Utilization of Colonoids Generated from *Apc*$^{min/+}$ Mice

Although we did not observe any changes in glucosylceramide in HT29/C1 cells treated with BFT, this was not entirely unexpected based on previous studies showing that cancer cells have a dysregulated sphingolipid metabolism.[38,50,122–126] In addition, because BFT did not increase viability, we propose that BFT may be more important for tumor formation than for cancer progression. To test this theory, we established colonoids from *Apc*$^{min/+}$ mice. *Apc*$^{min/+}$ mice have a mutation in *Apc*, which causes them to develop neoplasia in the intestines soon after birth.[177] Interestingly, even though these mice are frequently used to study colon cancer, they primarily develop tumors in the small intestine.[154] However, when they are colonized with ETBF, tumors will form in the distal colon.[91] Therefore, colonoids established from *Apc*$^{min/+}$ mice could be used as a pre-cancer model for BFT-induced carcinogenesis.

Shortly after *Apc*$^{min/+}$ colonoids were established, we began to notice dramatic morphology changes that were evident using bright field microscopy. The colonoids began growing much faster and larger than C57BL/6J colonoids, and the epithelial membrane began to compress. An example of this is shown in Figure 4.2, which shows a subset of colonoids growing during a 48-hour time period. These morphology changes were consistent with published data from another lab that generated colonoids from *Apc*$^{min/+}$ adenomas,[178] suggesting that our colonoids had already begun the transition to cancer.

Even though our colonoids were likely already adenomas, we decided to measure morphology changes after BFT treatment to determine if BFT would still illicit a response. When we added concentrated bacterial culture supernatants from ETBF*Δbft*, we did not observe any overt morphology changes (Figure 4.3A). However, when BFT was added, the colonoids underwent a dramatic morphology change (Figure 4.3B), similar to what we had previously shown in normal colonoids. This confirms previous findings that morphology changes are not dependent on glucosylceramide, but most likely reflect sudden loss of E-cadherin and adherens junctions.

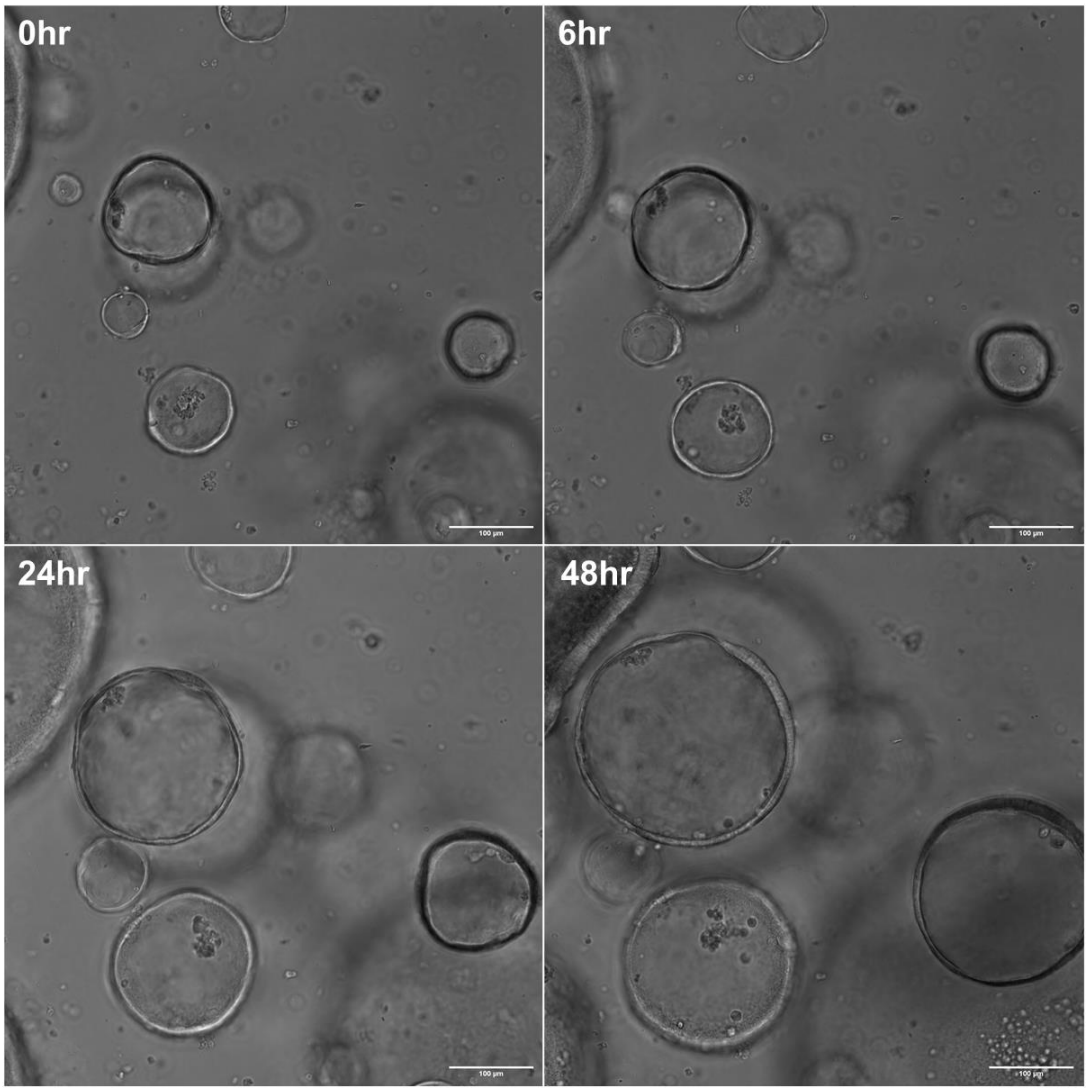

Figure 4.2: Colonoids from *Apc*$^{min/+}$ mice display a cystic morphology. *Apc*$^{min/+}$ colonoids were monitored for 48 hours using confocal microscopy. Colonoids grow to be quite large and display cystic morphology. Confocal images were captured using 10x magnification. Scale bar indicates a distance of 100µm.

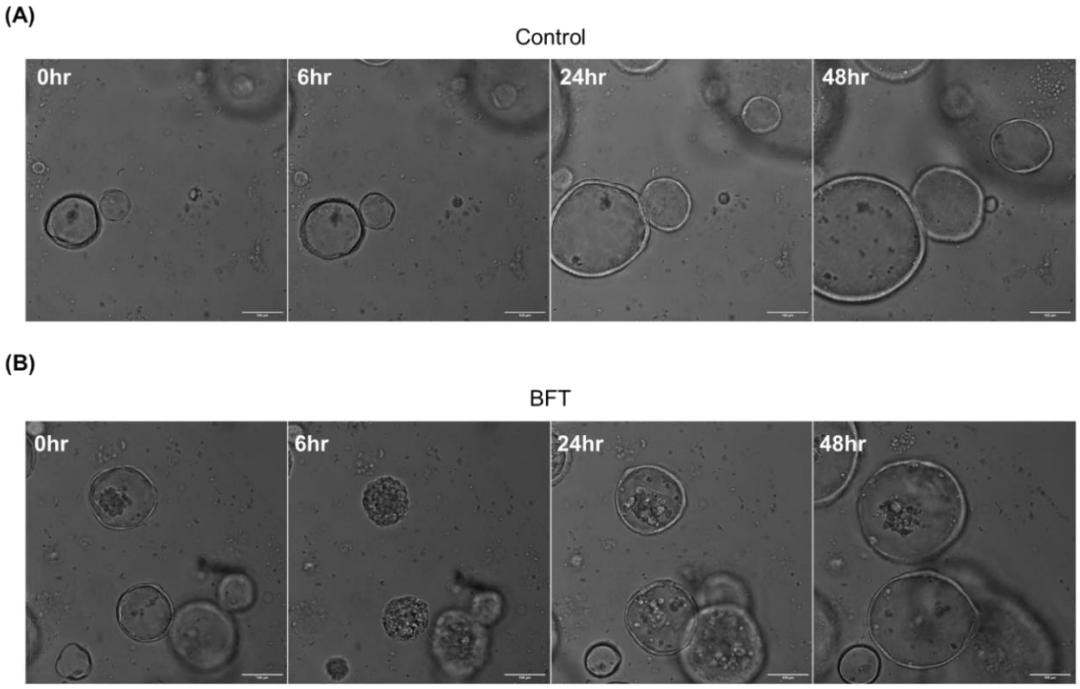

Figure 4.3: Colonoids from *Apc*$^{min/+}$ mice react strongly to BFT, but recover quickly. Colonoids treated with concentrated bacterial culture supernatant from ETBF*Δbft* (Control) (A) display no overt morphology changes in response to treatment. Colonoids treated with BFT undergo dramatic swelling and bubbling by six hours before returning to normal morphology by 24 hours (B). Control represents concentrated bacterial culture supernatant from ETBF*Δbft* and BFT represents concentrated bacterial culture supernatant from ETBF. Confocal images were captured using 10x magnification. Scale bar indicates a distance of 100µm.

One of the most striking differences between the BFT responses in *Apc*$^{min/+}$ and normal (C57BL/6J) colonoids was how quickly they returned to normal morphology. The *Apc*$^{min/+}$ colonoids recovered much faster, with near normal morphology after just 24 hours. In contrast, the majority of normal colonoids, which we investigated in chapter 3, treated with BFT still showed irregular morphologies 48 hours after treatment (Figure 3.5C).

Once we confirmed that BFT was still displaying activity on *Apc*$^{min/+}$ colonoids, we shifted our focus to the impact on sphingolipid metabolism. *Apc*$^{min/+}$ colonoids were treated for six hours with ETBF*Δbft* or ETBF concentrated bacterial culture supernatants, after which media was changed, and fresh growth medium was added for 18 hours. At 24 hours post-treatment, colonoids were collected and sphingolipids were extracted. Although glucosylceramide levels were high in both treatments, BFT did not further alter glucosylceramide levels when compared with control (Figure 4.4A). Consistent with our previous findings in normal colonoids, *Apc*$^{min/+}$ colonoids did not show altered levels of ceramide (Figure 4.4B) or sphingomyelin (Figure 4.4C) in response to BFT. We also measured mRNA expression of GCS and found that BFT increased GCS expression at three and six hours after treatment (Figure 4.4D).

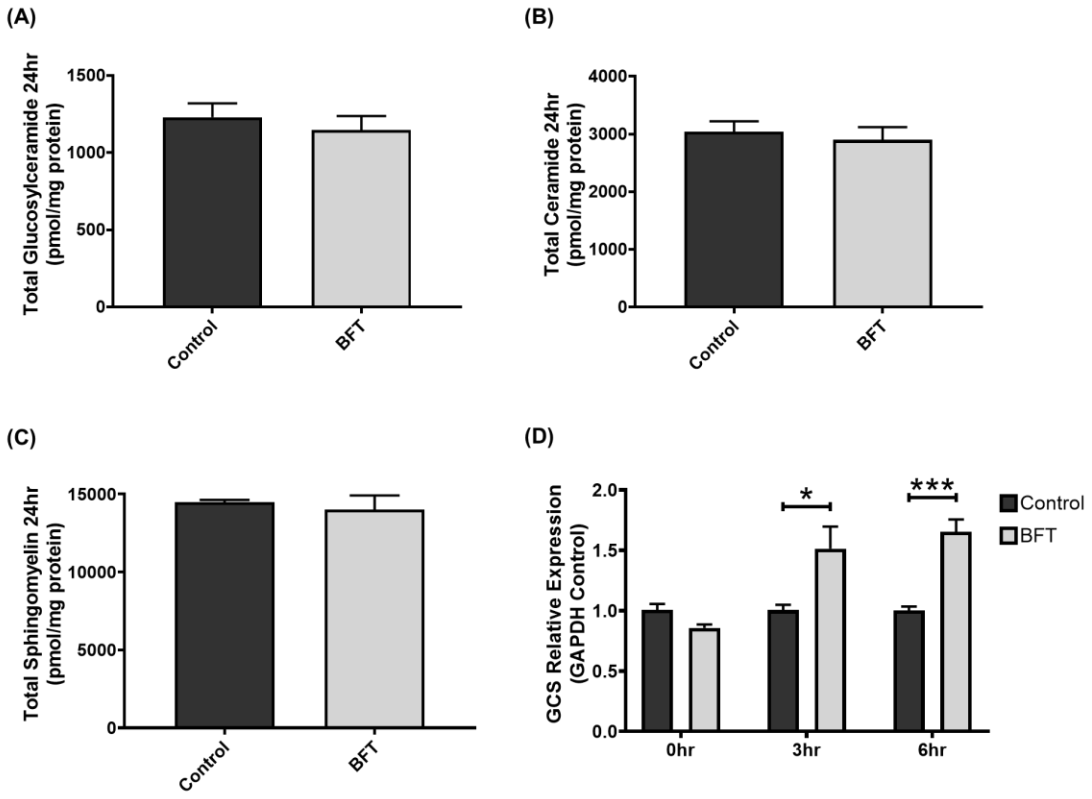

Figure 4.4: BFT does not alter sphingolipid levels in *Apc*$^{min/+}$ colonoids, but does increase GCS expression. Mass spectrometry analysis of *Apc*$^{min/+}$ colonoids treated with BFT did not change glucosylceramide (A), ceramide (B), or sphingomyelin (C) levels at 24 hours. GCS expression increased at three and six hours after BFT addition in *Apc*$^{min/+}$ colonoids (D). Single comparisons were made using an unpaired t-test. Statistical significance is indicated by asterisks: * ($p<0.05$) or *** ($p<0.001$). Control represents concentrated bacterial culture supernatant from ETBF*Δbft* and BFT represents concentrated bacterial culture supernatant from ETBF.

Based on our previous finding that glucosylceramide levels were increased in CECs after BFT exposure, it was surprising then that we did not observe increases in HT29/C1 cells or in colonoids generated from *Apc*$^{min/+}$ mice. One possibility is the conversion of glucosylceramide into higher-order glycosphingolipids. We will expand on the glycosphingolipid pathway in Chapter 5.2.2, but briefly, additional sugar molecules may be added to glucosylceramide to generate additional glycosphingolipids.

Glycosphingolipids have a wide variety of functions in healthy cells, but also in the progression of cancer. Measuring glycosphingolipids in cells requires different sphingolipid extraction protocols than those that we use for the main sphingolipids (ceramide/sphingomyelin/sphingosine/glucosylceramide), so measurement of these molecules will require additional optimization and testing before we're able to determine if glucosylceramide is being modified further in cancer cells.

Another explanation for this is that sphingolipid metabolism in cancer cells is notoriously dysregulated, and some genes, such as GCS, are overexpressed already.[36,38,50,122–126] Therefore, any stimulation of the pathway might not result in observable changes in lipid mass. In HT29/C1 cells, GCS expression did not change, suggesting that BFT activity on these cells does not activate the protective mechanisms involving glucosylceramide that we showed in normal cells. However, in *Apc*$^{min/+}$ derived colonoids, even though we did not see lipid changes in glucosylceramide, we did see increased expression of GCS in response to BFT. HT29/C1 cells and our *Apc*$^{min/+}$ derived colonoids are at different steps in cancer progression, with HT29/C1 cells representing late stage adenocarcinoma, while *Apc*$^{min/+}$ derived colonoids were likely early stage adenomas. Normal cells and early stage tumors may still rely on glucosylceramide to respond to BFT damage, while late stage tumors might be more resistant to this damage, but further studies will be necessary to confirm this hypothesis.

4.3: *Bacteroides fragilis* Toxin Stimulates Colon Epithelial Cells to Release Extracellular Vesicles Containing Glucosylceramide

4.3.1: Abstract

Extracellular vesicles (EVs) are small molecules released from cells across the body that are involved in cell-to-cell communication and the export of materials from cells. EVs include exosomes and microvesicles (MVs), which form using different pathways and have different size ranges. Independent of our studies in cancer cells, we discovered that BFT treatment of CECs promotes the production of EVs in the blood of C57BL/6J mice, and in the media of colonoids established from C57BL/6J mice. EVs isolated from BFT-treated samples displayed high levels of glucosylceramide and phosphatidylserine, a lipid frequently expressed on MVs. EVs generated from BFT-treated colonoids formed a unique cluster in the 300-500nm size range, a size consistent with MVs, but not exosomes. Further studies will be necessary to confirm the contents and functions of EVs produced in response to BFT, but we show for the first time here that BFT causes CECs to produce EVs.

4.3.2: Introduction

Our research has shown that ETBF, through production of BFT, causes levels of glucosylceramide to increase in colon epithelial cells. While this was a novel finding, this was not the first study to show that ETBF could influence host sphingolipid metabolism. Previously, another study found that ETBF would cause cells to produce “exosome-like”

particles which contained the signaling sphingolipid, S1P.[160] The authors suggested that the S1P contained within these particles was important for Th17 cell proliferation and recruitment, which is critical for ETBF-induced tumorigenesis.[92,160]

Extracellular vesicles (EVs) are lipid-containing particles released by cells that are involved in intercellular communication.[179] Exosomes and microvesicles (MVs) are the two major EVs produced by cells, where exosomes arise from the endosomal pathway and MVs form from plasma membrane blebbing.[180] The function of EVs has not been fully established at this point, but researchers have shown these particles play important roles in the development of many diseases, but most studies have focused on their role in cancer.[181,182] Membrane lipids, including sphingolipids, are an integral part of EV formation and release from cells. Sphingomyelin and ceramide are enriched in EV membranes, but other sphingolipids such as glucosylceramide may also be present.[183–185] Herein, we measured sphingolipids in the blood of mice colonized with ETBF and in the media of colonoids treated with BFT and found significant increases in glucosylceramide in both extracts. Further, isolation of EVs from colonoids treated with BFT contained high levels of glucosylceramide, highlighting an additional role for glucosylceramide in the cellular response to BFT.

4.3.3: Results and Discussion

BFT Increases Extracellular Glucosylceramide Levels in Mice and Colonoids

Because S1P is released extracellularly, we measured sphingolipids in the blood of mice colonized with PBS (sham control), ETBF*Δbft*, or ETBF for 1 week. We did not observe changes in S1P across our treatments (Figure 4.5A), but we did observe a significant increase in glucosylceramide (Figure 4.5B).

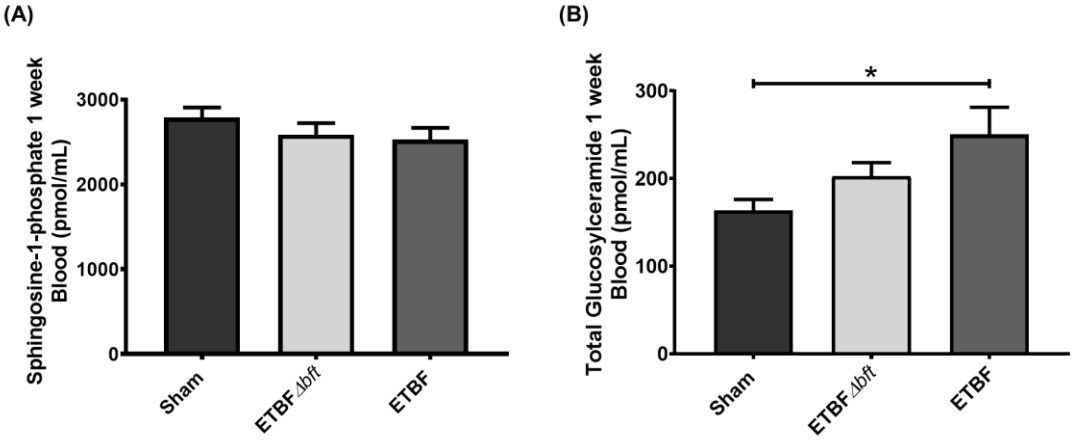

Figure 4.5: C57BL/6J mice colonized with ETBF for one week have increased glucosylceramide circulating in the blood. Colonization with C57BL/6J mice for one week with ETBF does not change sphingosine-1-phosphate (S1P) levels in the blood (A). ETBF increased glucosylceramide levels in the blood when compared with the sham (PBS) control (B). Group comparisons were performed using a one-way ANOVA and Tukey's multiple comparisons test. Statistical significance is indicated by asterisks: * ($p<0.05$). Error bars represent the standard deviation of the mean. Sham represents a PBS control.

Next, we treated colonoids with concentrated bacterial culture supernatants from ETBF*Δbft* and ETBF strains (herein referred to as control or BFT, respectively) and collected media at two or four hours after treatment. Sphingolipids were extracted from the media and, consistent with our *in vivo* results, S1P levels did not change at

either time point (Figure 4.6A), while BFT caused a significant increase in glucosylceramide that increased over time (Figure 4.6B). To determine if glucosylceramide levels in the media were increased over a longer period of time, we treated colonoids for six hours and collected the media. After collecting the media, colonoids received fresh growth medium for 18 hours, and then the media was collected again (24 hours after the initial treatment). Glucosylceramide levels were significantly increased in the six-hour BFT treatment when compared to the control (Figure 4.7A). However, by 24 hours, the increase was no longer statistically significant (Figure 4.7B). To exclude the possibility that the concentrated bacterial culture supernatants were the source of glucosylceramide, we treated colonoids with purified BFT2 and collected media at six and 24 hours after treatment. Glucosylceramide levels were significantly increased at six (Figure 4.7C) and 24 hours (Figure 4.7D) after treatment, confirming that our results were due to the presence of BFT, and not glucosylceramide present in the concentrated bacterial culture supernatants.

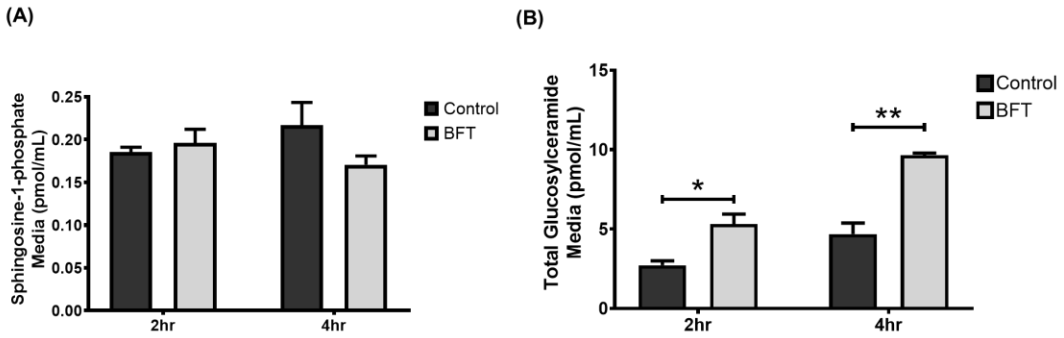

Figure 4.6: Colonoid treatment with BFT increases glucosylceramide levels in the media at early time points. Colonoids treated with BFT for two or four hours did not increase S1P levels in the media at either time point (A). BFT treatment significantly increased glucosylceramide in the colonoid media at two and four hours (B). Single comparisons were made using an unpaired t-test. Statistical significance is indicated by asterisks: * ($p<0.05$) or ** ($p<0.01$). Error bars represent the standard deviation of the mean. Control represents concentrated bacterial culture supernatant from ETBF*Δbft*, BFT represents concentrated bacterial culture supernatant from ETBF.

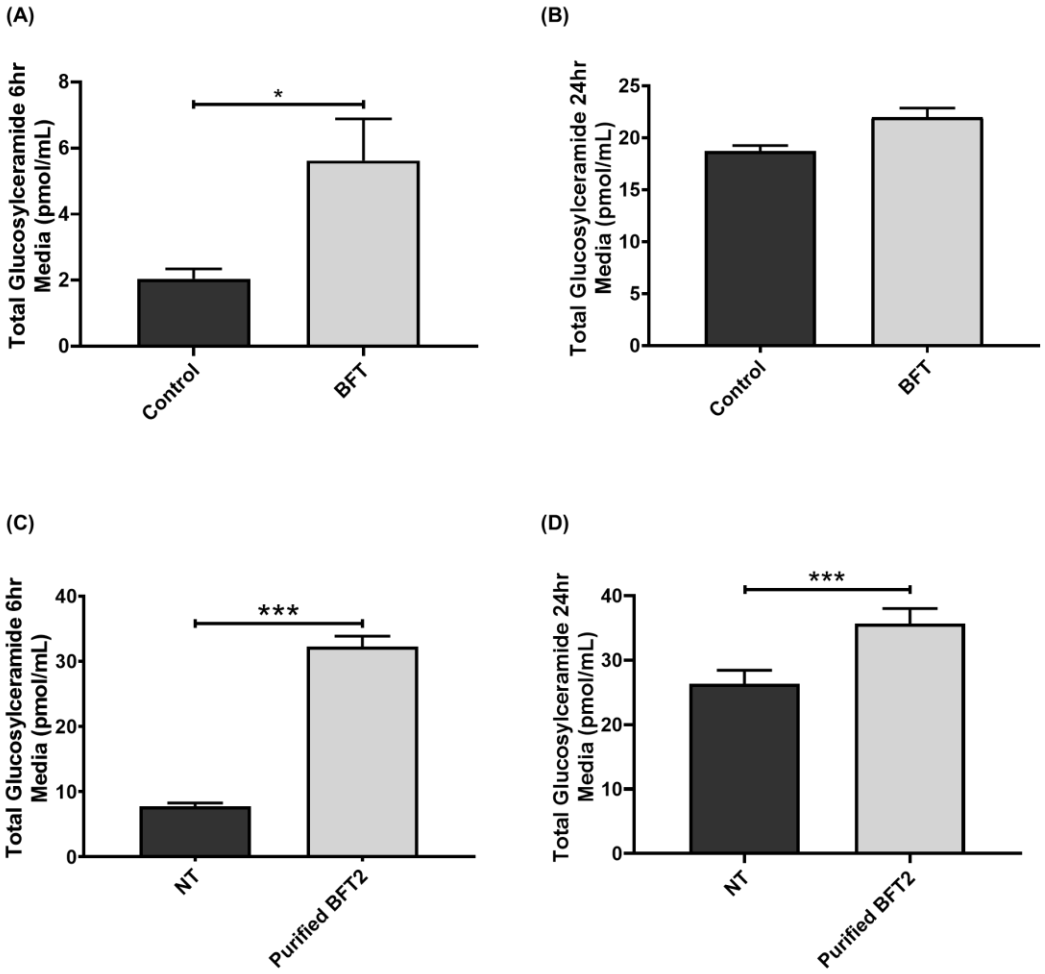

Figure 4.7: BFT, and purified BFT2, treatment of colonoids increases glucosylceramide levels in the media. Colonoids treated with BFT for six or 24 hours have significantly increased glucosylceramide levels in the media at six hours (A), but not 24 hours (B). Addition of purified *Bacteroides fragilis* toxin (Purified BFT2, isolated from ETBF strain 86-5443-2-2, see Materials and Methods for details) to colonoids significantly increases glucosylceramide release into the media at six (C) and 24 hours (D). Single comparisons were made using an unpaired t-test. Statistical significance is indicated by asterisks: * ($p<0.05$) or *** ($p<0.001$). Error bars represent the standard deviation of the mean. NT indicates no treatment was added. Control represents concentrated bacterial culture supernatant from ETBF*Δbft*, BFT represents concentrated bacterial culture supernatant from ETBF, and Purified BFT2 represents purified BFT from ETBF strain 86-5443-2-2 (see Materials and Methods).

Glucosylceramide is Released from Colonoids in Extracellular Vesicles after BFT Treatment

Because glucosylceramide is a membrane sphingolipid, we hypothesized that it would likely be contained within extracellular vesicles (EVs) in the blood and media. Colonoids were treated for six hours with ETBF*Δbft* or ETBF concentrated bacterial culture supernatants, media was collected, and EVs were isolated using ultracentrifugation based on a previously published protocol.[186] After isolation, dynamic light scattering was used to measure the size(s) of the resulting particles. We discovered that media from both treatments contained EVs (Figure 4.8A/B), with a size range consistent with microvesicles (MVs), a subset of EVs 100-1000nm in diameter that are produced by budding of the plasma membrane.[182,186] Interestingly, the number of particles was not too dissimilar between our two treatments, but BFT-treated CECs produced more EVs in the 300-500nm size range. Further studies are necessary to determine if the contents of EVs from each prep are different from one another.

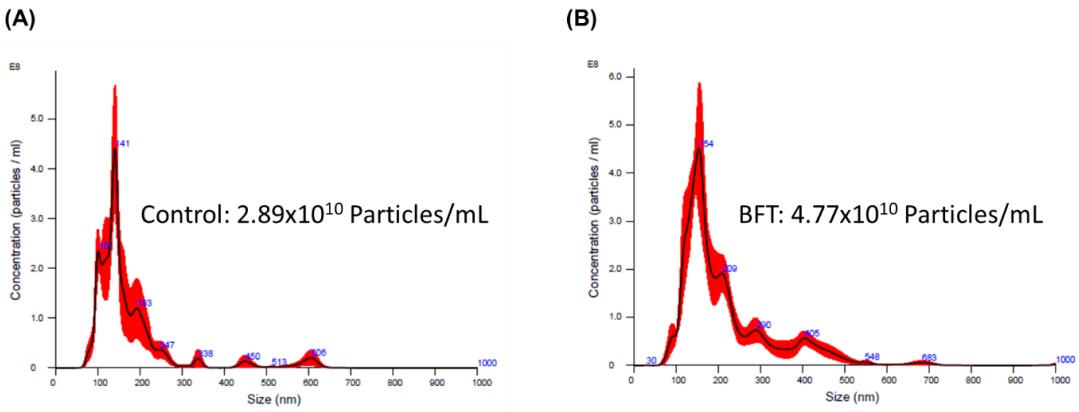

Figure 4.8: Treatment of colonoids with concentrated bacterial culture supernatants stimulates the release of extracellular vesicles from colonoids. Media from colonoids was evaluated using dynamic light scattering to determine the presence, size, and concentration of particles in the media. Concentrated bacterial supernatant from ETBF*Δbft* (Control) treated colonoids have extracellular vesicles (EVs) in the media (A). BFT treated colonoids also release EVs into the media, but there is a higher concentration of 300-500nm particles when compared to control (B). Control represents concentrated bacterial culture supernatant from ETBF*Δbft*, BFT represents concentrated bacterial culture supernatant from ETBF.

Once EVs were isolated, we measured the sphingolipids using mass spectrometry and found that EVs from BFT-treated colonoids contained significantly higher levels of glucosylceramide when compared to control (Figure 4.9A). Sphingomyelin, another membrane sphingolipid that can be associated with EVs,[187] was unaltered by BFT (Figure 4.9B). We also measured phosphatidylserine (PS), which is used as a marker for EVs,[188] and found that BFT significantly increased its presence (Figure 4.9C). Taken together, our data suggests that BFT causes CECs to produce EVs, and that these EVs contain high levels of glucosylceramide and phosphatidylserine.

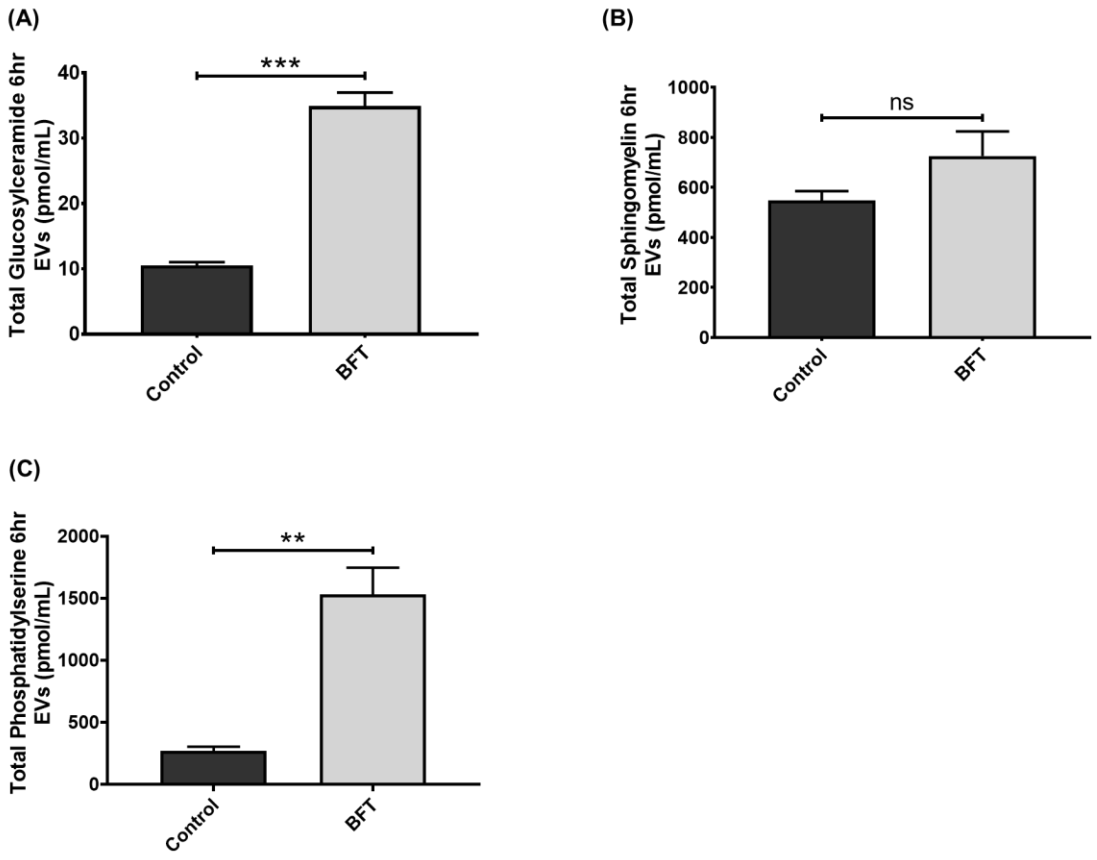

Figure 4.9: Extracellular vesicles from BFT-treated colonoids contain glucosylceramide and phosphatidylserine. EVs were purified from colonoid media and lipids were extracted. EVs from BFT treated colonoids had significantly higher levels of glucosylceramide (A), while sphingomyelin levels were not significantly different than control EVs (B). Phosphatidylserine levels were significantly higher in BFT colonoids (C). Error bars represent the standard deviation of the mean. Single comparisons were made using an unpaired t-test. Statistical significance is indicated by asterisks: ** ($p<0.01$) or *** ($p<0.001$). NS indicates non-significant results. Control represents concentrated bacterial culture supernatant from ETBF*Δbft* and BFT represents concentrated bacterial culture supernatant from ETBF.

Further studies are necessary to determine the role of glucosylceramide in EVs. Based on the size of the particles that we collected, we believe that the EVs were likely comprised of MVs and not exosomes. Since MVs are formed from the plasma membrane, the primary location for glucosylceramide in CECs,[51] increased

glucosylceramide levels in EVs may just be a reflection of the lipid profile of the membrane after BFT challenge. While a previous study reported S1P in BFT-induced EVs,[160] we were unable to replicate this finding. Despite this, it is possible that EVs without S1P may still recruit immune cells that could contribute to BFT tumorigenesis, but this will need to be confirmed experimentally. One major difference between our studies is that the Deng *et al.* study used EVs generated from a colon cancer cell line, raising questions about EV profile variability from normal versus cancerous cells. In support of this theory, other researchers have shown unique signaling roles for EVs generated by cancer cells, such as the initiation of metastasis,[179,181–183] further supporting differential roles of EVs in the progression of disease. Still, BFT-induced release of glucosylceramide within EVs is a novel finding that could have significant implications for cell-to-cell signaling, repair, and immune recruitment in host pathogen response. Although BFT did not increase glucosylceramide levels in cancer cells, our finding that BFT treatment increased glucosylceramide levels in EVs presents a new area to investigate, especially since EVs are frequently produced by cancer cells.

Chapter 5: Discussion

5.1: Summary of Results

In this study, we have demonstrated that glucosylceramide is a critically important regulator of epithelial barrier integrity in the colon during bacterial challenge. In order to achieve this, we used colonoids, a unique cell culture system that allowed us to interrogate the role of glucosylceramide in normal epithelial cells after exposure to *Bacteroides fragilis* toxin (BFT). Mice colonized with Enterotoxigenic *Bacteroides fragilis* (ETBF) had higher levels of glucosylceramide in the distal colon. Using a genetically-modified ETBF strain with the BFT gene knocked out (ETBF*Δbft*), we determined that the increase in glucosylceramide was dependent on the presence of BFT. We further confirmed these results in colonoids, using concentrated bacterial culture supernatants from ETBF and ETBF*Δbft* strains, as well as purified BFT.

After we established that glucosylceramide levels were increased in colonoids in response to BFT, we focused on why glucosylceramide was increasing in CECs. Using an inhibitor of glucosylceramide synthase (GCS), the enzyme responsible for generating glucosylceramide from ceramide, we found that GCS inhibition in the presence of BFT cause colonoids to burst. Because a loss of glucosylceramide caused colonoids to burst, we hypothesized that increasing glucosylceramide in cells would protect them from BFT-induced damage. Indeed, using an inhibitor of glucocerebrosidase, the enzyme responsible for breaking down glucosylceramide into ceramide, we increased levels of

glucosylceramide in colonoids and found that colonoids no longer burst with the GCS inhibitor (ibiglustat) and BFT.

We initially focused on apoptosis as a potential explanation for colonoid bursting events. However, we found that while BFT and ibiglustat did increase apoptosis, it did so in normal colonoids and colonoids treated with conduritol B epoxide (CBE), our GBA inhibitor. Because apoptosis alone couldn't explain our bursting events, we next focused on the main adherens junction protein, E-cadherin, which is known to be cleaved in CECs treated with BFT. Again, we saw cleavage, but results were similar in our normal and CBE colonoids. In addition to adherens junctions, tight junctions also play an important role in cell-to-cell adhesion and paracellular permeability. Tight junctions are the most apical of all of the junctional domains, so we questioned whether BFT and ibiglustat were triggering a loss of tight junction proteins. We found that tight junction protein 1 (TJP1), an important cytoplasmic mediator of tight junctions, was decreased in response to BFT and ibiglustat, but that this decrease did not occur in CBE treated colonoids. Other tight junction proteins, such as claudin-3 and occludin were measured, but were not altered in response to our treatments.

Based on our findings, we proposed a model by which BFT cleaves E-cadherin, increasing paracellular permeability. Tight junction proteins are able to maintain barrier integrity until E-cadherin expression returns, allowing cells to survive the BFT challenge. However, in the absence of glucosylceramide, TJP1 levels decrease and the second line

of defense, the tight junctions, are no longer able to maintain the epithelial barrier and colonoids burst open. By using CBE to increase levels of glucosylceramide within colonoids, TJP1 levels are stabilized throughout BFT-induced stress, and colonoids eventually return to normal morphology. Therefore, glucosylceramide serves to protect CECs exposed to BFT by stabilizing tight junction proteins.

In addition to our finding that glucosylceramide is increased in CECs, we also discovered that BFT stimulates the release of glucosylceramide from CECs in extracellular vesicles (EVs). Although the role of these EVs, as well as the importance of glucosylceramide within them, is unknown, this is a unique finding that we think could be important for cell-to-cell communication in response to pathogen-induced epithelial damage. Follow-up studies will be able to build upon our findings and determine the precise role(s) for glucosylceramide in the epithelium, and beyond, such as in EVs. In the following section, I detail some of the directions that I think are important for future researchers to consider, as well as present some additional data that highlights novel findings that did not fit in our original story.

5.2: Discussion and Future Directions

5.2.1: The Importance of Tight Junctions and Glucosylceramide in the Colon

The maintenance of the epithelial barrier might be the most important factor in determining the likelihood of developing BFT-induced disease. The feedback loop of

increased epithelial barrier permeability, followed by inflammation that further increases permeability, is a driver of both IBD and CRC.[51,99,100] A large number of tight junction proteins and adherens junction proteins are involved in maintaining the epithelial barrier. In Chapter 3, we focused mainly on E-cadherin, claudin-3, occludin, and TJP1. These targets were based on previous studies showing BFT-induced effects (E-cadherin cleavage and TJP1 localization changes)[147] or increased expression in the distal colon (claudin-3, occludin).[18] While mRNA expression changes do not always correlate with protein changes, we measured mRNA expression in colonoids treated with ETBF*Δbft* or ETBF concentrated bacterial culture supernatants for six hours to narrow down potential targets for further characterization in the BFT response. The results can be found in Figure 5.1, but briefly, TJP1, F11R/JAM, occludin, claudin-3, claudin-7, and claudin-12 all showed increased mRNA expression when colonoids were treated with BFT. Only one protein decreased its expression after BFT treatment, claudin-15. Interestingly, decreased claudin-15 expression is seen in colorectal cancer.[189]

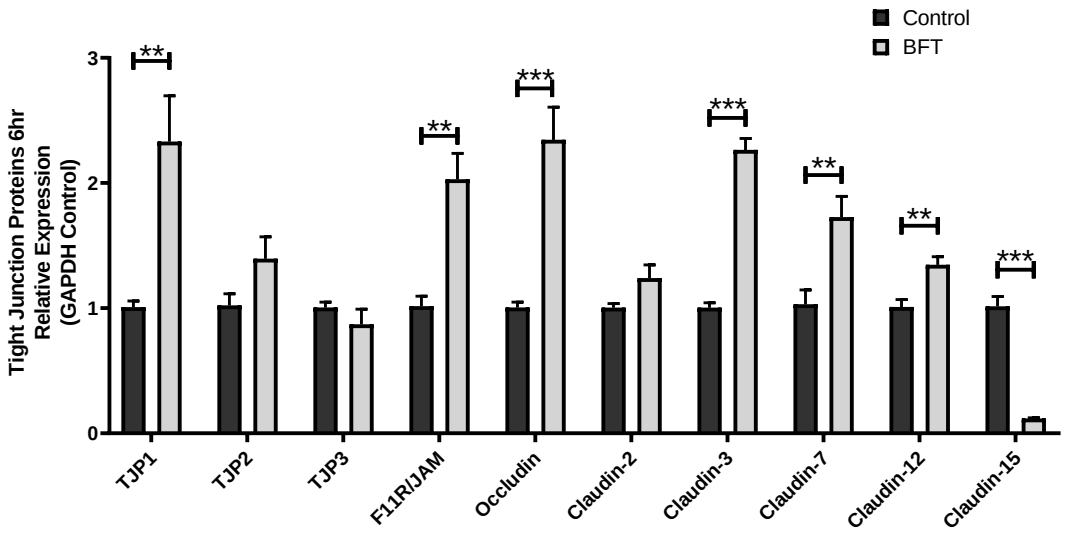

Figure 5.1: BFT alters mRNA expression of a number of tight junction proteins. Colonoids treated with concentrated bacterial culture supernatant from ETBF*Δbft* (Control) or ETBF (BFT) for six hours were collected to measure mRNA expression of major tight junction proteins. TJP1, F11R/JAM, occludin, claudin-3, cluadin-7, and claudin-12 all had significantly increased expression, while claudin-15 had significantly reduced expression. Error bars represent the standard deviation of the mean. Single comparisons were made using an unpaired t-test. Statistical significance is indicated by asterisks: ** ($p<0.01$) or *** ($p<0.001$). Control represents concentrated bacterial culture supernatant from ETBF*Δbft*, BFT represents concentrated bacterial culture supernatant from ETBF.

Based on these results, we performed western blots for claudin-3, occludin, and TJP1. The western blots and quantified data for these proteins are shown in Chapter 3 Figure 3.10. Although mRNA expression levels of claudin-3 and occludin were increased by BFT (Figure 5.1), protein levels did not reflect this increase. One possible explanation for this discrepancy is that the production and breakdown of the protein are in equilibrium during the dramatic morphology changes that occur in colonoids treated with BFT, highlighted by dramatic swelling and reorganization of the epithelial barrier.

A similar trend was also seen in TJP1, but, when GCS activity was inhibited by ibiglustat, TJP1 protein levels significantly decreased (Figure 3.10E,I). However, when a GBA inhibitor (CBE) was added to the cells, ibiglustat-induced decreases in TJP1 were no longer seen (Figure 3.10E,I). These results suggested that TJP1 was stabilized by glucosylceramide. However, the exact relationship between glucosylceramide and TJP1 is not currently known, and their association has not been documented in the literature. TJP1, glucosylceramide, glycosphingolipids (explained further in the following section), and sphingomyelin can all be found in membrane microdomains (sometimes referred to as lipid rafts).[190,191] We could envision then that disruption of these microdomains by loss of one of the components may weaken the membrane structure and result in destabilization of the membrane. Addition of methyl-β-cyclodextrin (mβCD) to cells depletes levels of membrane cholesterol, an important component of mammalian membranes and membrane microdomains,[192,193] and would allow us to begin to address this hypothesis. Treatment with mβCD can decrease TJP1 levels[194] and also initiate glycosphingolipid release from cells,[195] supporting our theory that these components may be interacting in a membrane microdomain.

While increased colonoid permeability can be measured in colonoids, the impact on disease initiation and progression is more difficult to determine. One of the major drawbacks of colonoids is the lack of all non-epithelial cells that are present in the colon. The lamina propria, the loose connective tissue that forms underneath the epithelium

and contains fibroblasts, lymphocytes, and macrophages, is an important mediator in the regulation of and response to microbial factors in the colon.[196] Bacterial translocation and epithelial barrier breakdown stimulates the release of cytokines by CECs to recruit immune cells to the area.[51,99,100] Methods to co-culture colonoids with immune cells are still extremely new, with initial publications revolving around methods to perform these experiments.[197,198] However, once researchers establish reproducible methods with higher throughput, this would make an excellent model system for studying BFT-induced disease progression. ETBF tumor formation in mice relies on IL-17A signaling by Th17 cells, a component which is missing from normal organoid cultures. In addition, even though STAT3 levels are increased in CECs in mice after ETBF colonization, STAT3 levels in cell cultures are not affected by BFT, highlighting another immune-dependent mechanism.[91]

In the meantime, murine studies will be necessary to determine if, and how, glucosylceramide is involved in inflammatory diseases of the colon. At the beginning of 2020, a global pandemic caused by severe acute respiratory syndrome virus 2 (SARS-Cov-2) led to mass quarantines and business suspensions across the world. One of the unfortunate side effects of this pandemic was the temporary shut-down of research labs around the country. Originally, we had planned to perform a large-scale animal experiment to determine if *Apc*$^{min/+}$ mice colonized with ETBF would still form tumors if they were treated using pharmacological inhibitors of GCS or GBA to reduce, or

increase, levels of glucosylceramide, respectively. Based on the protective effects of glucosylceramide in our models, increased glucosylceramide levels may support cancer cell survival by preventing apoptosis. Alternatively, increased glucosylceramide levels may help maintain the epithelial barrier and prevent ETBF-induced inflammation that promotes the progression of colitis to tumor development. However, regardless of the outcome, this experiment would be an incredibly useful starting point in further defining the role of glucosylceramide in CECs after BFT exposure.

5.2.2: Glycosphingolipids

This study revolved around a specific sphingolipid, glucosylceramide, and explored its function(s) in response to BFT challenge in CECs. While other major sphingolipids, such as ceramide, sphingomyelin, sphingosine, and sphingosine-1-phosphate were measured in all of our studies, there are still a number of sphingolipids that lie beyond these major species. Glycosphingolipids (GSLs) are a large class of sphingolipids that are formed by the attachment of a sugar molecule to ceramide.[164] The two main glycosphingolipids, which serve as the backbone for all other glycosphingolipids, are glucosylceramide and galactosylceramide. Glucosylceramide is formed by addition of a glucose molecule to ceramide by glucosylceramide synthase, while galactosylceramide is formed with galactose instead by galactosylceramide synthase. Galactosylceramide is an important component of the myelin sheath, but may also be expressed in other tissues, where its function is less clear.[161,164] Most studies have focused on its role in the nervous system

after noticing severe neurological defects in galactosylceramide synthase knockout mice.

Galactosylceramide may be modified further to form sulfatide. Sulfatide is abundant in the nervous system, due in large part to the localization of its precursor, galactosylceramide. However, sulfatide is also found in the gastrointestinal tract and is increased in colon cancer cells, correlating with metastatic potential and a worse prognosis for patients.[199–201] Increased sulfatide levels in colon tumors may come at the expense of galactosylceramide, as galactosylceramide levels were decreased.[201] Sulfatide is also a target for pathogenic bacteria, as a number of bacteria are able to bind to sulfatide, which is important for their ability to cause infection.[200] Although no studies have linked mammalian galactosylceramide (explained further in Section 5.2.4), or sulfatide, to *B. fragilis*, we believe that it would be valuable to measure these lipids in response to BFT addition, to definitively confirm that this pathway is not involved in our model.

The GSL pathway beyond glucosylceramide is much more complex than the galactosylceramide pathway, with glucosylceramide serving as the precursor lipid for over 400 additional GSLs.[45,202] Additional sugars, up to twenty, can be added to glucosylceramide to form higher-order GSLs with gangliosides being the most well studied.[202] Gangliosides are distinguished from other GSLs, which may contain similar sugar chains, by the addition of sialic acid. The nomenclature of gangliosides is

incredibly complex, and the IUPAC naming system is frequently ignored in favor of a shorter naming system based on important structural information.[203] We will use the common names for gangliosides from here on. An image adapted from Pasquel-Dávila *et al.* shows the beginning of the ganglioside pathway (Figure 5.2).

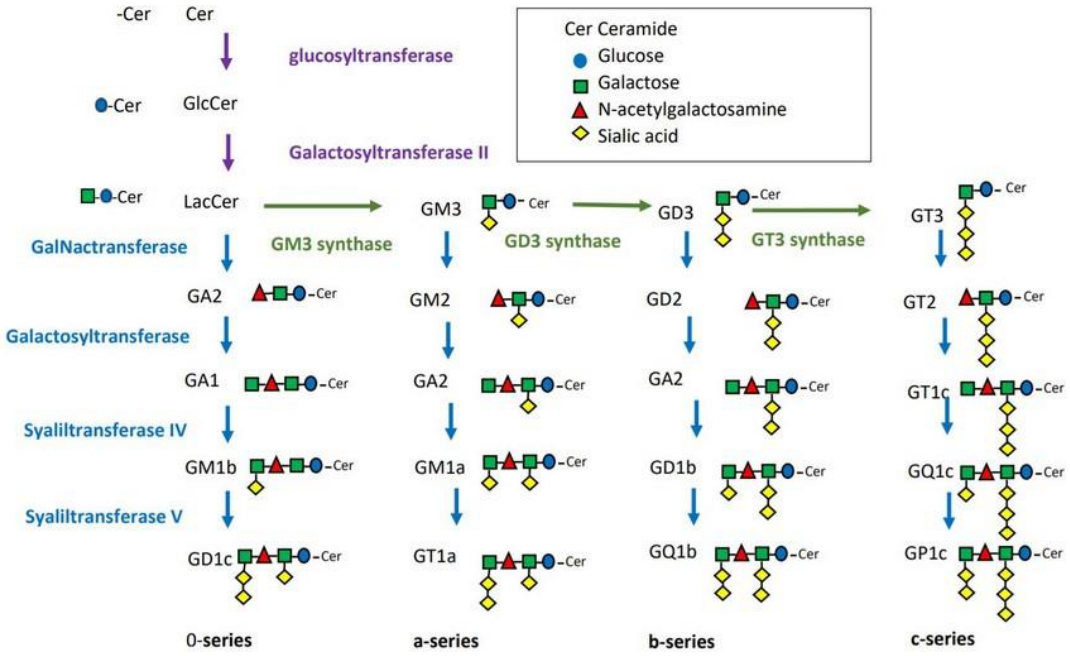

Figure 5.2: A graphical representation of the ganglioside pathway. This image is adapted from Pasquel-Dávila *et al.*[204] and displays the increasing complexity of the ganglioside pathway. GlcCer and glucosyltransferase are referred to as glucosylceramide and glucosylceramide synthase, respectively, within this document.

The primary location for gangliosides is the plasma membrane, where they expose their sugars to the environment.[164,203] Similar to galactosylceramide and sulfatide, gangliosides are highly expressed in the nervous system.[164,165] However, gangliosides can be found throughout the body, and are involved in many important cellular

functions such as proliferation, cell death, and cell-to-cell interactions.[165] Dysregulation of gangliosides is frequently seen in cancer, and, because of their expression on the outer surface of cells, have been used as cancer markers for targeted treamtents.[165,205]

Gangliosides are important for a number of critical functions of the intestine. Similar to the opposing roles of ceramide (pro-apoptotic) and glucosylceramide (pro-survival), many gangliosides have opposing functions. For example, GD3 is reduced in patients with IBD, while GM3 levels increase.[206] GD3, when obtained through the diet, decreases pro-inflammatory signaling in the intestines and protects against inflammation-associated damage.[206,207] In contrast, GM3 is associated with tight junction protein degradation,[207] which would decrease barrier integrity and likely promote inflammation.

Gangliosides can also serve as binding partners for bacterial toxins.[164] Examples include cholera toxin, botulinum toxins, tetanus toxins, and shiga toxin.[164,208,209] Because the binding partner for BFT is unknown, we initially questioned whether gangliosides may serve this purpose. However, morphological alterations, and thus, biological activity, are still observed when GCS activity is blocked, which would prevent the formation of glucosylceramide and the gangliosides beyond it. However, because we know that BFT alters glucosylceramide levels on its own, we hypothesize that BFT would also alter ganglioside production as well. Supporting this idea, we measured mRNA expression of B4Galt6, one of the preceding enzymes to the ganglioside pathway, and found that BFT increased B4Galt6 expression (Figure 5.3).

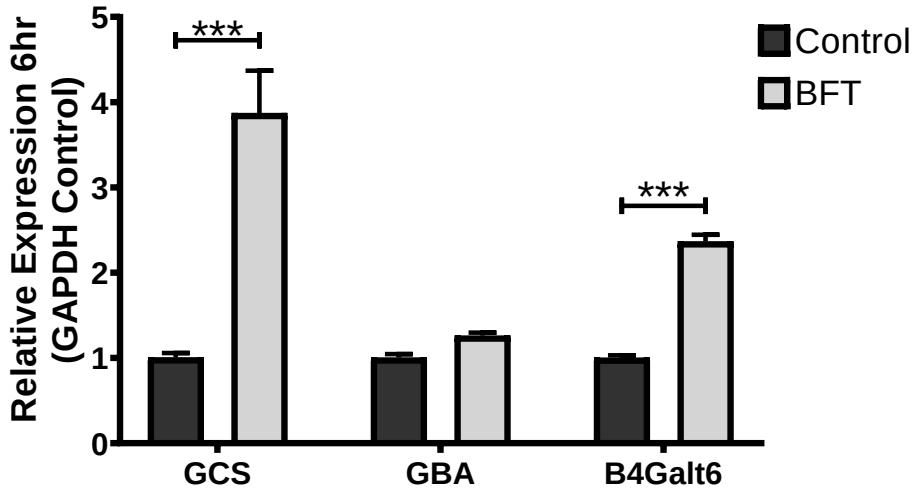

Figure 5.3: BFT increases GCS and B4Galt6 expression in colonoids. Colonoids treated with concentrated bacterial culture supernatant from ETBF*Δbft* (Control) or ETBF (BFT) for six hours were collected to measure mRNA expression of early glycosphingolipid enzymes. GCS and B4Galt6 were both significantly expressed, while GBA expression was not significantly altered when compared with control. Error bars represent the standard deviation of the mean. Single comparisons were made using an unpaired t-test. Statistical significance is indicated by asterisks: *** ($p<0.001$). Control represents concentrated bacterial culture supernatant from ETBF*Δbft*, BFT represents concentrated bacterial culture supernatant from ETBF.

In Chapter 4, we measured sphingolipids in a cancer cell line and colonoids generated from *Apc*$^{min/+}$ mice and found that glucosylceramide levels did not increase in response to BFT. However, in the *Apc*$^{min/+}$ colonoids, we still saw an increase in GCS expression relative to the control treatment (Figure 4.4D). The absence of changes in glucosylceramide levels following BFT treatment could be due to the overall abundance of the lipid, which would mask any minor increases, or it could be due to the conversion to higher order glycosphingolipids, such as gangliosides. Therefore, we propose that future studies measure gangliosides in addition to the more common sphingolipids.

GM3, mentioned above as a pro-inflammatory ganglioside in IBD, is one of the first gangliosides in the pathway, and serves as a precursor for the majority of gangliosides. Using a GM3 synthase knockout mouse model, which we maintain in our lab, we could determine if loss of the majority of gangliosides alters ETBF colonization, ETBF-induced inflammation, or hyperplasia in the colon attributed to ETBF. Using the same mouse model, we could isolate and establish GM3 synthase knockout colonoids, which would allow us to interrogate more specific cell signaling events that occur in response to BFT. The most obvious experiment is a simple morphology experiment to determine if BFT activity is still seen (colonoid swelling and cellular rounding). If the morphological response is still present, this would further support our argument above that BFT is not binding to gangliosides.

Based on the overlapping roles of GSLs and sphingolipids in maintaining the epithelial barrier, including the regulation of inflammatory responses, we believe that GSLs are an important target for future studies with ETBF. Although we do not believe that gangliosides are the elusive BFT receptor, we do believe that they may still play an important role in ETBF pathogenesis.

5.2.3: Extracellular Vesicles

We showed that ETBF, through production of BFT, stimulates the release of extracellular vesicles from CECs (Chapter 4.3). However, the purpose of these EVs still needs to be

determined. Extracellular vesicles are a unique way for cells to export genetic material, proteins, and lipids into the environment or to other cells.[210] Extracellular vesicles are typically grouped into two categories: exosomes and microvesicles. Exosomes are smaller in size than microvesicles, with a typical diameter of around 30-100 nm.[211] Microvesicles are larger, with sizes that can approach 1-2µm.[183] Based on the size of the particles that we found, we believe that our EVs were predominantly MVs. Further supporting this idea was the enrichment of phosphatidylserine, a lipid frequently found in MVs,[212] in our samples. While the overall number of EVs released after treatment with ETBF*Δbft* or ETBF concentrated bacterial culture supernatants were similar, BFT increased the population of larger EVs, indicated by a higher peak in the 300-500 nm size range (Figure 4.8). The increased size could likely be attributed to differential cargo or membrane composition of EVs exposed to BFT.

Dr. Sears' lab has previously shown that a chemokine gradient forms in response to ETBF colonization of *Apc*$^{min/+}$ mice, with expression increasing from proximal to distal colon.[91] The production of EVs by CECs exposed to BFT after ETBF colonization could facilitate chemokine signaling. Microvesicles can transport chemokine receptors between cells or stimulate the release of chemokines by recipient cells.[211] Because ETBF colonization is higher in the proximal colon,[91] production of EVs by CECs exposed to ETBF in the proximal colon could travel along the colon, exposing downstream CECs in the distal colon to increased numbers of chemokines. This hypothesis could be tested

using inhibitors for EV release, such as Y27632 for MVs and GW4869 for exosomes, and measuring chemokines along the colon.[212] However, due to overlapping molecular mechanisms in the MV and exosome pathways, inhibition of both pathways might be more successful than attempting to target either individually.

Another role for EVs in response to BFT is to package and remove the toxin from the cell. This has previously been shown with other bacterial toxins, where they demonstrated that active toxin was shed in MVs, while inactivated toxin was endocytosed and degraded internally.[213] The precise fate of BFT is not known, although a previous study using fluorescently labeled BFT found localization at the plasma membrane for up to three hours after addition. After three hours, signal was detected intracellularly, suggesting internalization of the toxin. By 24 hours, toxin signaling was greatly reduced in the membrane and intracellularly.[150] The overall loss of BFT signaling by 24 hours correlates with a return to normal morphology that we see in HT29/C1 cells and in colonoids (data not shown; Figure 3.5C). Using a similar experiment, we propose adding fluorescently labeled BFT to colonoids and monitoring BFT localization in two ways. The first is cellular localization within the colonoid. This would allow tracking of internalized BFT if it becomes endocytosed. The second is to collect the growth medium from the samples at different time intervals, purify EVs from the medium, and then monitor fluorescence in the EV fraction and in the remaining media after purification. If BFT is being removed from cells in EVs, signal would be expected in the EV fraction and

not in the media. To strengthen these findings, a western blot using an anti-BFT antibody would confirm BFT presence in EVs. If EVs are indeed involved in removing BFT from cells, inhibition of exosome and/or MV release from cells would theoretically lead to a build-up of intracellular BFT, either in the cytosol or in the membrane. Finally, the importance of glucosylceramide throughout this process could be evaluated using GCS inhibitors to decrease the glucosylceramide levels within the cells.

As mentioned briefly in Chapter 4.3, one study found that ETBF treatment of colon cancer cells promoted the production and release of EVs containing S1P. These EVs also contained CCL20 and PGE2, which were involved in Th17 cell recruitment and expansion.[160] Although we did not observe S1P increases in the blood of ETBF colonized C57BL/6J mice, or in the media of colonoids treated with BFT, their model was focused on EVs generated by cancer cells. EVs are frequently used by cancer cells to control and modulate their environment,[180,181,187,210] so it would not be surprising if the contents from their EVs were different than ours that were generated from normal mice. Using *Apc*$^{min/+}$ colonoids would allow us to compare EVs generated from normal mice and those generated from a pre-cancer/early cancer mouse model. Observed differences between the two populations could potentially allow EVs to serve as cancer biomarkers. One hypothesis would be that glucosylceramide levels are increased in EVs generated by healthy tissue after BFT treatment, while an increase in S1P could signify cancer EVs.

5.2.4: Bacterial Sphingolipids

When this project began, we used very crude bacterial culture supernatants to determine if the media from ETBF strains, which contained BFT, would alter sphingolipid metabolism in CECs. Before we switched to a more concentrated bacterial culture supernatant, we discovered that the bacterial media was introducing an odd-chain length (17-19 carbon) sphingolipid to our cells (Figure 5.4). This odd-chain length is not produced naturally by mammalian cells, indicating that the sphingolipid was coming from the bacteria or the bacterial media. When we examined the bacterial media alone, we did not detect the odd-chain length sphingolipids, indicating that the source was the bacteria (data not shown).

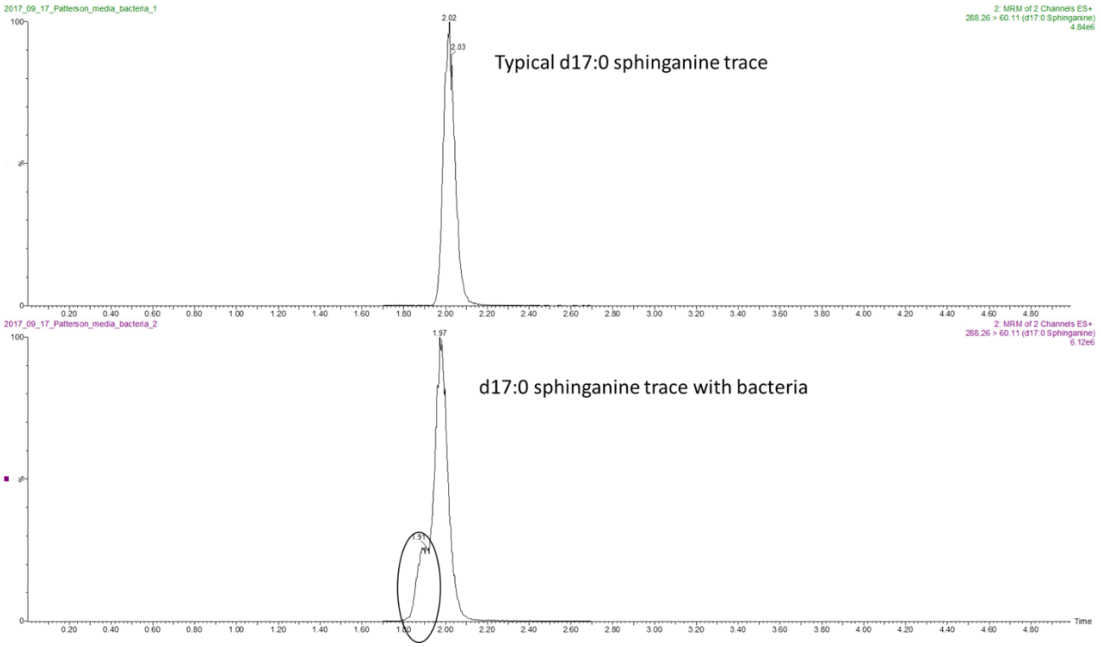

Figure 5.4: Mass spectrum of HT29/C1 cells treated with bacterial cultured media shows a unique peak in the internal standard. HT29/C1 cells were collected and sphingolipids were extracted. A shoulder was detected on the d17:0 sphinganine peak from the internal standard controls, indicating the presence of an additional sphingolipid.

A literature search revealed that *B*. *fragilis* is one of a select group of bacteria that are able to produce its own sphingolipids. Other *Bacteroides* species can also produce sphingolipids, indicating that this is not specific to *B. fragilis*, but the sphingolipids produced by each member may still differ.[214] In 2013, researchers discovered that *B. fragilis* produces α-galactosylceramide, a sphingolipid previously only known to be produced by a sponge.[169] This lipid is an agonist for iNKT cells, allowing the bacteria to communicate directly with the host immune system.[167,169] The researchers that discovered α-galactosylceramide also found that *B. fragilis* produced dihydrosphingosine, dihydroceramide, and ceramide phosphorylethanolamine.

Interestingly, they noted the presence of a homologous protein to mammalian sphingosine kinase, the enzyme responsible for adding a phosphate to sphingosine to form sphingosine-1-phosphate. However, when they attempted to knock out this gene, they were unsuccessful.[169] In our samples, we saw dihydrosphingosine (Figure 5.5), dihydroceramide (Figure 5.6), and dihydrohexosylceramide (likely α-galactosylceramide; Figure 5.7).

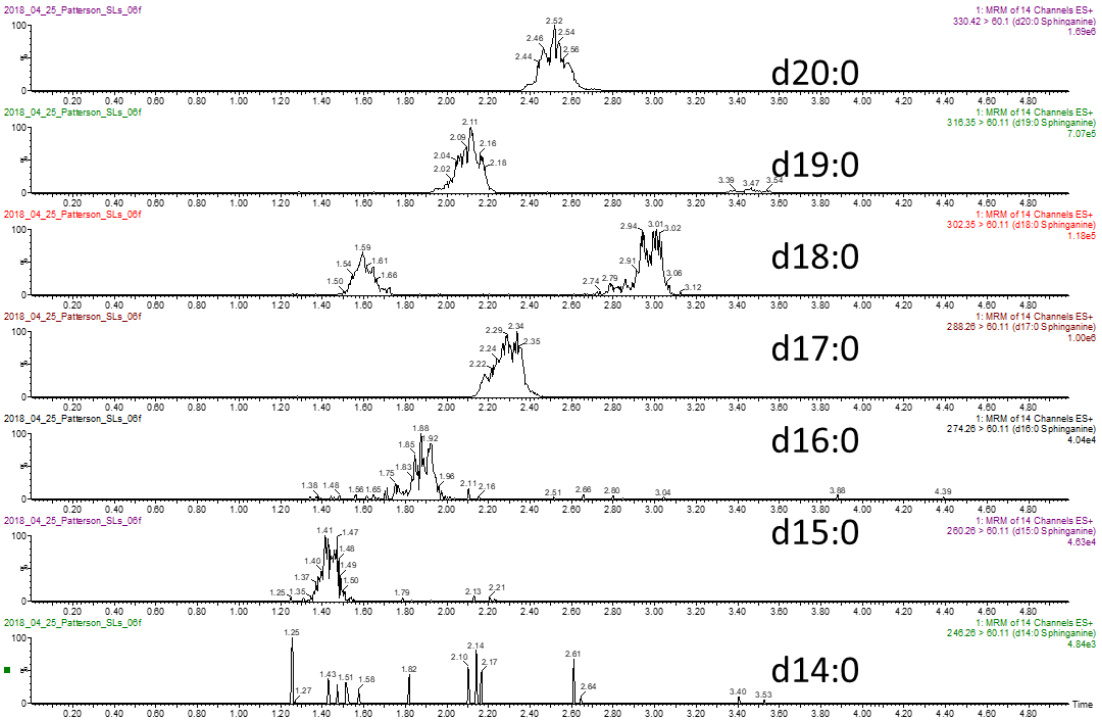

Figure 5.5: ETBF produces dihydrosphingosine. Mass spectrum of ETBF displaying the presence of dihydrosphingosine with varying chain lengths, with d17:0 being the most abundant.

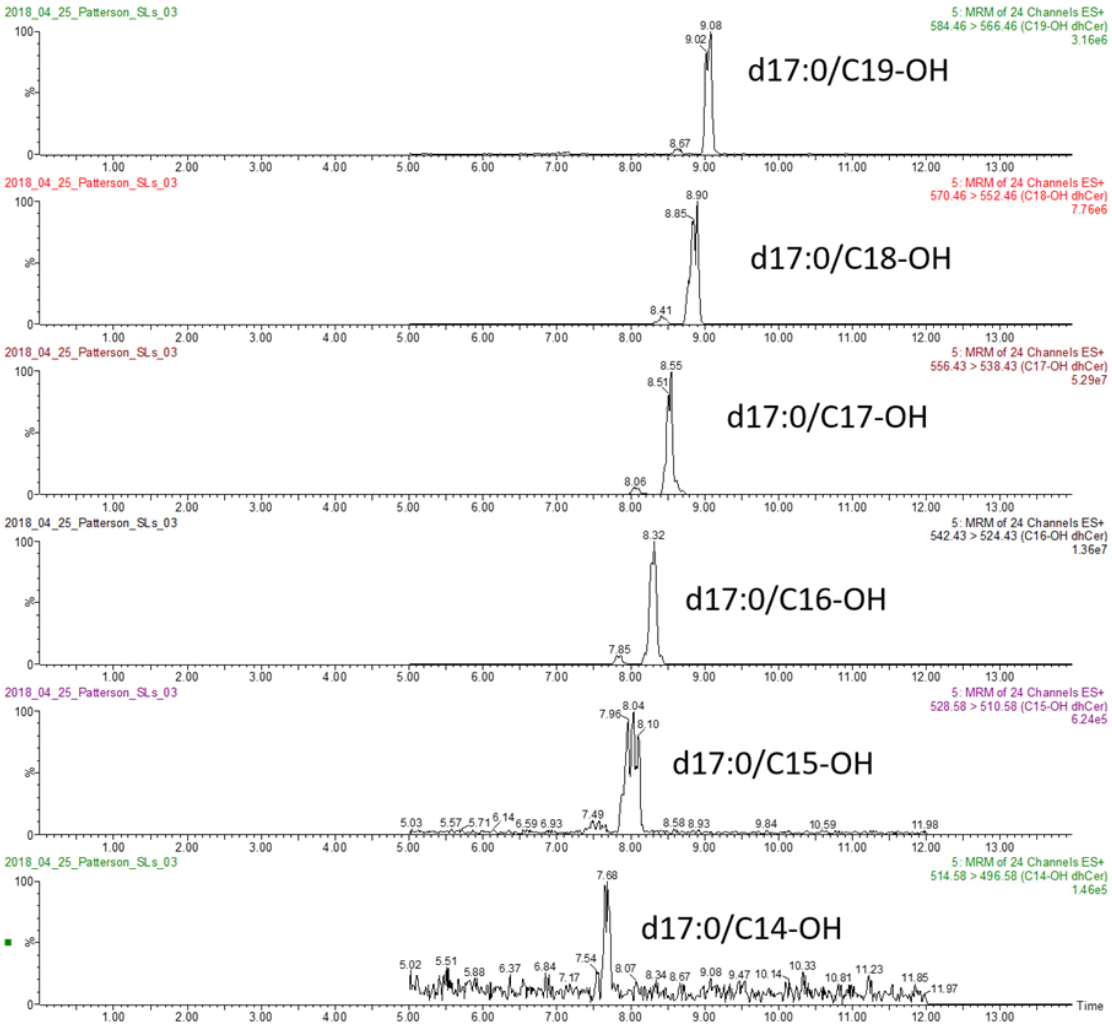

Figure 5.6: ETBF produces dihydroceramide. Mass spectrum of ETBF displaying the presence of dihydrosphingosine with varying chain lengths, with d17:0/C17-OH being the most abundant.

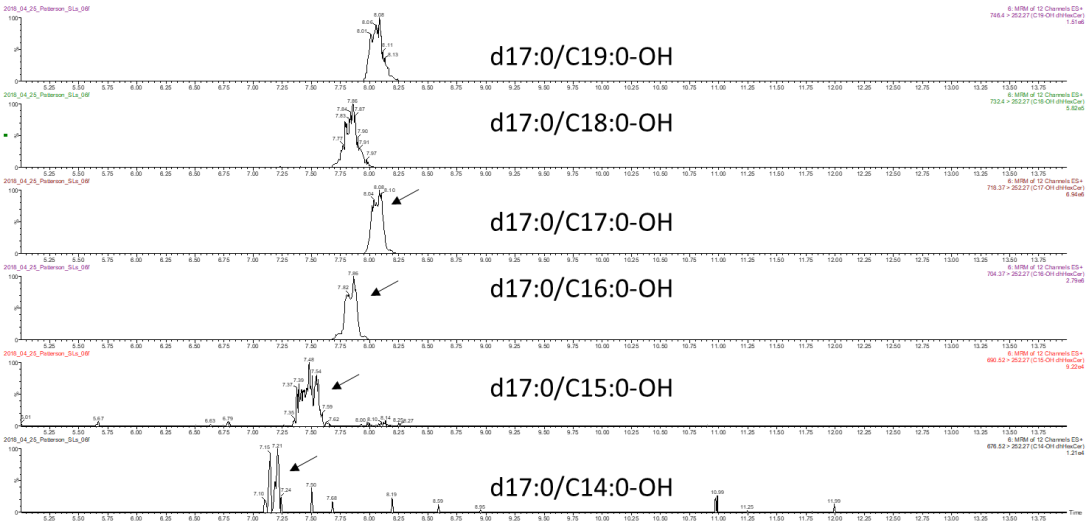

Figure 5.7: ETBF produces dihydrohexosylceramides. Mass spectrum of ETBF displaying the presence of dihydrosphingosine with varying chain lengths, with d17:0/C17-OH being the most abundant.

We attempted to determine if *B. fragilis* strains could produce S1P by adding sphingosine to the bacteria. In a pilot experiment (n=1), we were able to detect S1P levels in both strains cultured with sphingosine (Figure 5.8).

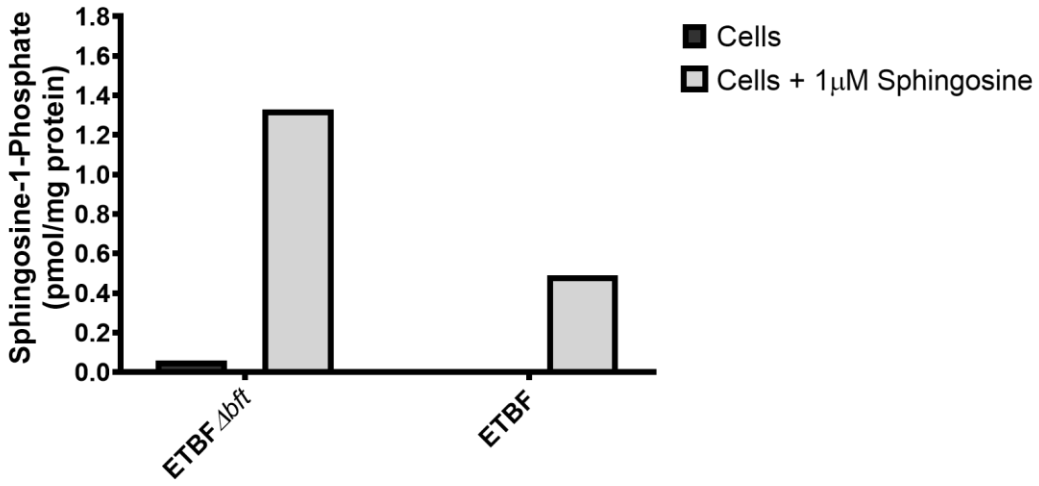

Figure 5.8: ETBF*Δbft* and ETBF treated with sphingosine produce S1P. Bacteria were treated with 1μM sphingosine for one hour and then cells were collected and lipids were extracted. Bacteria treated with sphingosine have higher levels of S1P than their untreated controls.

Because S1P is an extracellular lipid, we looked for changes in the bacterial media as well. Surprisingly, we found that when bacteria were present, S1P signals were dramatically decreased (Figure 5.9). This finding suggests that the bacteria have the ability to break down S1P, a previously unknown capability of bacteria. The implications of this finding are significant, as it would allow bacteria to intercept mammalian signaling sphingolipids that are released extracellularly to communicate with and recruit immune cells.[215]

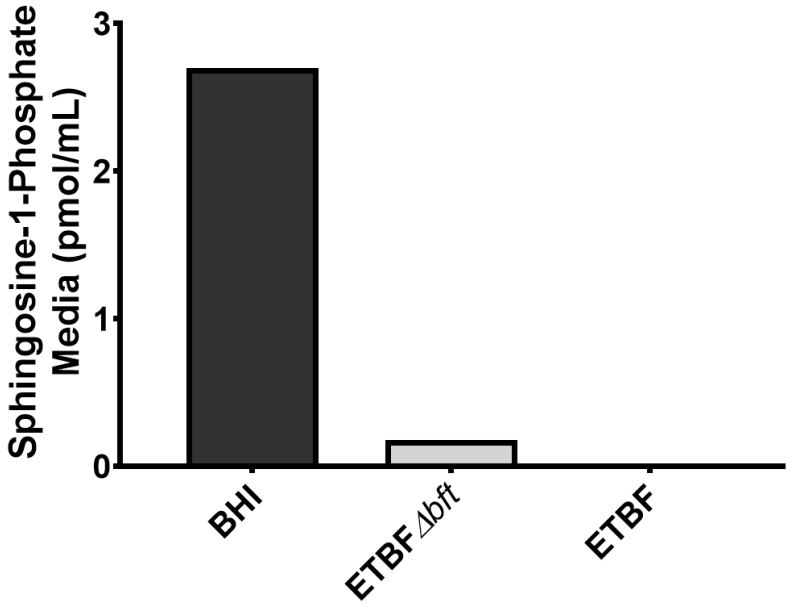

Figure 5.9: ETBF*Δbft* and ETBF break down S1P in bacterial growth media. Bacterial media was collected from cultured ETBF*Δbft* and ETBF strains and analyzed using mass spectrometry for S1P. S1P levels were dramatically reduced in both bacterial tubes, while control media (BHI) still had S1P remaining.

While most of the research on *B. fragilis* sphingolipids focuses on α-galactosylceramide, few studies mention the role of the other sphingolipids that it produces. Other researchers have suggested that *B. fragilis* sphingolipids are useful for bacterial survival in the gut, which can even be incorporated into the host membrane.[167,168,170] We saw inclusion of bacterial sphingolipids in HT29/C1 cells, but the role of these sphingolipids within these cells is currently unknown. We can speculate that the inclusion of bacterial sphingolipids, with odd-chain lengths, would disrupt normal membrane function. Because we know that maintenance of the epithelium is critical in the colon, especially in response to BFT, determining if these lipids alter normal function is important.

One of our biggest findings was the ability of *B. fragilis* to generate and break down S1P. To date, no other studies have shown this phenomenon, and follow-up studies are already underway within our lab to confirm, and expand on, these results.

In conclusion, this study highlights the importance of sphingolipids for interkingdom interactions between the host and the bacteria that colonize the colon.

Chapter 6: Works Cited

1. Barrett KEBT-RM in BS. Gastrointestinal (GI) Physiology. In: Elsevier; 2014. doi:https://doi.org/10.1016/B978-0-12-801238-3.00042-8

2. Fedoruk MJ, Hong S. Gastrointestinal System. In: Wexler PBT-E of T (Third E, ed. Oxford: Academic Press; 2014:702-705. doi:https://doi.org/10.1016/B978-0-12-386454-3.00026-9

3. Greenwald D, Brandt LJ. Gastrointestinal System: Function and Dysfunction. In: Birren JEBT-E of G (Second E, ed. New York: Elsevier; 2007:581-592. doi:https://doi.org/10.1016/B0-12-370870-2/00076-7

4. Carrington E V, Scott SM. Physiology and function of the colon. *Adv Nutr Diet Gastroenterol*. August 2014:28-32. doi:doi:10.1002/9781118872796.ch1.5

5. Reed KK, Wickham R. Review of the Gastrointestinal Tract: From Macro to Micro. *Semin Oncol Nurs*. 2009;25(1):3-14. doi:https://doi.org/10.1016/j.soncn.2008.10.002

6. Bassotti G, Battaglia E. Physiology of the Colon BT - Colon, Rectum and Anus: Anatomic, Physiologic and Diagnostic Bases for Disease Management. In: Ratto C, Parello A, Donisi L, Litta F, eds. Cham: Springer International Publishing; 2017:43-53. doi:10.1007/978-3-319-09807-4_7

7. Thomas RM, Jobin C. The Microbiome and Cancer: Is the “Oncobiome” Mirage Real? *TRENDS in CANCER: TRECAN*. 2015;1(1):24-35. doi:10.1016/j.trecan.2015.07.005

8. Cani PD. Human gut microbiome: hopes, threats and promises. *Gut*. 2018;67(9):1716 LP - 1725. doi:10.1136/gutjnl-2018-316723

9. Allaire JM, Crowley SM, Law HT, Chang S-Y, Ko H-J, Vallance BA. The Intestinal Epithelium: Central Coordinator of Mucosal Immunity. *Trends Immunol*. 2018;39(9):677-696. doi:10.1016/j.it.2018.04.002

10. Zachos NC, Kovbasnjuk O, Foulke-Abel J, et al. Human Enteroids/Colonoids and Intestinal Organoids Functionally Recapitulate Normal Intestinal Physiology and Pathophysiology. *J Biol Chem*. 2016;291(8):3759-3766. doi:10.1074/jbc.R114.635995

11. van der Flier LG, Clevers H. Stem Cells, Self-Renewal, and Differentiation in the Intestinal Epithelium. *Annu Rev Physiol*. 2009;71(1):241-260. doi:10.1146/annurev.physiol.010908.163145

12. Miyoshi J, Takai Y. Molecular perspective on tight-junction assembly and epithelial polarity. *Adv Drug Deliv Rev*. 2005;57(6):815-855. doi:https://doi.org/10.1016/j.addr.2005.01.008

13. Campbell HK, Maiers JL, DeMali KA. Interplay between tight junctions & adherens junctions. *Exp Cell Res*. 2017;358(1):39-44. doi:10.1016/j.yexcr.2017.03.061

14. Niessen CM. Tight Junctions/Adherens Junctions: Basic Structure and Function. *J Invest Dermatol*. 2007;127(11):2525-2532. doi:https://doi.org/10.1038/sj.jid.5700865

15. Hartsock A, Nelson WJ. Adherens and tight junctions: structure, function and connections to the actin cytoskeleton. *Biochim Biophys Acta*. 2008;1778(3):660-669. doi:10.1016/j.bbamem.2007.07.012

16. Peterson LW, Artis D. Intestinal epithelial cells: regulators of barrier function and immune homeostasis. *Nat Rev Immunol*. 2014;14(3):141-153. doi:10.1038/nri3608

17. Schulzke JD, Gitter AH, Mankertz J, et al. Epithelial transport and barrier function in occludin-deficient mice. *Biochim Biophys Acta - Biomembr*. 2005;1669(1):34-42. doi:https://doi.org/10.1016/j.bbamem.2005.01.008

18. Holmes JL, Van Itallie CM, Rasmussen JE, Anderson JM. Claudin profiling in the mouse during postnatal intestinal development and along the gastrointestinal tract reveals complex expression patterns. *Gene Expr Patterns*. 2006;6(6):581-588. doi:https://doi.org/10.1016/j.modgep.2005.12.001

19. Zihni C, Mills C, Matter K, Balda MS. Tight junctions: from simple barriers to multifunctional molecular gates. *Nat Rev Mol Cell Biol*. 2016;17(9):564-580. doi:10.1038/nrm.2016.80

20. Hervé J-C, Derangeon M, Sarrouilhe D, Bourmeyster N. Influence of the scaffolding protein Zonula Occludens (ZOs) on membrane channels. *Biochim Biophys Acta - Biomembr*. 2014;1838(2):595-604. doi:https://doi.org/10.1016/j.bbamem.2013.07.006

21. Bauer H, Zweimueller-Mayer J, Steinbacher P, Lametschwandtner A, Bauer HC. The dual role of zonula occludens (ZO) proteins. *J Biomed Biotechnol*. 2010;2010:402593. doi:10.1155/2010/402593

22. Daulagala AC, Bridges MC, Kourtidis A. E-cadherin Beyond Structure: A Signaling Hub in Colon Homeostasis and Disease. *Int J Mol Sci*. 2019;20(11):2756. doi:10.3390/ijms20112756

23. Takai Y, Nakanishi H. Nectin and afadin: novel organizers of intercellular junctions. *J Cell Sci*. 2003;116(1):17 LP - 27. doi:10.1242/jcs.00167

24. Irie K, Shimizu K, Sakisaka T, Ikeda W, Takai Y. Roles and modes of action of nectins in cell–cell adhesion. *Semin Cell Dev Biol*. 2004;15(6):643-656.

doi:https://doi.org/10.1016/j.semcdb.2004.09.002

25. Yagi T, Takeichi M. Cadherin superfamily genes: functions, genomic organization, and neurologic diversity. *Genes Dev*. 2000;14(10):1169-1180. doi:10.1101/gad.14.10.1169

26. Gumbiner BM. Regulation of cadherin-mediated adhesion in morphogenesis. *Nat Rev Mol Cell Biol*. 2005;6(8):622-634. doi:10.1038/nrm1699

27. Halbleib JM, Nelson WJ. Cadherins in development: cell adhesion, sorting, and tissue morphogenesis. *Genes Dev*. 2006;20(23):3199-3214. doi:10.1101/gad.1486806

28. Kemler R. Classical cadherins. *Semin Cell Biol*. 1992;3(3):149-155. doi:https://doi.org/10.1016/S1043-4682(10)80011-X

29. Tan CW, Hirokawa Y, Gardiner BS, Smith DW, Burgess AW. Colon Cryptogenesis: Asymmetric Budding. *PLoS One*. 2013;8(10):e78519. https://doi.org/10.1371/journal.pone.0078519.

30. Harris TJC, Tepass U. Adherens junctions: from molecules to morphogenesis. *Nat Rev Mol Cell Biol*. 2010;11(7):502-514. doi:10.1038/nrm2927

31. Ando-Akatsuka Y, Yonemura S, Itoh M, Furuse M, Tsukita S. Differential behavior of E-cadherin and occludin in their colocalization with ZO-1 during the establishment of epithelial cell polarity. *J Cell Physiol*. 1999;179(2):115-125. doi:10.1002/(SICI)1097-4652(199905)179:2<115::AID-JCP1>3.0.CO;2-T

32. Rajasekaran AK, Hojo M, Huima T, Rodriguez-Boulan E. Catenins and zonula occludens-1 form a complex during early stages in the assembly of tight junctions. *J Cell Biol*. 1996;132(3):451-463. doi:10.1083/jcb.132.3.451

33. Hawn MT, Umar A, Carethers JM, et al. Evidence for a Connection between the Mismatch Repair System and the G2 Cell Cycle Checkpoint. *Cancer Res* . 1995;55(17):3721-3725. http://cancerres.aacrjournals.org/content/55/17/3721.abstract.

34. Maiers JL, Peng X, Fanning AS, DeMali KA. ZO-1 recruitment to α-catenin--a novel mechanism for coupling the assembly of tight junctions to adherens junctions. *J Cell Sci*. 2013;126(Pt 17):3904-3915. doi:10.1242/jcs.126565

35. Capaldo CT, Macara IG. Depletion of E-cadherin disrupts establishment but not maintenance of cell junctions in Madin-Darby canine kidney epithelial cells. *Mol Biol Cell*. 2007;18(1):189-200. doi:10.1091/mbc.e06-05-0471

36. Morad S a F, Cabot MC. Ceramide-orchestrated signalling in cancer cells. *Nat Rev*

Cancer. 2013;13(1):51-65. doi:10.1038/nrc3398

37. Ogretmen B. Sphingolipid metabolism in cancer signalling and therapy. *Nat Rev Cancer*. 2018;18(1):33-50. doi:10.1038/nrc.2017.96

38. Ryland LK, Fox TE, Liu X, Loughran TP, Kester M. Dysregulation of sphingolipid metabolism in cancer. *Cancer Biol Ther*. 2011;11(2):138-149. doi:10.4161/cbt.11.2.14624

39. Camp ER, Patterson LD, Kester M, Voelkel-Johnson C. Therapeutic implications of bioactive sphingolipids: A focus on colorectal cancer. *Cancer Biol Ther*. 2017;18(9):640-650. doi:10.1080/15384047.2017.1345396

40. Pralhada Rao R, Vaidyanathan N, Rengasamy M, Mammen Oommen A, Somaiya N, Jagannath MR. Sphingolipid metabolic pathway: an overview of major roles played in human diseases. *J Lipids*. 2013;2013:178910. doi:10.1155/2013/178910

41. Hannun YA, Obeid LM. Sphingolipids and their metabolism in physiology and disease. *Nat Rev Mol Cell Biol*. 2018;19(3):175-191. doi:10.1038/nrm.2017.107

42. Pralhada Rao R, Vaidyanathan N, Rengasamy M, Mammen Oommen A, Somaiya N, Jagannath MR. Sphingolipid metabolic pathway: an overview of major roles played in human diseases. *J Lipids*. 2013;2013:178910. doi:10.1155/2013/178910

43. Ségui B, Andrieu-Abadie N, Jaffrézou J-P, Benoist H, Levade T. Sphingolipids as modulators of cancer cell death: Potential therapeutic targets. *Biochim Biophys Acta - Biomembr*. 2006;1758(12):2104-2120. doi:https://doi.org/10.1016/j.bbamem.2006.05.024

44. Hla T, Dannenberg AJ. Sphingolipid signaling in metabolic disorders. *Cell Metab*. 2012;16(4):420-434. doi:10.1016/j.cmet.2012.06.017

45. Ichikawa S, Hirabayashi Y. Glucosylceramide synthase and glycosphingolipid synthesis. *Trends Cell Biol*. 1998. doi:10.1016/S0962-8924(98)01249-5

46. Stirnemann J, Belmatoug N, Camou F, et al. A Review of Gaucher Disease Pathophysiology, Clinical Presentation and Treatments. *Int J Mol Sci*. 2017;18(2):441. doi:10.3390/ijms18020441

47. Yamashita T, Wada R, Sasaki T, et al. A vital role for glycosphingolipid synthesis during development and differentiation. *Proc Natl Acad Sci U S A*. 1999;96(16):9142-9147. doi:10.1073/pnas.96.16.9142

48. Messner MC, Cabot MC. Glucosylceramide in Humans. In: Chalfant C, Poeta M Del, eds. New York, NY: Springer New York; 2010:156-164. doi:10.1007/978-1-4419-6741-1_11

49. Chujor CSN, Feingold KR, Elias PM, Holleran WM. Glucosylceramide synthase activity in murine epidermis: quantitation, localization, regulation, and requirement for barrier homeostasis. *J Lipid Res*. 1998;39(2):277-285. http://www.jlr.org/content/39/2/277.abstract.

50. Duan RD, Nilsson Å. Metabolism of sphingolipids in the gut and its relation to inflammation and cancer development. *Prog Lipid Res*. 2009;48(1):62-72. doi:10.1016/j.plipres.2008.04.003

51. Abdel Hadi L, Di Vito C, Riboni L. Fostering Inflammatory Bowel Disease: Sphingolipid Strategies to Join Forces. *Mediators Inflamm*. 2016;2016:3827684. doi:10.1155/2016/3827684

52. Jennemann R, Kaden S, Sandhoff R, et al. Glycosphingolipids Are Essential for Intestinal Endocytic Function. *J Biol Chem*. 2012;287(39):32598-32616. doi:10.1074/jbc.M112.371005

53. IDETA R, SAKUTA T, NAKANO Y, UCHIYAMA T. Orally Administered Glucosylceramide Improves the Skin Barrier Function by Upregulating Genes Associated with the Tight Junction and Cornified Envelope Formation. *Biosci Biotechnol Biochem*. 2011;75(8):1516-1523. doi:10.1271/bbb.110215

54. KAWADA C, HASEGAWA T, WATANABE M, NOMURA Y. Dietary Glucosylceramide Enhances Tight Junction Function in Skin Epidermis via Induction of Claudin-1. *Biosci Biotechnol Biochem*. 2013;77(4):867-869. doi:10.1271/bbb.120874

55. Popovic Z V, Rabionet M, Jennemann R, et al. Glucosylceramide Synthase Is Involved in Development of Invariant Natural Killer T Cells. *Front Immunol*. 2017;8:848. https://www.frontiersin.org/article/10.3389/fimmu.2017.00848.

56. Hiippala K, Jouhten H, Ronkainen A, et al. The Potential of Gut Commensals in Reinforcing Intestinal Barrier Function and Alleviating Inflammation. *Nutrients*. 2018;10(8):988. doi:10.3390/nu10080988

57. Sekirov I, Russell SL, Antunes LCM, Finlay BB. Gut Microbiota in Health and Disease. *Physiol Rev*. 2010;90(3):859-904. doi:10.1152/physrev.00045.2009

58. Ding R, Goh W-R, Wu R, et al. Revisit gut microbiota and its impact on human health and disease. *J Food Drug Anal*. 2019;27(3):623-631. doi:https://doi.org/10.1016/j.jfda.2018.12.012

59. Jobin C. Colorectal cancer: Looking for answers in the microbiota. *Cancer Discov*. 2013;3(4):384-387. doi:10.1158/2159-8290.CD-13-0042

60. Okumura R, Takeda K. Roles of intestinal epithelial cells in the maintenance of gut homeostasis. *Exp Mol Med*. 2017;49(5):e338-e338. doi:10.1038/emm.2017.20

61. Durack J, Lynch S V. The gut microbiome: Relationships with disease and opportunities for therapy. *J Exp Med*. 2018;216(1):20-40. doi:10.1084/jem.20180448

62. Tuddenham S, Sears CL. The intestinal microbiome and health. *Curr Opin Infect Dis*. 2015;28(5):464-470. doi:10.1097/QCO.0000000000000196

63. Karlsson FH, Tremaroli V, Nookaew I, et al. Gut metagenome in European women with normal, impaired and diabetic glucose control. *Nature*. 2013;498(7452):99-103. http://dx.doi.org/10.1038/nature12198.

64. Arthur JC, Gharaibeh RZ, Muhlbauer M, et al. Microbial genomic analysis reveals the essential role of inflammation in bacteria-induced colorectal cancer. 2015;73(4):389-400. doi:10.1530/ERC-14-0411.Persistent

65. Garrett WS. The gut microbiota and colon cancer. *Science (80-)*. 2019;364(6446):1133 LP - 1135. doi:10.1126/science.aaw2367

66. König J, Wells J, Cani PD, et al. Human Intestinal Barrier Function in Health and Disease. *Clin Transl Gastroenterol*. 2016;7(10):e196-e196. doi:10.1038/ctg.2016.54

67. Wang Z, Klipfell E, Bennett BJ, et al. Gut flora metabolism of phosphatidylcholine promotes cardiovascular disease. *Nature*. 2011;472(7341):57-63. doi:10.1038/nature09922

68. Kostic AD, Xavier RJ, Gevers D. The Microbiome in Inflammatory Bowel Diseases: Current Status and the Future Ahead. *Gastroenterology*. 2014;146(6):1489-1499. doi:10.1053/j.gastro.2014.02.009

69. Simrén M, Barbara G, Flint HJ, et al. Intestinal microbiota in functional bowel disorders: a Rome foundation report. *Gut*. 2013;62(1):159-176. doi:10.1136/gutjnl-2012-302167

70. Le Chatelier E, Nielsen T, Qin J, et al. Richness of human gut microbiome correlates with metabolic markers. *Nature*. 2013;500(7464):541-546. http://dx.doi.org/10.1038/nature12506.

71. Ulluwishewa D, Anderson RC, McNabb WC, Moughan PJ, Wells JM, Roy NC. Regulation of Tight Junction Permeability by Intestinal Bacteria and Dietary Components. *J Nutr*. 2011;141(5):769-776. doi:10.3945/jn.110.135657

72. Thevaranjan N, Puchta A, Schulz C, et al. Age-Associated Microbial Dysbiosis Promotes Intestinal Permeability, Systemic Inflammation, and Macrophage Dysfunction. *Cell Host Microbe*. 2017;21(4):455-466.e4. doi:10.1016/j.chom.2017.03.002

73. Chang C-S, Kao C-Y. Current understanding of the gut microbiota shaping mechanisms. *J Biomed Sci*. 2019;26(1):59. doi:10.1186/s12929-019-0554-5

74. Birchenough GMH, Johansson ME V, Gustafsson JK, Bergström JH, Hansson GC. New developments in goblet cell mucus secretion and function. *Mucosal Immunol*. 2015;8(4):712-719. doi:10.1038/mi.2015.32

75. Sonnenburg JL, Angenent LT, Gordon JI. Getting a grip on things: how do communities of bacterial symbionts become established in our intestine? *Nat Immunol*. 2004;5(6):569-573. doi:10.1038/ni1079

76. Macfarlane S, Woodmansey EJ, Macfarlane GT. Colonization of Mucin by Human Intestinal Bacteria and Establishment of Biofilm Communities in a Two-Stage Continuous Culture System. *Appl Environ Microbiol*. 2005;71(11):7483 LP - 7492. doi:10.1128/AEM.71.11.7483-7492.2005

77. Sicard J-F, Le Bihan G, Vogeleer P, Jacques M, Harel J. Interactions of Intestinal Bacteria with Components of the Intestinal Mucus. *Front Cell Infect Microbiol*. 2017;7:387. https://www.frontiersin.org/article/10.3389/fcimb.2017.00387.

78. Schroeder BO. Fight them or feed them: how the intestinal mucus layer manages the gut microbiota. *Gastroenterol Rep*. 2019;7(1):3-12. doi:10.1093/gastro/goy052

79. Mowat AM, Agace WW. Regional specialization within the intestinal immune system. *Nat Rev Immunol*. 2014;14(10):667-685. doi:10.1038/nri3738

80. Pott J, Hornef M. Innate immune signalling at the intestinal epithelium in homeostasis and disease. *EMBO Rep*. 2012;13(8):684-698. doi:10.1038/embor.2012.96

81. Blander JM. Death in the intestinal epithelium-basic biology and implications for inflammatory bowel disease. *FEBS J*. 2016;283(14):2720-2730. doi:10.1111/febs.13771

82. Pruteanu M, Shanahan F. Digestion of epithelial tight junction proteins by the commensal Clostridium perfringens. *Am J Physiol Liver Physiol*. 2013;305(10):G740-G748. doi:10.1152/ajpgi.00316.2012

83. Catalioto R-M, Giuliani CAM and S. Intestinal Epithelial Barrier Dysfunction in Disease and Possible Therapeutical Interventions. *Curr Med Chem*. 2011;18(3):398-426. doi:http://dx.doi.org/10.2174/092986711794839179

84. Bansal T, Alaniz RC, Wood TK, Jayaraman A. The bacterial signal indole increases epithelial-cell tight-junction resistance and attenuates indicators of inflammation. *Proc Natl Acad Sci U S A*. 2010;107(1):228-233. doi:10.1073/pnas.0906112107

85. Sears CL, Geis AL, Housseau F. Bacteroides fragilis subverts mucosal biology: from symbiont to colon carcinogenesis. *J Clin Invest*. 2014;124(10):4166-4172. doi:10.1172/JCI72334

86. Sears CL, Islam S, Saha A, et al. Association of Enterotoxigenic Bacteroides fragilis Infection with Inflammatory Diarrhea. *Clin Infect Dis*. 2008;47(6):797-803. http://cid.oxfordjournals.org/content/47/6/797.abstract.

87. Zhang W, Zhu B, Xu J, et al. Bacteroides fragilis Protects Against Antibiotic-Associated Diarrhea in Rats by Modulating Intestinal Defenses. *Front Immunol*. 2018;9:1040. https://www.frontiersin.org/article/10.3389/fimmu.2018.01040.

88. Sears CL. Enterotoxigenic Bacteroides fragilis: a Rogue among Symbiotes. *Clin Microbiol Rev*. 2009;22(2):349 LP - 369. doi:10.1128/CMR.00053-08

89. Zitomersky NL, Coyne MJ, Comstock LE. Longitudinal analysis of the prevalence, maintenance, and IgA response to species of the order Bacteroidales in the human gut. *Infect Immun*. 2011;79(5):2012-2020. doi:10.1128/IAI.01348-10

90. Sears CL. The toxins of Bacteroides fragilis. *Toxicon*. 2001;39(11):1737-1746. doi:http://dx.doi.org/10.1016/S0041-0101(01)00160-X

91. Chung L, Thiele Orberg E, Geis AL, et al. Bacteroides fragilis Toxin Coordinates a Pro-carcinogenic Inflammatory Cascade via Targeting of Colonic Epithelial Cells. *Cell Host Microbe*. 2018;23(2):203-214.e5. doi:10.1016/j.chom.2018.01.007

92. Wu S, Rhee K, Albesiano E, et al. A human colonic commensal promotes colon tumorigenesis via activation of T helper type 17 T cell responses. *Nat Med*. 2009;15(9):1016-1022. doi:10.1038/nm.2015.A

93. Rhee K-J, Wu S, Wu X, et al. Induction of persistent colitis by a human commensal, enterotoxigenic Bacteroides fragilis, in wild-type C57BL/6 mice. *Infect Immun*. 2009;77(4):1708-1718. doi:10.1128/IAI.00814-08

94. Wu S, Lim K-C, Huang J, Saidi RF, Sears CL. Bacteroides fragilis enterotoxin cleaves the zonula adherens protein, E-cadherin. *Proc Natl Acad Sci U S A*. 1998;95(25):14979-14984. http://www.ncbi.nlm.nih.gov/pmc/articles/PMC24561/.

95. Wu S, Dreyfus LA, Tzianabos AO, Hayashi C, Sears CL. Diversity of the Metalloprotease Toxin Produced by Enterotoxigenic Bacteroides fragilis. *Infect Immun*. 2002;70(5):2463-2471. doi:10.1128/IAI.70.5.2463-2471.2002

96. Wells C, van de Westerlo E, Jechorek R, Feltis B, Wilkins T, Erlandsen S. Bacteroides fragilis enterotoxin modulates epithelial permeability and bacterial

internalization by HT-29 enterocytes. *Gastroenterology*. 1996;110(5):1429-1437. doi:10.1053/GAST.1996.V110.PM8613048

97. Obiso Jr RJ, Azghani AO, Wilkins TD. The Bacteroides fragilis toxin fragilysin disrupts the paracellular barrier of epithelial cells. *Infect Immun*. 1997;65(4):1431-1439. https://www.ncbi.nlm.nih.gov/pubmed/9119484.

98. Wu S, Morin PJ, Maouyo D, Sears CL. Bacteroides fragilis enterotoxin induces c-Myc expression and cellular proliferation. *Gastroenterology*. 2003;124(2):392-400. doi:10.1053/gast.2003.50047

99. Suzuki T. Regulation of intestinal epithelial permeability by tight junctions. *Cell Mol Life Sci*. 2013;70(4):631-659. doi:10.1007/s00018-012-1070-x

100. Guan Q. A Comprehensive Review and Update on the Pathogenesis of Inflammatory Bowel Disease. *J Immunol Res*. 2019;2019:7247238. doi:10.1155/2019/7247238

101. Spiller R, Major G. IBS and IBD — separate entities or on a spectrum? *Nat Rev Gastroenterol Hepatol*. 2016;13(10):613-621. doi:10.1038/nrgastro.2016.141

102. Odenwald MA, Turner JR. The intestinal epithelial barrier: a therapeutic target? *Nat Rev Gastroenterol Hepatol*. 2017;14(1):9-21. doi:10.1038/nrgastro.2016.169

103. Ni J, Wu GD, Albenberg L, Tomov VT. Gut microbiota and IBD: causation or correlation? *Nat Rev Gastroenterol Hepatol*. 2017;14(10):573-584. doi:10.1038/nrgastro.2017.88

104. Zhu L, Han J, Li L, Wang Y, Li Y, Zhang S. Claudin Family Participates in the Pathogenesis of Inflammatory Bowel Diseases and Colitis-Associated Colorectal Cancer. *Front Immunol*. 2019;10:1441. doi:10.3389/fimmu.2019.01441

105. Franzosa EA, Sirota-Madi A, Avila-Pacheco J, et al. Gut microbiome structure and metabolic activity in inflammatory bowel disease. *Nat Microbiol*. 2019;4(2):293-305. doi:10.1038/s41564-018-0306-4

106. Kolho K-L, Pessia A, Jaakkola T, de Vos WM, Velagapudi V. Faecal and Serum Metabolomics in Paediatric Inflammatory Bowel Disease. *J Crohn's Colitis*. 2016;11(3):321-334. doi:10.1093/ecco-jcc/jjw158

107. Nishida A, Inoue R, Inatomi O, Bamba S, Naito Y, Andoh A. Gut microbiota in the pathogenesis of inflammatory bowel disease. *Clin J Gastroenterol*. 2018;11(1):1-10. doi:10.1007/s12328-017-0813-5

108. Francino MP. Antibiotics and the Human Gut Microbiome: Dysbioses and Accumulation of Resistances. *Front Microbiol*. 2016;6:1543.

doi:10.3389/fmicb.2015.01543

109. Siegel RL, Miller KD, Goding Sauer A, et al. Colorectal cancer statistics, 2020. *CA Cancer J Clin*. 2020;70(3):145-164. doi:10.3322/caac.21601

110. Frank SA. *Dynamics of Cancer: Incidence, Inheritance, and Evolution*. Vol 1. Princeton University Press; 2007.

111. Brenner H, Kloor M, Pox CP. Colorectal cancer. *Lancet*. 2014;383(9927):1490-1502. doi:10.1016/S0140-6736(13)61649-9

112. Testa U, Pelosi E, Castelli G. Colorectal cancer: genetic abnormalities, tumor progression, tumor heterogeneity, clonal evolution and tumor-initiating cells. *Med Sci (Basel, Switzerland)*. 2018;6(2):31. doi:10.3390/medsci6020031

113. Fearon ER. Molecular Genetics of Colorectal Cancer. *Annu Rev Pathol Mech Dis*. 2011;6(1):479-507. doi:10.1146/annurev-pathol-011110-130235

114. Danielsen SA, Eide PW, Nesbakken A, Guren T, Leithe E, Lothe RA. Portrait of the PI3K/AKT pathway in colorectal cancer. *Biochim Biophys Acta - Rev Cancer*. 2015;1855(1):104-121. doi:http://dx.doi.org/10.1016/j.bbcan.2014.09.008

115. Carvalho B, Sillars-Hardebol AH, Postma C, et al. Colorectal adenoma to carcinoma progression is accompanied by changes in gene expression associated with ageing, chromosomal instability, and fatty acid metabolism. *Cell Oncol (Dordr)*. 2012;35(1):53-63. doi:10.1007/s13402-011-0065-1

116. Xie Y-H, Chen Y-X, Fang J-Y. Comprehensive review of targeted therapy for colorectal cancer. *Signal Transduct Target Ther*. 2020;5(1):22. doi:10.1038/s41392-020-0116-z

117. Dekker E, Tanis PJ, Vleugels JLA, Kasi PM, Wallace MB. Colorectal cancer. *Lancet*. 2019;394(10207):1467-1480. doi:10.1016/S0140-6736(19)32319-0

118. Grivennikov SI, Wang K, Mucida D, et al. Adenoma-linked barrier defects and microbial products drive IL-23/IL-17-mediated tumour growth. *Nature*. 2012;491(7423):254-258. doi:10.1038/nature11465

119. Bhat AA, Uppada S, Achkar IW, et al. Tight Junction Proteins and Signaling Pathways in Cancer and Inflammation: A Functional Crosstalk. *Front Physiol*. 2019;9:1942. https://www.frontiersin.org/article/10.3389/fphys.2018.01942.

120. Salvador E, Burek M, Förster CY. Tight Junctions and the Tumor Microenvironment. *Curr Pathobiol Rep*. 2016;4:135-145. doi:10.1007/s40139-016-0106-6

121. Choi C-HR, Bakir I Al, Hart AL, Graham TA. Clonal evolution of colorectal cancer in

IBD. *Nat Rev Gastroenterol Hepatol*. 2017;14(4):218-229. doi:10.1038/nrgastro.2017.1

122. Machala M, Procházková J, Hofmanová J, et al. Colon Cancer and Perturbations of the Sphingolipid Metabolism. *Int J Mol Sci*. 2019;20(23). doi:10.3390/ijms20236051

123. Gouazé V, Yu JY, Bleicher RJ, et al. Overexpression of glucosylceramide synthase and P-glycoprotein in cancer cells selected for resistance to natural product chemotherapy. *Mol Cancer Ther*. 2004;3(5):633-640. http://mct.aacrjournals.org/content/3/5/633.abstract.

124. Kovbasnjuk O, Mourtazina R, Baibakov B, et al. The glycosphingolipid globotriaosylceramide in the metastatic transformation of colon cancer. *Proc Natl Acad Sci U S A*. 2005;102(52):19087-19092. doi:10.1073/pnas.0506474102

125. Morjani H, Aouali N, Belhoussine R, Veldman RJ, Levade T, Manfait M. Elevation of glucosylceramide in multidrug-resistant cancer cells and accumulation in cytoplasmic droplets. *Int J Cancer*. 2001;94(2):157-165. doi:10.1002/ijc.1449

126. Beckham TH, Cheng JC, Marrison ST, Norris JS, Liu X. Interdiction of sphingolipid metabolism to improve standard cancer therapies. *Adv Cancer Res*. 2013;117:1-36. doi:10.1016/B978-0-12-394274-6.00001-7

127. García-Barros M, Coant N, Truman J-P, Snider AJ, Hannun YA. Sphingolipids in colon cancer. *Biochim Biophys Acta*. 2014;1841(5):773-782. doi:10.1016/j.bbalip.2013.09.007

128. Duan RD. Anticancer compounds and sphingolipid metabolism in the colon. *In Vivo (Brooklyn)*. 2005;19(1):293-300.

129. Garris CS, Blaho VA, Hla T, Han MH. Sphingosine-1-phosphate receptor 1 signalling in T cells: trafficking and beyond. *Immunology*. 2014;142(3):347-353. doi:10.1111/imm.12272

130. Gouaze V, Liu Y-Y, Prickett CS, Yu JY, Giuliano AE, Cabot MC. Glucosylceramide synthase blockade down-regulates P-glycoprotein and resensitizes multidrug-resistant breast cancer cells to anticancer drugs. *Cancer Res*. 2005;65(9):3861-3867. doi:10.1158/0008-5472.CAN-04-2329

131. Medico E, Russo M, Picco G, et al. The molecular landscape of colorectal cancer cell lines unveils clinically actionable kinase targets. *Nat Commun*. 2015;6(1):7002. doi:10.1038/ncomms8002

132. Fan H, Demirci U, Chen P. Emerging organoid models: leaping forward in cancer research. *J Hematol Oncol*. 2019;12(1):142. doi:10.1186/s13045-019-0832-4

133. In JG, Foulke-Abel J, Estes MK, Zachos NC, Kovbasnjuk O, Donowitz M. Human mini-guts: new insights into intestinal physiology and host-pathogen interactions. *Nat Rev Gastroenterol Hepatol*. 2016;13(11):633-642. doi:10.1038/nrgastro.2016.142

134. Yoo J-H, Donowitz M. Intestinal enteroids/organoids: A novel platform for drug discovery in inflammatory bowel diseases. *World J Gastroenterol*. 2019;25(30):4125-4147. doi:10.3748/wjg.v25.i30.4125

135. Wallach TE, Bayrer JR. Intestinal Organoids: New Frontiers in the Study of Intestinal Disease and Physiology. *J Pediatr Gastroenterol Nutr*. 2017;64(2):180-185. doi:10.1097/MPG.0000000000001411

136. Sato T, Stange DE, Ferrante M, et al. Long-term Expansion of Epithelial Organoids From Human Colon, Adenoma, Adenocarcinoma, and Barrett's Epithelium. *Gastroenterology*. 2011;141(5):1762-1772. doi:10.1053/j.gastro.2011.07.050

137. In JG, Foulke-Abel J, Clarke E, Kovbasnjuk O. Human Colonoid Monolayers to Study Interactions Between Pathogens, Commensals, and Host Intestinal Epithelium. *J Vis Exp*. 2019;(146):10.3791/59357. doi:10.3791/59357

138. Shawki A, McCole DF. Mechanisms of Intestinal Epithelial Barrier Dysfunction by Adherent-Invasive Escherichia coli. *Cell Mol Gastroenterol Hepatol*. 2016;3(1):41-50. doi:10.1016/j.jcmgh.2016.10.004

139. Allen J, Hao S, Sears CL, Timp W. Epigenetic Changes Induced by Bacteroides fragilis Toxin. *Infect Immun*. 2019;87(6):e00447-18. doi:10.1128/IAI.00447-18

140. Myers LL, Shoop DS. Association of enterotoxigenic Bacteroides fragilis with diarrheal disease in young pigs. *Am J Vet Res*. 1987;48(5):774-775. http://europepmc.org/abstract/MED/3592377.

141. Pearson JM, Tan S-F, Sharma A, et al. Ceramide Analogue SACLAC Modulates Sphingolipid Levels and MCL-1 Splicing to Induce Apoptosis in Acute Myeloid Leukemia. *Mol Cancer Res*. 2020;18(3):352 LP - 363. doi:10.1158/1541-7786.MCR-19-0619

142. Merrill AH, Sullards MC, Allegood JC, Kelly S, Wang E. Sphingolipidomics: High-throughput, structure-specific, and quantitative analysis of sphingolipids by liquid chromatography tandem mass spectrometry. *Methods*. 2005;36(2):207-224. doi:10.1016/J.YMETH.2005.01.009

143. Allen J, Hao S, Sears CL, Timp W. Epigenetic Changes Induced by Bacteroides fragilis Toxin. *Infect Immun*. 2019;87(6):e00447-18. doi:10.1128/IAI.00447-18

144. In J, Foulke-Abel J, Zachos NC, et al. Enterohemorrhagic Escherichia coli reduce

mucus and intermicrovillar bridges in human stem cell-derived colonoids. *Cell Mol Gastroenterol Hepatol*. 2016;2(1):48-62.e3. doi:10.1016/j.jcmgh.2015.10.001

145. Franco AA, Cheng RK, Goodman A, Sears CL. Modulation of bft expression by the Bacteroides fragilis pathogenicity island and its flanking region. *Mol Microbiol*. 2002;45(4):1067-1077. doi:10.1046/j.1365-2958.2002.03077.x

146. Franco AA, Buckwold SL, Shin JW, Ascon M, Sears CL. Mutation of the zinc-binding metalloprotease motif affects Bacteroides fragilis toxin activity but does not affect propeptide processing. *Infect Immun*. 2005;73(8):5273-5277. doi:10.1128/IAI.73.8.5273-5277.2005

147. Wu S, Lim KC, Huang J, Saidi RF, Sears CL. Bacteroides fragilis enterotoxin cleaves the zonula adherens protein, E-cadherin. *Proc Natl Acad Sci U S A*. 1998;95(25):14979-14984. doi:10.1073/pnas.95.25.14979

148. Schneider CA, Rasband WS, Eliceiri KW. NIH Image to ImageJ: 25 years of image analysis. *Nat Methods*. 2012;9(7):671-675. doi:10.1038/nmeth.2089

149. Chan JL, Wu S, Geis AL, et al. Non-toxigenic Bacteroides fragilis (NTBF) administration reduces bacteria-driven chronic colitis and tumor development independent of polysaccharide A. *Mucosal Immunol*. 2019;12(1):164-177. doi:10.1038/s41385-018-0085-5

150. Wu S, Shin J, Zhang G, Cohen M, Franco A, Sears CL. The Bacteroides fragilis Toxin Binds to a Specific Intestinal Epithelial Cell Receptor . *Infect Immun*. 2006;74(9):5382-5390. doi:10.1128/IAI.00060-06

151. Jennemann R, Kaden S, Sandhoff R, et al. Glycosphingolipids are essential for intestinal endocytic function. *J Biol Chem*. 2012;287(39):32598-32616. doi:10.1074/jbc.M112.371005

152. García-Barros M, Coant N, Truman J-P, Snider AJ, Hannun YA. Sphingolipids in colon cancer. *Biochim Biophys Acta*. 2014;1841(5):773-782. doi:10.1016/j.bbalip.2013.09.007

153. Wu S, Rhee K-J, Albesiano E, et al. A human colonic commensal promotes colon tumorigenesis via activation of T helper type 17 T cell responses. *Nat Med*. 2009;15(9):1016-1022. doi:10.1038/nm.2015

154. Housseau F, Sears CL. Enterotoxigenic Bacteroides fragilis (ETBF)-mediated colitis in Min (Apc+/-) mice: a human commensal-based murine model of colon carcinogenesis. *Cell Cycle*. 2010;9(1):3-5. doi:10.4161/cc.9.1.10352

155. Vardi A, Zigdon H, Meshcheriakova A, et al. Delineating pathological pathways in a chemically induced mouse model of Gaucher disease. *J Pathol*.

2016;239(4):496-509. doi:10.1002/path.4751

156. Porter AG, Jänicke RU. Emerging roles of caspase-3 in apoptosis. *Cell Death Differ*. 1999;6(2):99-104. doi:10.1038/sj.cdd.4400476

157. Chambers FG, Koshy SS, Saidi RF, Clark DP, Moore RD, Sears CL. Bacteroides fragilis toxin exhibits polar activity on monolayers of human intestinal epithelial cells (T84 cells) in vitro. *Infect Immun*. 1997;65(9):3561 LP - 3570. http://iai.asm.org/content/65/9/3561.abstract.

158. Co JY, Margalef-Català M, Li X, et al. Controlling Epithelial Polarity: A Human Enteroid Model for Host-Pathogen Interactions. *Cell Rep*. 2019;26(9):2509-2520.e4. doi:10.1016/j.celrep.2019.01.108

159. Liu L, Saitz-Rojas W, Smith R, et al. Mucus layer modeling of human colonoids during infection with enteroaggragative E. coli. *Sci Rep*. 2020;10(1):10533. doi:10.1038/s41598-020-67104-4

160. Deng Z, Mu J, Tseng M, et al. Enterobacteria-secreted particles induce production of exosome-like S1P-containing particles by intestinal epithelium to drive Th17-mediated tumorigenesis. *Nat Commun*. 2015;6:6956. doi:10.1038/ncomms7956

161. Shayman JA. Glucosylceramide and Galactosylceramide Synthase BT - Sphingolipid Biology. In: Hirabayashi Y, Igarashi Y, Merrill AH, eds. Tokyo: Springer Japan; 2006:83-94. doi:10.1007/4-431-34200-1_6

162. von Gerichten J, Schlosser K, Lamprecht D, et al. Diastereomer-specific quantification of bioactive hexosylceramides from bacteria and mammals. *J Lipid Res*. 2017;58(6):1247-1258. doi:10.1194/jlr.D076190

163. Itier J-M, Ret G, Viale S, et al. Effective clearance of GL-3 in a human iPSC-derived cardiomyocyte model of Fabry disease. *J Inherit Metab Dis*. 2014;37(6):1013-1022. doi:10.1007/s10545-014-9724-5

164. Schnaar RL, Kinoshita T. Glycosphingolipids. In: Varki A, Cummings RD, Esko JD et al., ed. *Essentials of Glycobiology*. 3rd ed. Cold Spring Harbor Laboratory Press; 2017. https://www.ncbi.nlm.nih.gov/books/NBK453016/ doi: 10.1101/glycobiology.3e.011.

165. Daniotti JL, Vilcaes AA, Torres Demichelis V, Ruggiero FM, Rodriguez-Walker M. Glycosylation of glycolipids in cancer: basis for development of novel therapeutic approaches. *Front Oncol*. 2013;3:306. doi:10.3389/fonc.2013.00306

166. Hakomori S, Handa K, Iwabuchi K, Yamamura S, Prinetti A. New insights in glycosphingolipid function: “glycosignaling domain,” a cell surface assembly of glycosphingolipids with signal transducer molecules, involved in cell adhesion

coupled with signaling. *Glycobiology*. 1998;8(10):xi-xviii. doi:10.1093/oxfordjournals.glycob.a018822

167. An D, Oh SF, Olszak T, et al. Sphingolipids from a symbiotic microbe regulate homeostasis of host intestinal natural killer T cells. *Cell*. 2014;156(1-2):123-133. doi:10.1016/j.cell.2013.11.042

168. An D, Na C, Bielawski J, Hannun Y a, Kasper DL. Membrane sphingolipids as essential molecular signals for Bacteroides survival in the intestine. *Proc Natl Acad Sci U S A*. 2011;108 Suppl:4666-4671. doi:10.1073/pnas.1001501107

169. Wieland Brown LC, Penaranda C, Kashyap PC, et al. Production of α-Galactosylceramide by a Prominent Member of the Human Gut Microbiota. *PLOS Biol*. 2013;11(7):e1001610. https://doi.org/10.1371/journal.pbio.1001610.

170. Heaver SL, Johnson EL, Ley RE. Sphingolipids in host–microbial interactions. *Curr Opin Microbiol*. 2018;43:92-99. doi:10.1016/J.MIB.2017.12.011

171. Zschiebsch K, Fischer C, Pickert G, et al. Tetrahydrobiopterin Attenuates DSS-evoked Colitis in Mice by Rebalancing Redox and Lipid Signalling. *J Crohn's Colitis*. 2016;10(8):965-978. doi:10.1093/ecco-jcc/jjw056

172. Arai K, Mizobuchi Y, Tokuji Y, et al. Effects of Dietary Plant-Origin Glucosylceramide on Bowel Inflammation in DSS-Treated Mice. *J Oleo Sci*. 2015;64(7):737-742. doi:10.5650/jos.ess15005

173. Zigmond E, Preston S, Pappo O, et al. Beta-glucosylceramide: a novel method for enhancement of natural killer T lymphoycte plasticity in murine models of immune-mediated disorders. *Gut*. 2007;56(1):82-89. doi:10.1136/gut.2006.095497

174. Landy J, Ronde E, English N, et al. Tight junctions in inflammatory bowel diseases and inflammatory bowel disease associated colorectal cancer. *World J Gastroenterol*. 2016;22(11):3117-3126. doi:10.3748/wjg.v22.i11.3117

175. Patterson L, Allen J, Posey I, et al. Glucosylceramide production maintains colon integrity in response to Bacteroides fragilis toxin-induced colon epithelial cell signaling. *FASEB J*. 2020;34(12):15922-15945. doi:https://doi.org/10.1096/fj.202001669R

176. Fogh J, Trempe G. New human tumor cell lines. In: *Human Tumor Cells in Vitro*. Springer; 1975:115-159.

177. Yamada Y, Mori H. Multistep carcinogenesis of the colon in ApcMin/+ mouse. *Cancer Sci*. 2007;98(1):6-10. doi:10.1111/j.1349-7006.2006.00348.x

178. Tan CW, Hirokawa Y, Burgess AW. Analysis of Wnt signalling dynamics during colon crypt development in 3D culture. *Sci Rep*. 2015;5(1):11036. doi:10.1038/srep11036

179. Raposo G, Stoorvogel W. Extracellular vesicles: exosomes, microvesicles, and friends. *J Cell Biol*. 2013;200(4):373-383. doi:10.1083/jcb.201211138

180. Ståhl A-L, Johansson K, Mossberg M, Kahn R, Karpman D. Exosomes and microvesicles in normal physiology, pathophysiology, and renal diseases. *Pediatr Nephrol*. 2019;34(1):11-30. doi:10.1007/s00467-017-3816-z

181. Becker A, Thakur BK, Weiss JM, Kim HS, Peinado H, Lyden D. Extracellular Vesicles in Cancer: Cell-to-Cell Mediators of Metastasis. *Cancer Cell*. 2016;30(6):836-848. doi:10.1016/j.ccell.2016.10.009

182. Naito Y, Yoshioka Y, Yamamoto Y, Ochiya T. How cancer cells dictate their microenvironment: present roles of extracellular vesicles. *Cell Mol Life Sci*. 2017;74(4):697-713. doi:10.1007/s00018-016-2346-3

183. Latifkar A, Hur YH, Sanchez JC, Cerione RA, Antonyak MA. New insights into extracellular vesicle biogenesis and function. *J Cell Sci*. 2019;132(13):jcs222406. doi:10.1242/jcs.222406

184. Gerlach JQ, Griffin MD. Getting to know the extracellular vesicle glycome. *Mol Biosyst*. 2016;12(4):1071-1081. doi:10.1039/C5MB00835B

185. Skotland T, Hessvik NP, Sandvig K, Llorente A. Exosomal lipid composition and the role of ether lipids and phosphoinositides in exosome biology. *J Lipid Res*. 2019;60(1):9-18. doi:10.1194/jlr.R084343

186. Konoshenko MY, Lekchnov EA, Vlassov A V, Laktionov PP. Isolation of Extracellular Vesicles: General Methodologies and Latest Trends. *Biomed Res Int*. 2018;2018:8545347. doi:10.1155/2018/8545347

187. Tamkovich SN, Tutanov OS, Laktionov PP. Exosomes: Generation, structure, transport, biological activity, and diagnostic application. *Biochem Suppl Ser A Membr Cell Biol*. 2016;10(3):163-173. doi:10.1134/S1990747816020112

188. Matsumura S, Minamisawa T, Suga K, et al. Subtypes of tumour cell-derived small extracellular vesicles having differently externalized phosphatidylserine. *J Extracell vesicles*. 2019;8(1):1579541. doi:10.1080/20013078.2019.1579541

189. Bujko M, Kober P, Mikula M, Ligaj M, Ostrowski J, Siedlecki Aleksander J. Expression changes of cell-cell adhesion-related genes in colorectal tumors. *Oncol Lett*. 2015;9(6):2463-2470. doi:10.3892/ol.2015.3107

190. Nusrat A, Parkos CA, Verkade P, et al. Tight junctions are membrane microdomains. *J Cell Sci*. 2000;113(10):1771 LP - 1781. http://jcs.biologists.org/content/113/10/1771.abstract.

191. Yu RK, Tsai Y-T, Ariga T, Yanagisawa M. Structures, Biosynthesis, and Functions of Gangliosides-an Overview. *J Oleo Sci*. 2011;60(10):537-544. doi:10.5650/jos.60.537

192. Mahammad S, Parmryd I. Cholesterol Depletion Using Methyl-β-cyclodextrin BT - Methods in Membrane Lipids. In: Owen DM, ed. New York, NY: Springer New York; 2015:91-102. doi:10.1007/978-1-4939-1752-5_8

193. Simons K, Ehehalt R. Cholesterol, lipid rafts, and disease. *J Clin Invest*. 2002;110(5):597-603. doi:10.1172/JCI16390

194. Maruyama M, Ishida K, Watanabe Y, Nishikawa M, Takakura Y. Effects of Methyl-β-cyclodextrin Treatment on Secretion Profile of Interferon-β and Zonula Occuludin-1 Architecture in Madin–Darby Canine Kidney Cell Monolayers. *Biol Pharm Bull*. 2009;32(5):910-915. doi:10.1248/bpb.32.910

195. Ottico E, Prinetti A, Prioni S, et al. Dynamics of membrane lipid domains in neuronal cells differentiated in culture. *J Lipid Res* . 2003;44(11):2142-2151. doi:10.1194/jlr.M300247-JLR200

196. Okumura R, Takeda K. Maintenance of gut homeostasis by the mucosal immune system. *Proc Jpn Acad Ser B Phys Biol Sci*. 2016;92(9):423-435. doi:10.2183/pjab.92.423

197. Fiorini E, Veghini L, Corbo V. Modeling Cell Communication in Cancer With Organoids: Making the Complex Simple . *Front Cell Dev Biol* . 2020;8:166. https://www.frontiersin.org/article/10.3389/fcell.2020.00166.

198. Cattaneo CM, Dijkstra KK, Fanchi LF, et al. Tumor organoid–T-cell coculture systems. *Nat Protoc*. 2020;15(1):15-39. doi:10.1038/s41596-019-0232-9

199. Morichika H, Hamanaka Y, Tai T, Ishizuka I. Sulfatides as a predictive factor of lymph node metastasis in patients with colorectal adenocarcinoma. *Cancer*. 1996;78(1):43-47. doi:10.1002/(SICI)1097-0142(19960701)78:1<43::AID-CNCR8>3.0.CO;2-I

200. Takahashi T, Suzuki T. Role of sulfatide in normal and pathological cells and tissues. *J Lipid Res*. 2012;53(8):1437-1450. doi:10.1194/jlr.R026682

201. Siddiqui B, Whitehead JS, Kim YS. Glycosphingolipids in human colonic adenocarcinoma. *J Biol Chem* . 1978;253(7):2168-2175. http://www.jbc.org/content/253/7/2168.short.

202. D'Angelo G, Capasso S, Sticco L, Russo D. Glycosphingolipids: synthesis and functions. *FEBS J*. 2013;280(24):6338-6353. doi:10.1111/febs.12559

203. Kolter T. Ganglioside biochemistry. *Int Sch Res Not*. 2012;2012.

204. Pasquel-Dávila D, Yanez-Vaca S, Espinosa-Hidalgo N, Buenaventura E. Gangliosides generalities and role in cancer therapies. *Bionatura*. 2019;02. doi:10.21931/RB/CS/2019.02.01.28

205. Groux-Degroote S, Guérardel Y, Delannoy P. Gangliosides: Structures, Biosynthesis, Analysis, and Roles in Cancer. *ChemBioChem*. 2017;18(13):1146-1154. doi:10.1002/cbic.201600705

206. Miklavcic JJ, Hart TDL, Lees GM, et al. Increased catabolism and decreased unsaturation of ganglioside in patients with inflammatory bowel disease. *World J Gastroenterol*. 2015;21(35):10080-10090. doi:10.3748/wjg.v21.i35.10080

207. Miklavcic JJ, Schnabl KL, Mazurak VC, Thomson ABR, Clandinin MT. Dietary ganglioside reduces proinflammatory signaling in the intestine. *J Nutr Metab*. 2012;2012:280286. doi:10.1155/2012/280286

208. Schnaar RL. Chapter Three - The Biology of Gangliosides. In: Baker DCBT-A in CC and B, ed. *Sialic Acids, Part II: Biological and Biomedical Aspects*. Vol 76. Academic Press; 2019:113-148. doi:https://doi.org/10.1016/bs.accb.2018.09.002

209. Saragovi HU, Gagnon M. Gangliosides: therapeutic agents or therapeutic targets? *Expert Opin Ther Pat*. 2002;12(8):1215-1223. doi:10.1517/13543776.12.8.1215

210. D'Souza-Schorey C, Clancy JW. Tumor-derived microvesicles: shedding light on novel microenvironment modulators and prospective cancer biomarkers. *Genes Dev* . 2012;26(12):1287-1299. doi:10.1101/gad.192351.112

211. Tricarico C, Clancy J, D'Souza-Schorey C. Biology and biogenesis of shed microvesicles. *Small GTPases*. 2017;8(4):220-232. doi:10.1080/21541248.2016.1215283

212. Catalano M, O'Driscoll L. Inhibiting extracellular vesicles formation and release: a review of EV inhibitors. *J Extracell vesicles*. 2019;9(1):1703244. doi:10.1080/20013078.2019.1703244

213. Romero M, Keyel M, Shi G, et al. Intrinsic repair protects cells from pore-forming toxins by microvesicle shedding. *Cell Death Differ*. 2017;24(5):798-808. doi:10.1038/cdd.2017.11

214. Olsen I, Jantzen E. Sphingolipids in Bacteria and Fungi. *Anaerobe*. 2001;7(2):103-112. doi:http://dx.doi.org/10.1006/anae.2001.0376

215. Mendelson K, Evans T, Hla T. Sphingosine 1-phosphate signalling. *Development*. 2013;141(1):5-9. http://dev.biologists.org/content/141/1/5.abstract.